RISK TERRITORIALISATION

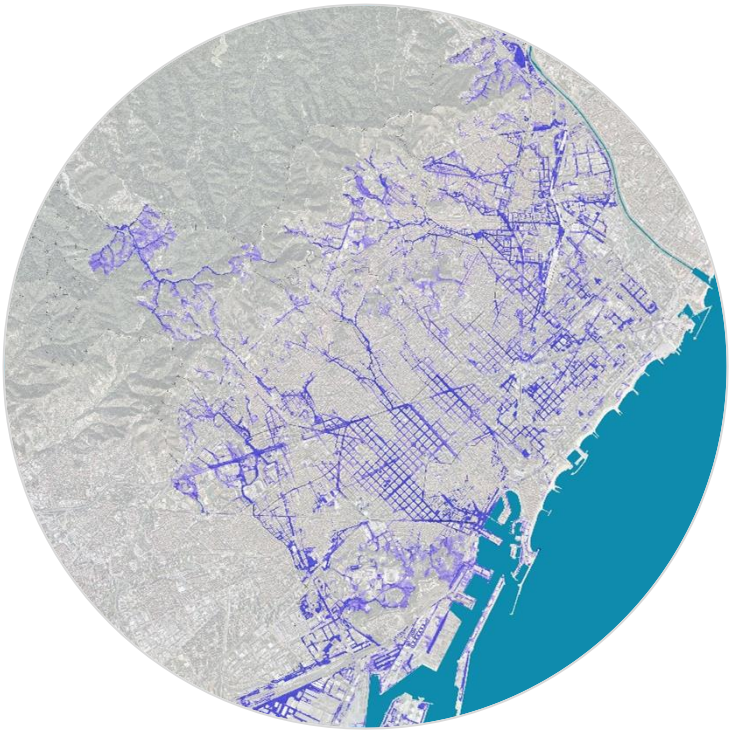

Executive summary of the results for the climate change impact analysis in Barcelona, developed within the European RESCCUE project framework

July 2021

RESCCUE

Department of
Urban Resilience

Ajuntament de Barcelona

Index of figures

Index of maps

1 Introduction

The main goal of the RESCCUE project is to help cities become more resilient to not only the physical, but also the social and economic challenges arising from climate change impacts, generating methodologies that are applicable to various types of cities with different exposures to climate change. More specifically, RESCCUE aims to improve the urban resilience of our cities, through a series of models and tools that assess the impact of climate change on various strategic urban sectors, such as the water cycle (water treatment, water supply, urban drainage, waste-water treatment), transport, energy supplies and solid waste. Secondly, the project studies how these urban services are interconnected, in order to assess urban resilience for the current situation and for different future climate-change and adaptation scenarios.

The initial basis for the entire process of assessing the city's resilience is acquiring detailed knowledge about the behaviour of our urban systems when subjected to extreme climate events. In order to achieve this goal, the project has produced, calibrated and validated a series of detailed sectorial models, based on various future climate change scenarios, extracted from new climate projections, as well as the current situation. The use of sectorial models (or the integration of several sectorial models) can help to fully understand the hazard exposure related to extreme climate events and, lastly, how they can be used to assess the multiple risks that could affect Barcelona city in the future. The project focused on analyzing water-related impactsin three different areas: **flood risk**, **drought risk and sea level rise risk**.

Within the framework of flood risk, a multi-risk assessment of various sectors exposed to the effects of climate change was carried out, for four different scenarios: **The current scenario**: deals with today's situation; **the future scenario**: raises the future changes brought about by climate change, based on new climate projections; **Adaptation Scenario 1**: lists the improvements resulting from the introduction of SUDS (sustainable urban drainage systems) with regard to the future scenario, and **Adaptation Scenario 2** is based on introducing structural measures in the drainage system, in addition to the SUDS, in relation to the future scenario.

The four scenarios considered for flood risk have been developed for the **T1, T10, T50, T100 and T500** return periods. However, depending on the sector being assessed and its particular characteristics, only the most significant return periods are considered in this document.

In the case of the rise in sea level, the analysed scenarios consider the 2070-2100 temporal horizon for Representative Concentration Pathways (RCPs) 4.5 and 8.5 from 5th IPCC Report.

2 Methodology

Figure 1 shows the conceptual framework for the risk assessment and the definitions used.

Figure 1. *Methodology used for developing the risk analysis.*

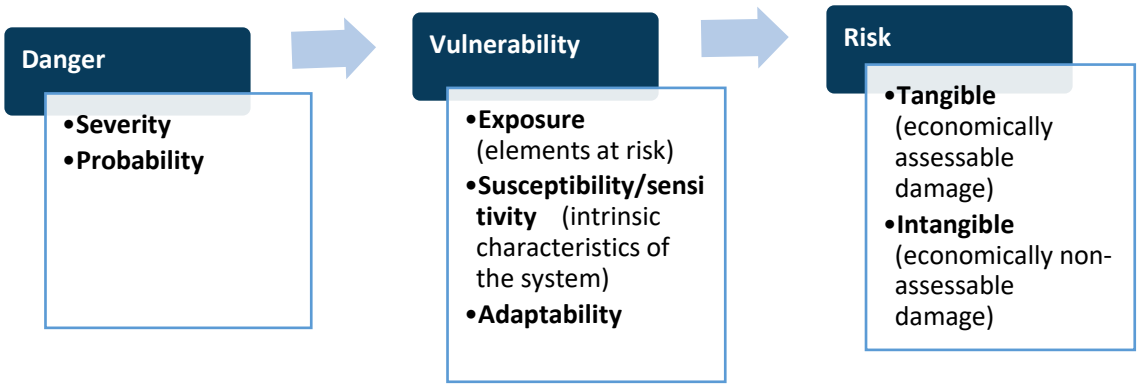

The risk of climate-related impacts are the result of the interaction of hazards associated with climate itself (including extreme events and change trends) with the vulnerability of human and natural systems.

A **climate hazard** is considered to be any condition of a climate variable that may cause an adverse effect: as a first step, the selection of relevant climate variables serve as a basis for obtaining the climate indexes needed for the haxards analysis process. For every hazard related to climate, one or more relevant index are identified, such as the probability of occurrence or exceeding the threshold values. The indexes are calculated for a defined climate period and can be combined with other parameters in order to assess various scales of hazard.

Vulnerability refers to the propensity of exposed elements (such as human beings, their ways of life and their assets) to suffer adverse effects when they are affected by hazardous events. This corresponds to the inventory of elements present in areas where dangerous events may occur (flooding, drought and a rise in sea level, in our case), which may negatively affect them (possibly damaged or displaced). These values depend on the presence of people, ecosystems, environmental services and resources, infrastructures and economic, social and cultural assets in places that could be negatively affected. **Susceptibility (or sensitivity)** is the degree to which the system is affected, which depends on the intrinsic characteristics of its exposed elements within the area where hazardous events may occur, while the **adaptability** of a system is its capacity to endure and overcome any disruption, such as flooding, and maintain significant levels of efficiency in its social, economic, environmental and physical components.

Lastly, the process of **risk assessment** takes into account the magnitude and probability of impacts associated with the previously identified risks, with the aim of evaluating the importance of the affected assets, identifying them and locating them on a risk map. This map is developed by overlapping the hazard map and the vulnerability map. The result of this process is a map that establishes different risk levels in specific areas of the city for the several fields studied, based on the combination of hazard and vulnerability levels. Figure 2 shows the concept of the risk map as a combination of hazard and vulnerability:

Figure 2. *Methodology for generating risk maps based on the combination of hazard maps and vulnerability maps.*

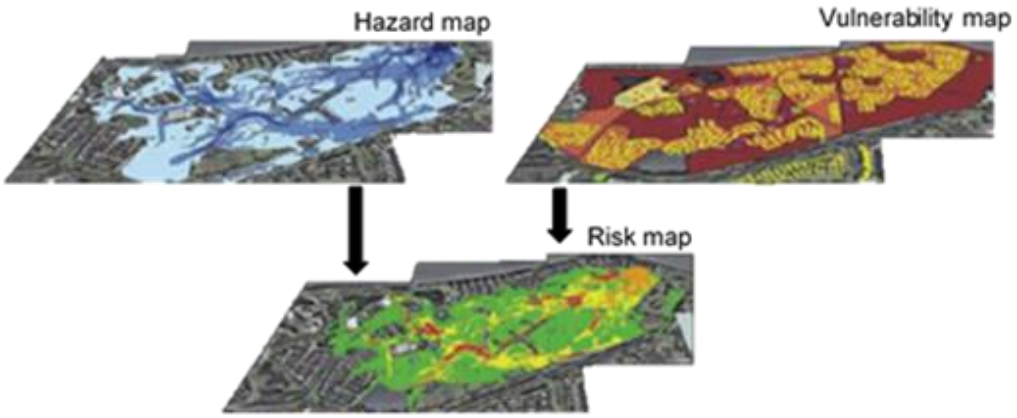

The results are classified by tangible damage (economic damage to assets) or intangible damage (damage that cannot be economically evaluated, e.g. the expansion of high-risk areas, social impacts on vulnerable groups or the loss of human lives). The results of the analysis and the monetisation of the risks arising from the impact of climate change, developed as part of the RESCCUE project, may be consulted at: *RESCCUE Deliverable 3.5 Impact assessments of multiple hazards in case study areas* (https://toolkit.resccue.eu/resccue-deliverables).

ADAPTATION SCENARIOS

The urban flooding model makes possible the simulation of climate change scenarios, applying different adaptation measures and provide information about the **reduction of flood risk,** depending on the measures applied. More specifically, two different adaptation scenarios have been considered: **Adaptation Scenario 1,** which provides for the improvement of the implementationof sustainable urban drainage systems, and **Adaptation Scenario 2**, which proposes the incorporation of structural measures in the drainage network system, in addition to the SUDS, regarding the future scenario.

3 Impact analysis derived from floods caused by rainfall episodes

3.1 Urban flood model

The mathematical modelling of Barcelona's urban drainage system is used as a basis for the risk analysis of flooding and the assessment of the impacts on assets and people caused by these floods. The urban-drainage model developed in the RESCCUE project is the result of the participation of BCASA as a project partner, which agreed to supply the RESCCUE project with the results of the PDISBA model (Barcelona Master drainage plan), therefore both projects take advantage from the developed methodologies and their results are consistent.

The main characteristic of the new urban drainage model is the modelling of the city's entire drainage network, including both the primary and secondary networks, and also the characterization of all the singular elements it includes (grilles, drains, rainwater retention tanks, valves, pumping stations, etc.). The model, denominated as 1D/2D, combines the water flow simulation of the underground sewer system with the circulation model for surface water, which provides information on the hydrological variables of depth, velocity and extension of floodable areas of the city during torrential rain events.

Within the framework of the PDISBA, the calibration of the urban drainage model was developed based on the design rainfall corresponding to a 10-year return period (T10), produced from historical pluviometric data provided by BCASA (Figure 3).

Figure 3. *Comparison between design rainfall for the current scenario (T10) and the future scenario (T10 CC), corresponding to the 10-year return period and the 2071-2100 temporal horizon.*

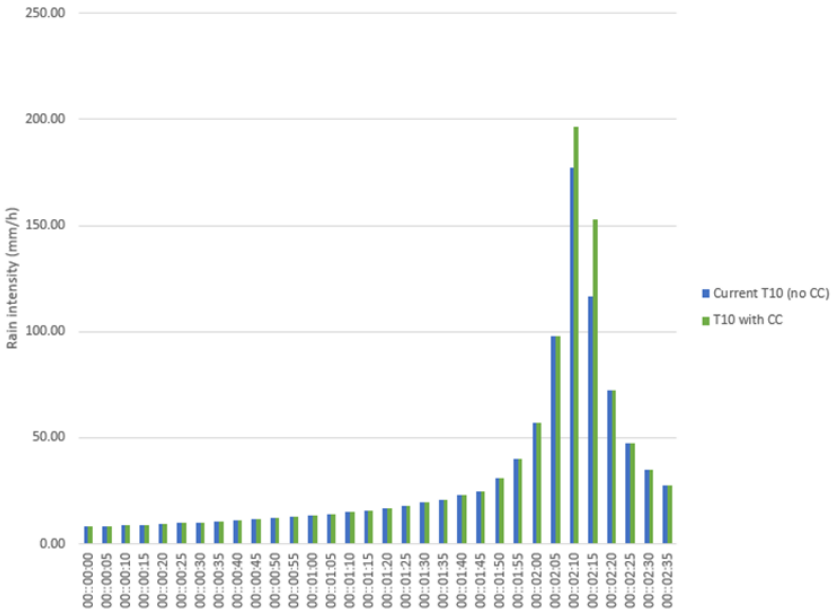

Once the mode had been validated, the different return periods (T1, T10, T50, T100, T500) were simulated for the current scenario and the future climate-change scenario, applying the climate-change factors obtained from the climate rainfall projections in a statistical regression analysis of 20 rainfall series provided for 10 forced global climate models for RCP 4.5 and 8.5, previously validated for the 1976-2005 historical period.

The behaviour of the drainage system for each associated rainfall episode was extracted from the simulation of the differents design rainfalls produced, for the current and future scenarios (Figure 4):

Figure 4. *Behaviour of the drainage network for the current and future scenarios (metres of drain system).*

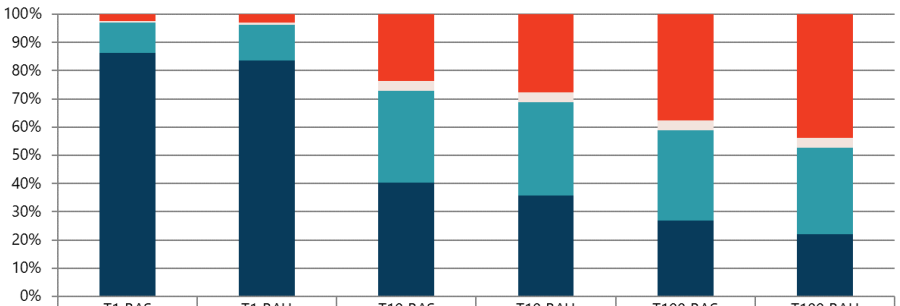

	T1 BAS	T1 BAU	T10 BAS	T10 BAU	T100 BAS	T100 BAU
4-Sobre terreny	2%	3%	24%	28%	38%	44%
3-0.5 m sota terreny	1%	1%	3%	3%	4%	4%
2-Pressio	11%	13%	33%	33%	32%	31%
1-Làmina lliure	86%	83%	40%	36%	27%	22%

Logically, as the return period increases, there are fewer sections of main sewers that function under free flow, as they become increasingly more in demand. In the simulation of the future climate-change scenario, for the 10-year return period (T10), it can be seen that the drainage system functions worsened in comparison with the current situation, so that there is up to a 28% increase in sections where the water flows on the surface, a 3% increase in the sections where water flows 50 cm below the surface and a 33% increase in sections that function under pressure. The rest of the network, 36%, functions properly.

According to the new climate projections produced as part of the project, the intensity of torrential rain episodes in the city is forecast to increase by between 20% and 40%. Taking into account that the drainage system already starts to suffer major overflows with rainfall for a 10-year return period, this increase in rainfall intensity would mean an increase in the floodable areas of the city.

The urban drainage model enables us to analyse the behaviour of surface water by parameterising the velocity and depth of the water, and to determine the extension of floodable areas in the city. The following maps show how the analysed hydrological variables (water velocity and depth) vary for the most significant return periods: T10 to represent a normal frequency and T100 to represent a reduced frequency, for both the current and future scenarios:

Map 1. *Urban flooding for the current scenario, with a T10 return period.*

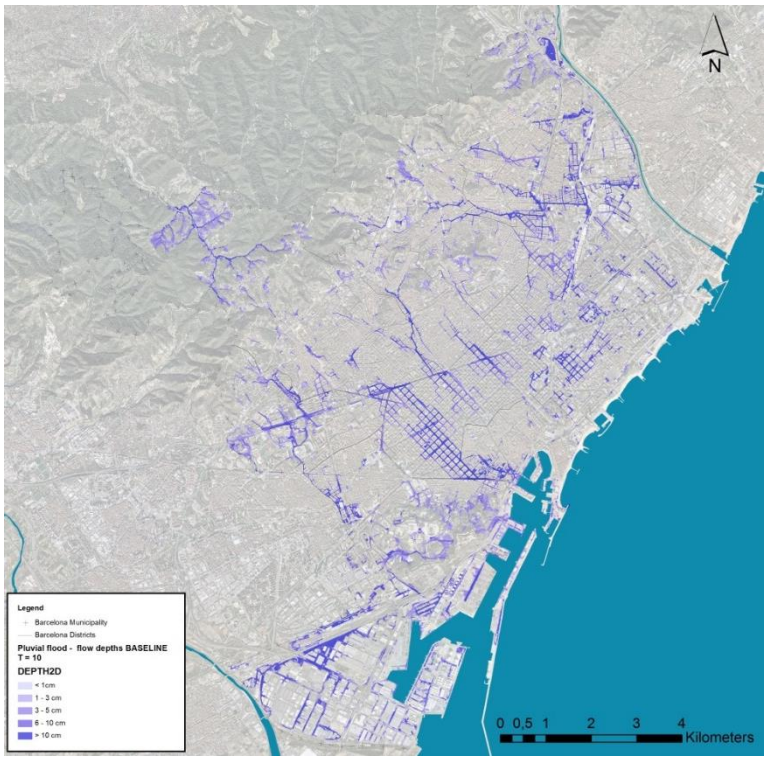

Map 2. *Urban flooding for the future scenario, with a T10 return period.*

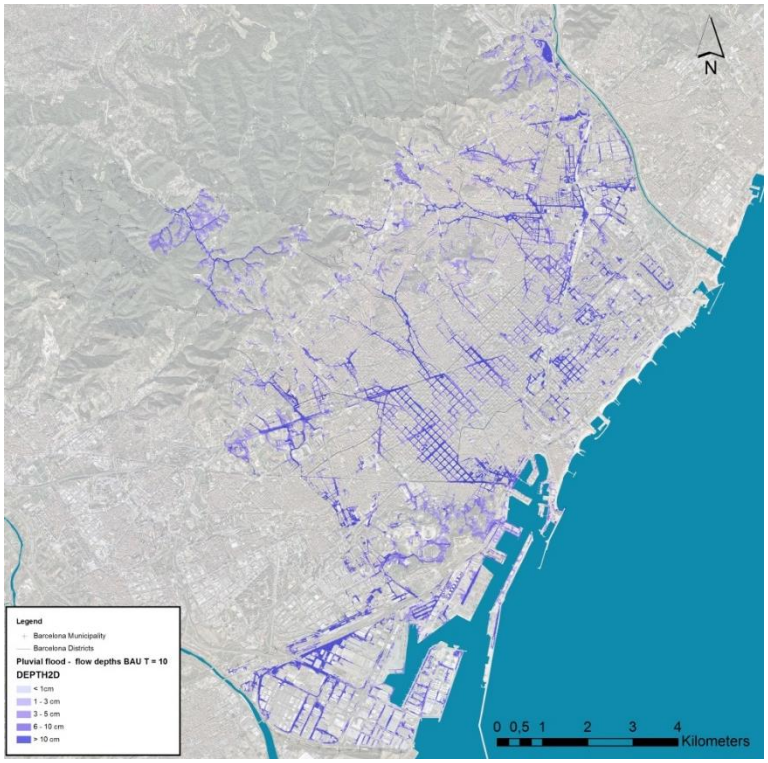

Map 3. *Urban flooding for the current scenario, with a T100 return period.*

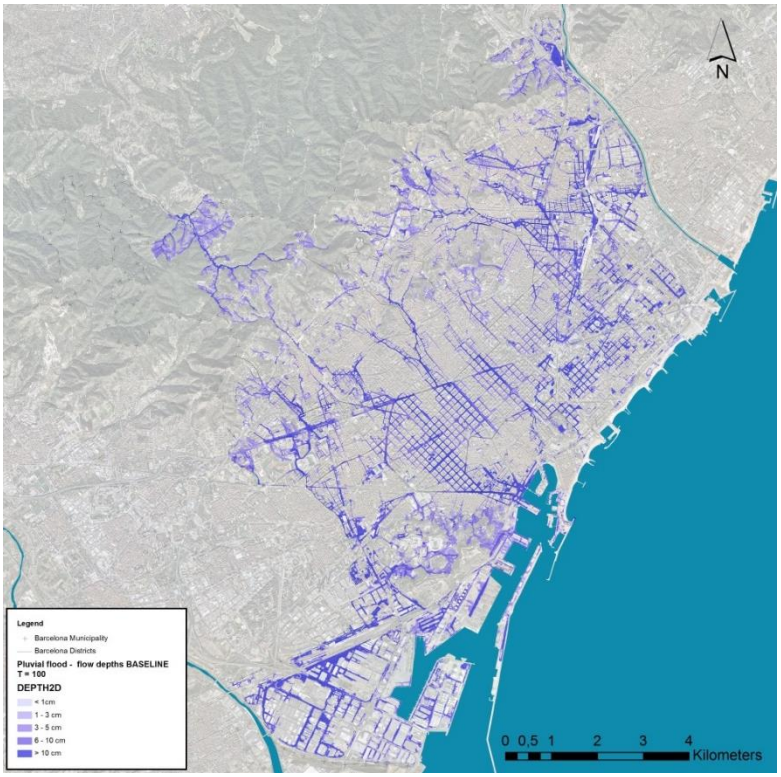

Map 4. *Urban flooding for the future scenario, with a T100 return period.*

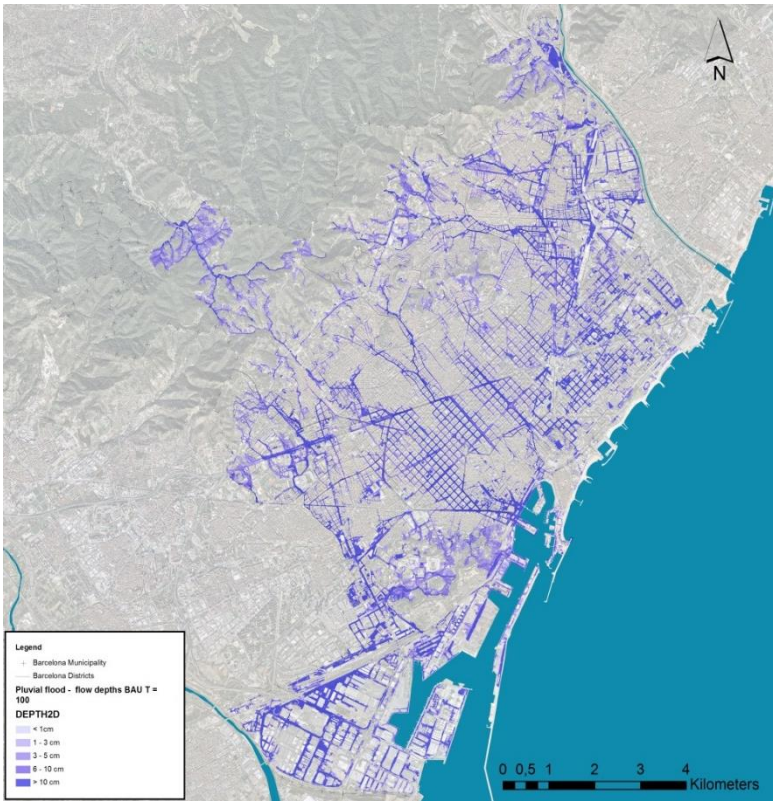

The maps make it possible to identify the city's major critical points, in terms of the malfunctioning of the drainage network, which can be summarised as follows:

1. Diagonal - Plaça de Francesc Macià
2. Urgell/Casanova /Av. Roma
3. Ronda de Sant Pau – Av. Paral·lel
4. The area surrounding Carrer de Sant Pau
5. Diagonal (Bruc - Roger de Flor)
6. Clot - Navas
7. Via Augusta - Príncep d'Astúries - Rambla del Prat
8. The area surrounding Rambla de Prim
9. Plaça de Llucmajor
10. Tajo - Cartellà
11. Carrer de Parcerisa
12. Carrer de la Riera Blanca
13. The area surrounding the Seat factory (Zona Franca)
14. Torrent de Tapioles

Map 5. *The major critical points in the city.*

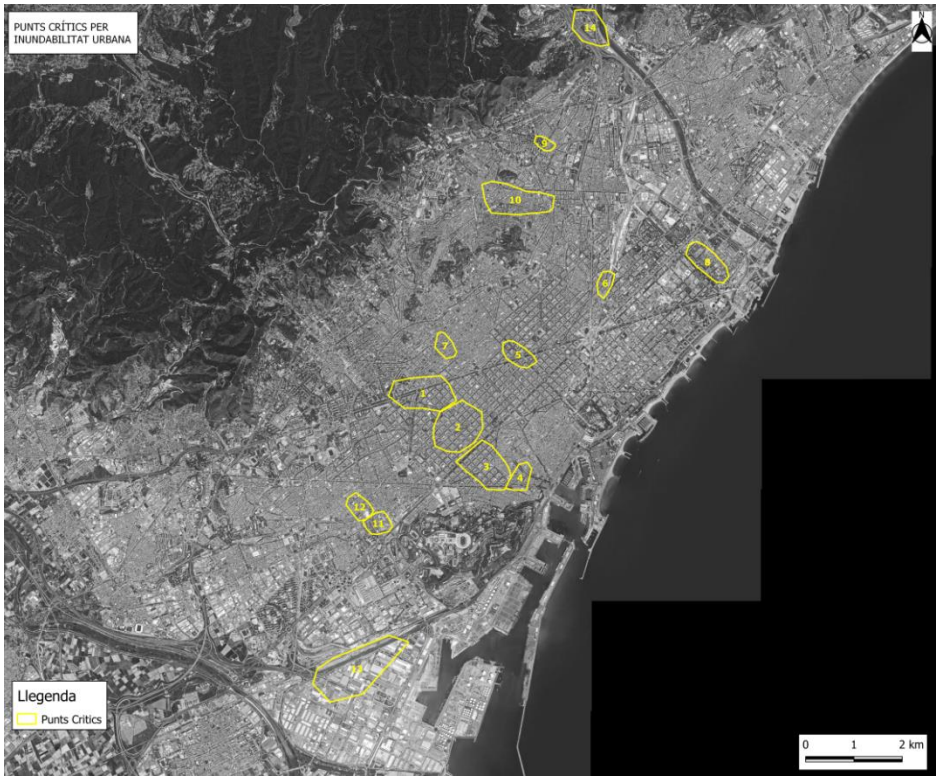

In the potential context of climate change, the effects of flooding for the city have been assessed by means of a multi-risk approach, and the results of this evaluation are presented in terms of hazard, vulnerability and through the use of risk maps for the urban services affected in the case of flooding: mobility and waste, as well as the effects on people (pedestrians and vehicles) and on water quality, in order to assess the socio-economic impacts of discharges into the receiving environment. The flooding simulation results show that Barcelona could suffer a significant increase in these impacts. For example, an increase in the maximum intensity of torrential rainfall of between 12% and 16% could mean increases of over 25% to 30% in terms of social impacts (intangible damage, such as an increase in the areas classified as high risk) and economic losses (tangible damage expresses in monetary terms).

Here are the main result of the analysis of the impacts caused by flooding in Barcelona city.

3.2 Risk to people: the stability of pedestrians and vehicles.

The study on how flooding affects the stability of pedestrians and vehicles is based on the results of the hydrodynamic model in which water velocity and depth are the main hydrological variables affecting the stability of pedestrians and vehicles in the case of urban rainwater flooding, so that surface run-off is characterised by a high flow velocity and a low flow depth. Figure 6 shows how flow velocity and water depth are turned into a hazard level, according to the thresholds[1] proposed for the study, for pedestrians (a) and vehicles (b):

Figure 5. *Risk matrix for pedestrians (a) and vehicles (b) according to the hydrological variables of flow and depth.*

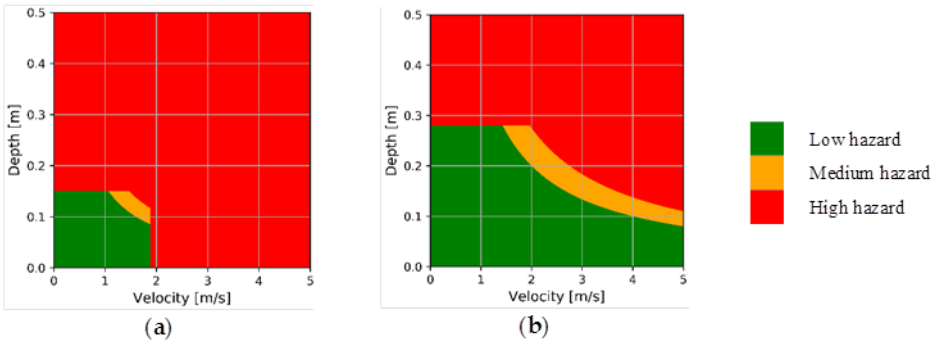

The following **risk maps** show the level of probability that a pedestrian would lose stability, and could therefore fall and be carried away by the flow of water. The high-risk areas indicate those areas where the hydrodynamic variables are able to cause loss of stability in a person, depending on the intensity of the rainfall episode, characterised by its return period. The following map shows the high-risk areas for pedestrians, for all the simulated return periods:

[1] Russo, B., Gómez, M., Macchione, F., 2013. Pedestrian hazard criteria for flooded urban areas. Nat. Hazards 69, 251–265. https://doi.org/10.1007/s11069-013-0702-2
Martínez-Gomariz, E.; Gómez, M.; Russo, B. Experimental study of the stability of pedestrians exposed to urban pluvial flooding. Nat. Hazards 2016, 82, 1259–1278.
Martínez-Gomariz, E.; Gómez, M.; Russo, B.; Djordjević, S. A new experiments-based methodology to define the stability threshold for any vehicle exposed to flooding. Urban Water J. 2017, 14, 930–939.

Map 6. *High-risk areas for pedestrians, for the current scenario and the simulated T1, T10 and T100 return periods*

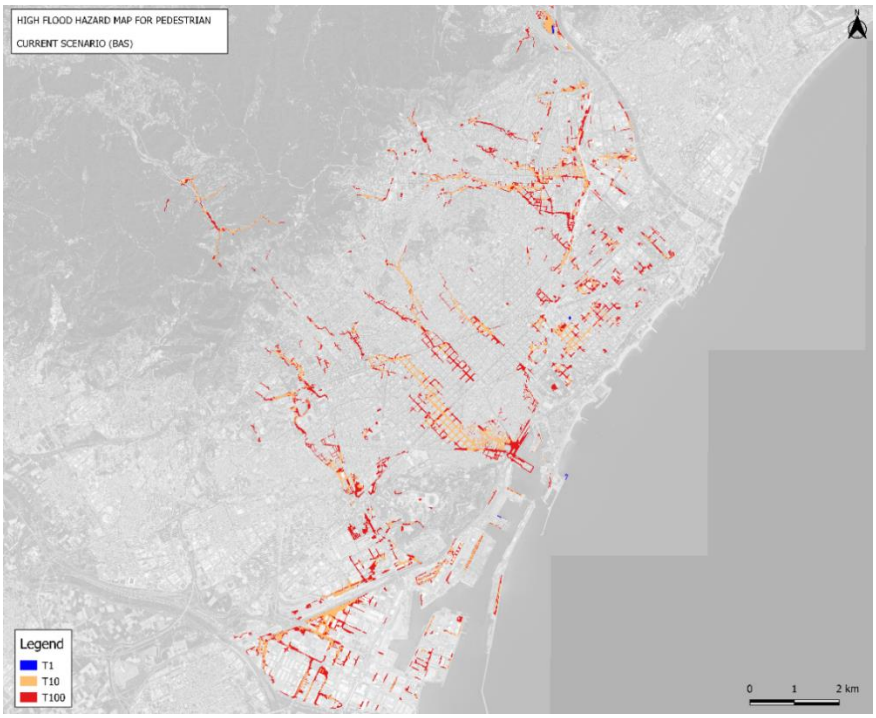

Map 7. *High-risk areas for pedestrians, for the future scenario and the simulated T1, T10 and T100 return periods*

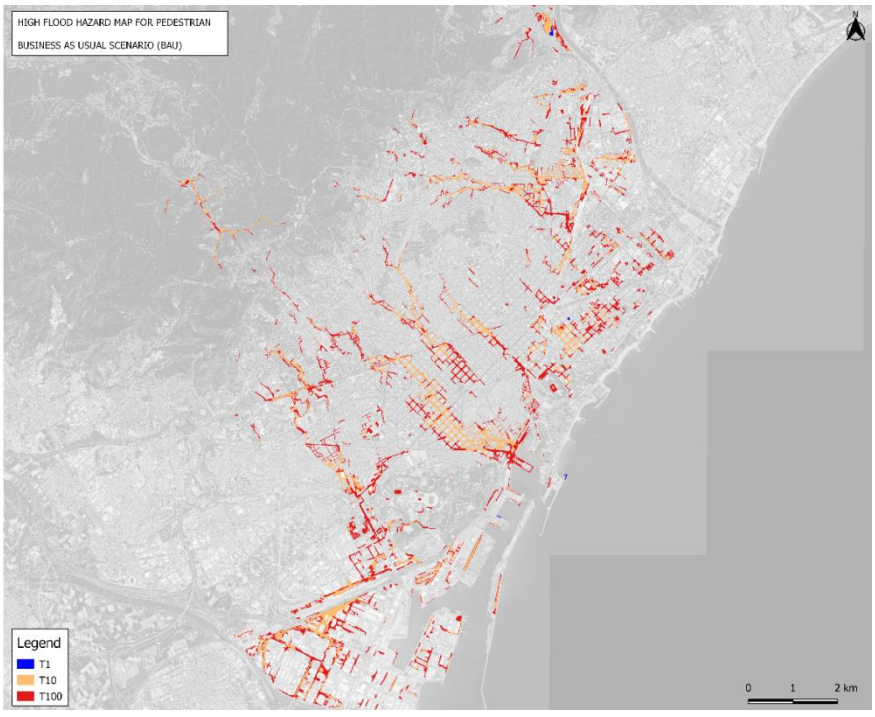

The following graph summarises the results of the risk maps for pedestrians, classified by risk level:

Figure 6. *Total surface area (as a %) of risk levels for pedestrians, for the current (BAS) and future (BAU) scenarios, with all the simulated return periods.*

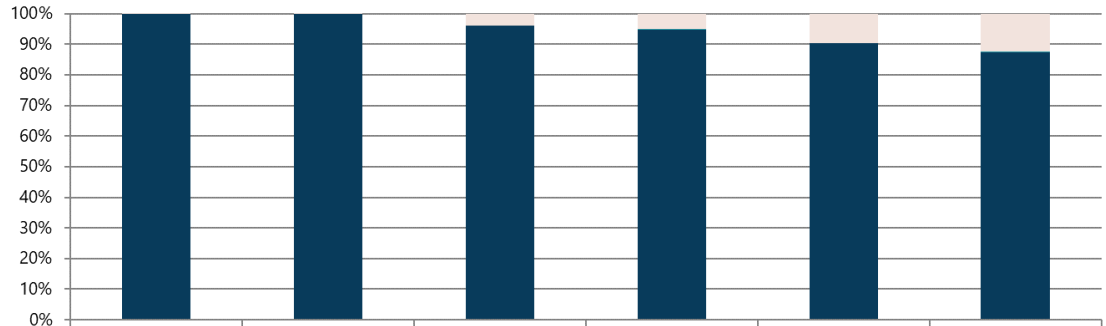

	T1 BAS	T1 BAU	T10 BAS	T10 BAU	T100 BAS	T100 BAU
Alt	0.1%	0.1%	3.9%	5.1%	9.5%	12.4%
Mitjà	0.0%	0.0%	0.1%	0.1%	0.1%	0.2%
Baix	99.9%	99.9%	96.0%	94.8%	90.3%	87.4%

For the one-year (T1) return period, for both the current and future scenarios, the high-risk areas are anecdotal (0.02% and 0.03% of the surface area, respectively). Therefore, climate change does not mean any worsening of the existing situation.

For the T10 return period, the high-risk areas total 240 ha, which is 3.9% of the city's total transitable surface area. No new high-risk areas appear due to the action of climate change, but the existing ones increase equally in all the city's neighbourhoods to a total of 312 ha, which is 5.1% of the total surface area. This is a 30% increase in the high-risk surface area.

In the case of the T100, the current situation gets notably worsened, as new high-risk areas appear and the existing T10 high-risk areas get considerably larger, reaching 9.5% of Barcelona's total surface area (585 ha). For the future scenario, once again a 30% increase in the transitable surface area with a high risk for pedestrians, to a figure of 12.4% of the total surface area (762 ha).

Map 8. *High-risk areas for vehicles, for the current scenario and the simulated T1, T10 and T100 return periods*

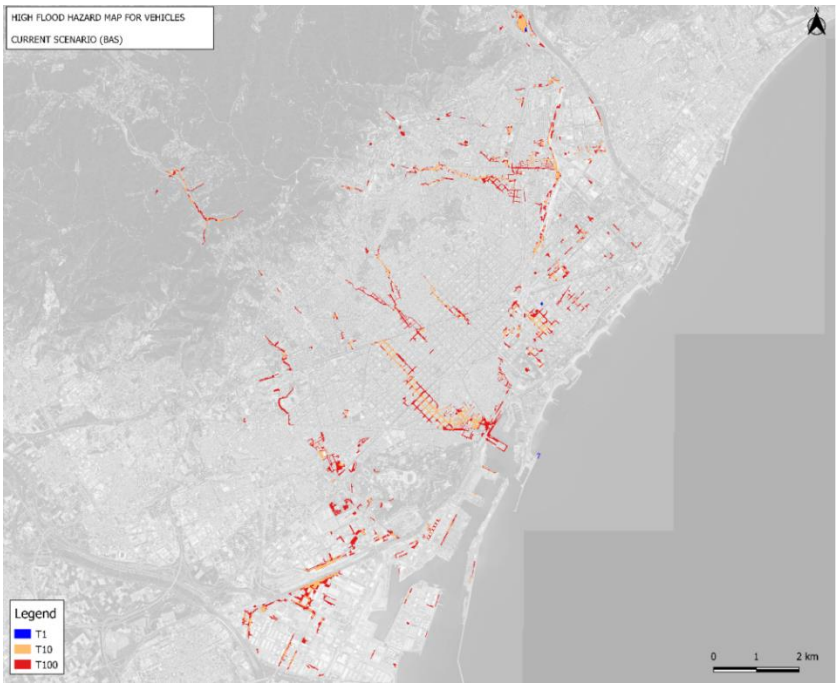

The following risk maps show the probability of a vehicle being swept away by the flow of surface water:

Map 9. *High-risk areas for vehicles, for the future scenario and the simulated T1, T10 and T100 return periods*

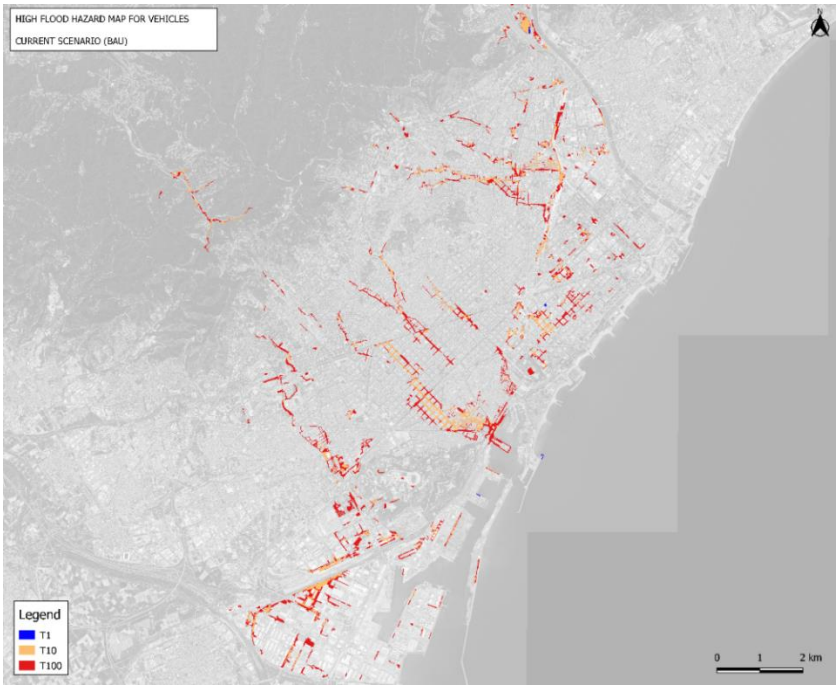

Once again, the high-risk areas for T1 are irrelevant. In regard to the T10, the high-risk areas are the same as for risk to pedestrians, but here they extend along a lower number of streets. This means, for the current situation, a surface area of 110 ha (1.8% of the total), and 148 ha (2.4%) for the future scenario, which is an increase of 34%.

Figure 7. *Total surface area (as a %) of risk levels for vehicles in the current and future scenarios, for the most significant return periods.*

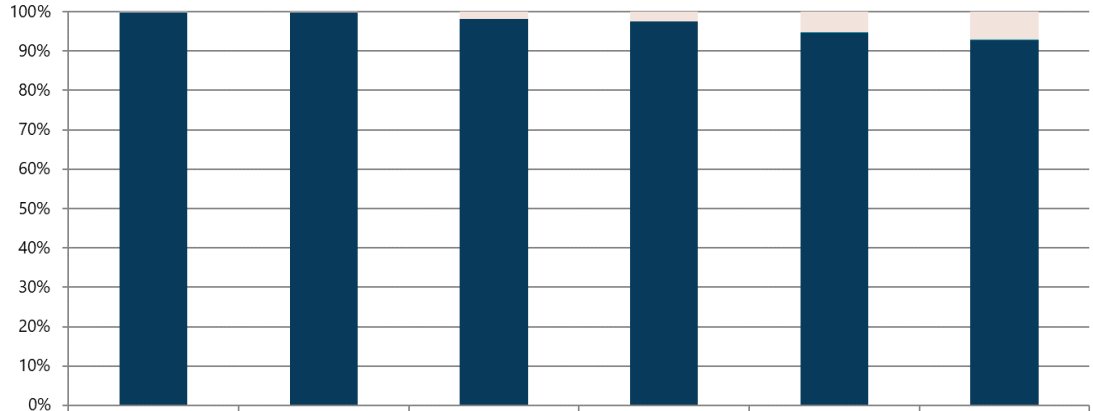

	T1 BAS	T1 BAU	T10 BAS	T10 BAU	T100 BAS	T100 BAU
Alt	0.1%	0.1%	1.8%	2.4%	5.2%	7.1%
Mitjà	0.0%	0.0%	0.1%	0.1%	0.2%	0.2%
Baix	99.9%	99.9%	98.1%	97.5%	94.6%	92.7%

In the case of the T100, the risk trend for pedestrians is reproduced, increasing to 318 ha (5.2%) for the current scenario and 433 ha (7.1%) for the future scenario, so that the increase is once again approximately 35%.

Therefore, once the results for the pedestrian and vehicle risk areas have been analysed, it can be concluded that:

- There is an analogous behaviour between the risk to pedestrians and the risk to vehicles.
- The medium-risk areas are irrelevant in all return periods.
- The total high-risk surface area for pedestrians is twice as big than the high-risk area for vehicles, which shows that pedestrians are not as stable as vehicles, which show a greater resistance to slippage.
- The high-risk areas are irrelevant in T1, even in the future scenario. This is due to the fact that the city's drainage system is designed for a T10 design period. Therefore, at T1, there is no appreciable climate change impact caused by an increase in the design rainfall, as the system has the capacity to absorb it without any problems.
- However, from T10 onwards, there is a proportional increase in risk for all the return periods, of around 30-35%.

The next step defines the **vulnerability** of people considered to be at risk in this study. Various levels of vulnerability are established, according to people's exposure (density of people) and their physical characteristics (sensitivity), taking into account indicators such as the percentage of people at a critical age, the population density and the percentage of foreigners. The vulnerability assessment also considers the presence of vulnerable infrastructures, such as schools, hospitals or senior-citizen centres. Figure 8 shows the vulnerability criteria for pedestrians exposed to urban flooding:

Figure 8. *Vulnerability criteria for pedestrians exposed to urban flooding.*

	VULNERABILITY FOR PEDESTRIANS IN CENSAL AREAS FOR BARCELONA CITY			
Vulnerability index / score	A. Population density (person/km²)	B. % areas of infrastructures vulnerability	C. % of people with critical age	D. % of foreign people
1 (low)	≤ 384,62	0%	≤ 25%	≤ 10%
2 (medium)	384,62 <X≤ 15,747	0% < X ≤ 15%	25% < X ≤ 33%	10% < X ≤ 25%
3 (high)	> 15,747	> 15%	> 33%	> 25%

Furthermore, vehicle stability can compromise people's safety, and therefore the flow of traffic (indicator of exposure) is analysed in order to define the vulnerability levels of each street. Figure 9 shows the vulnerability criteria for vehicles exposed to urban flooding:

Figure 9. *Vulnerability criteria for vehicles exposed to urban flooding.*

	VULNERABILITY FOR VEHICLES
Vulnerability index / score	Vehicular flow intensity (VFI) (veh/day)
1 (low)	< 5,000
2 (medium)	5,000 ≤ X ≤ 10,000
3 (high)	> 10,000

The vulnerability maps show the vulnerability of pedestrians or vehicles when they are exposed to rainwater flooding in specific areas of the city and establish three qualitative levels: low, medium and high.

Map 10. *Vulnerability map for pedestrians.*

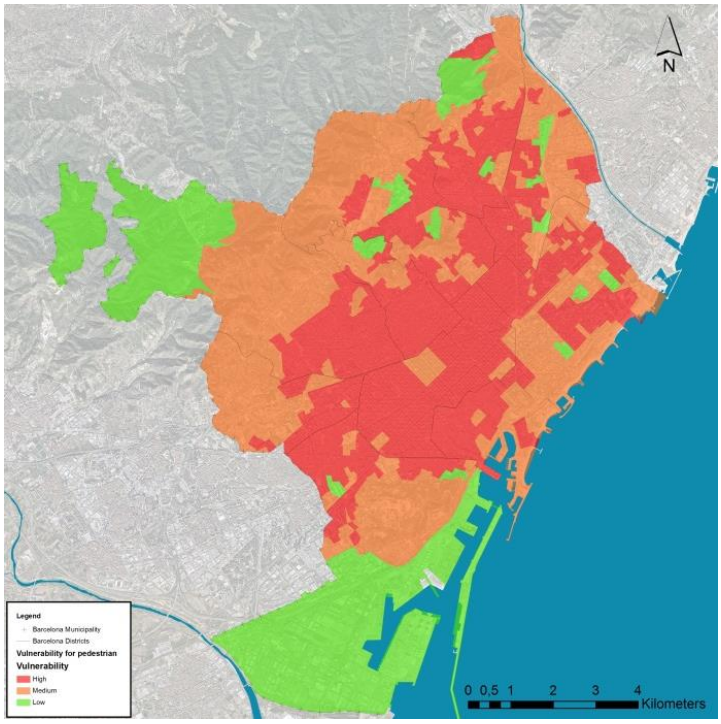

In regard to the vulnerability map for pedestrians, the largest weighting is allocated to population density (50%), which shows that the most vulnerable areas for pedestrians practically coincide with the neighbourhood areas with the highest population density.

Map 11. *Vulnerability map for vehicles*

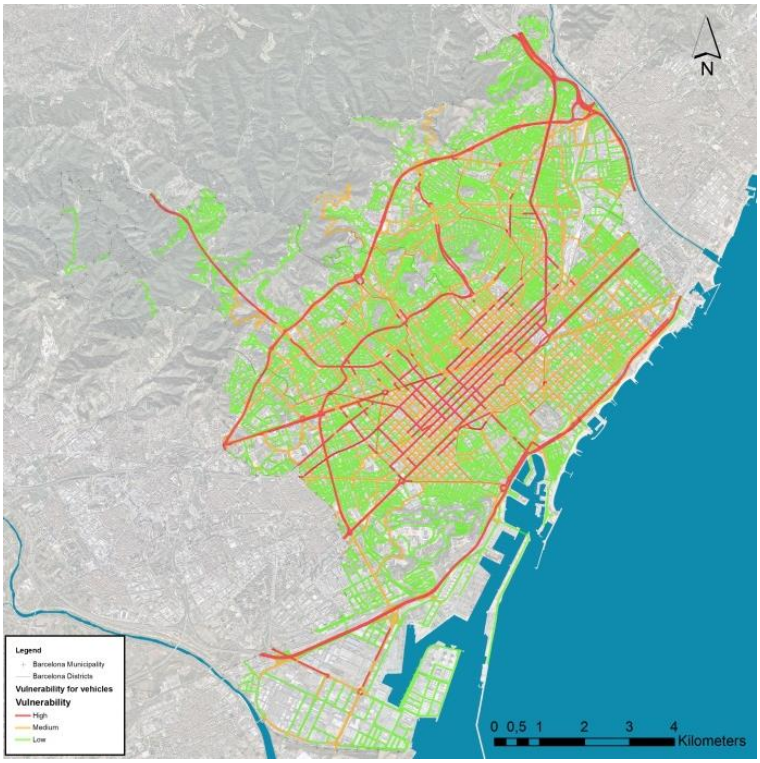

In regard to the vulnerability map for vehicles, the roads with most traffic are also the most vulnerable ones.

Once risk and vulnerability have been defined, the **risk maps** are developed. This results in a qualitative map that establishes three risk levels in specific areas of the city, for pedestrians or vehicles, based on a combination of the risk level caused by rainwater flooding and the vulnerability level. Figure 10 shows the various risk levels as a result of the combination of hazard caused by flooding and the level of vulnerability:

Figure 10. *Risk levels.*

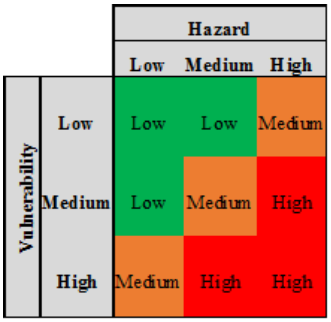

Here are the various risk maps for pedestrians and vehicles, for the current scenario and the climate-change scenario, and for the T10 and T100 return periods:

Map 12. *Risk map for pedestrians in the current scenario, with a T10 return period.*

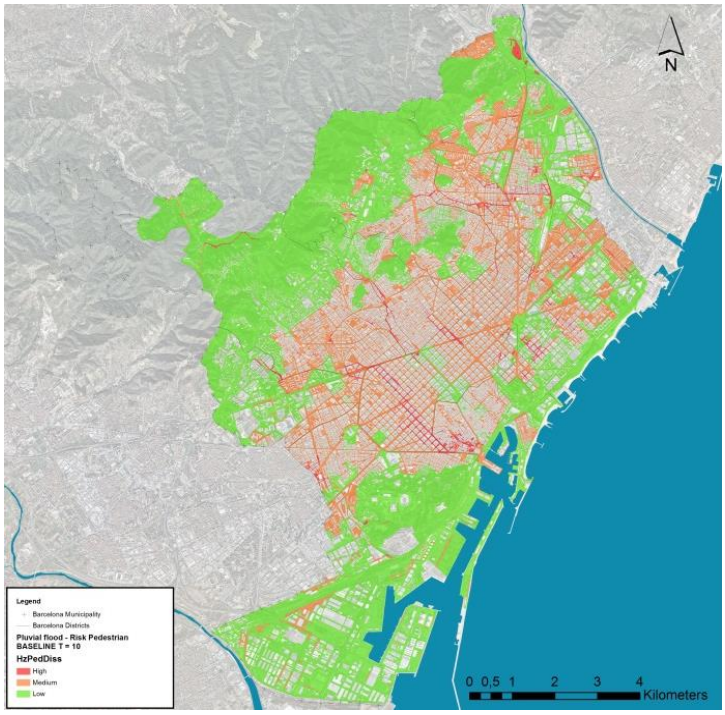

Map 13. *Risk map for pedestrians in the future scenario, with a T10 return period.*

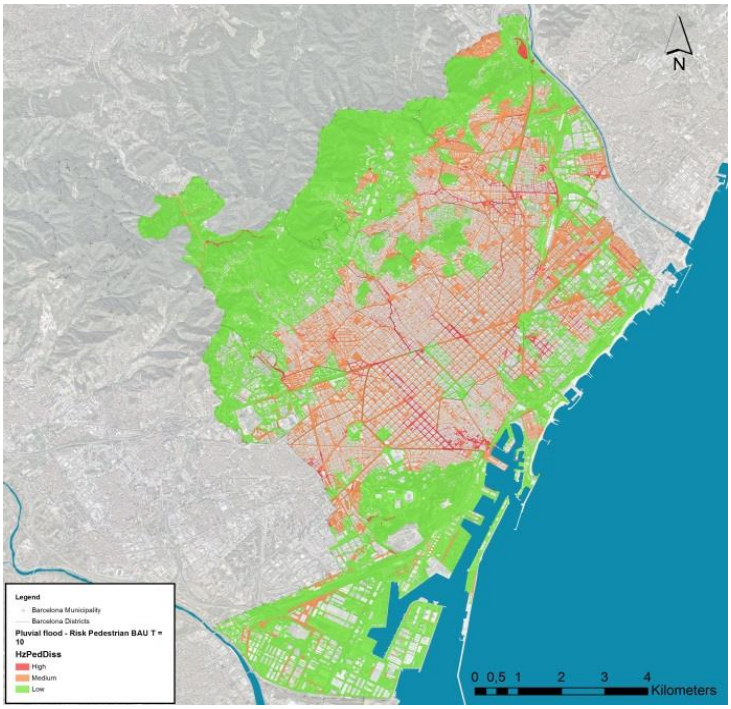

Map 14. *Risk map for pedestrians in the current scenario, with a T100 return period.*

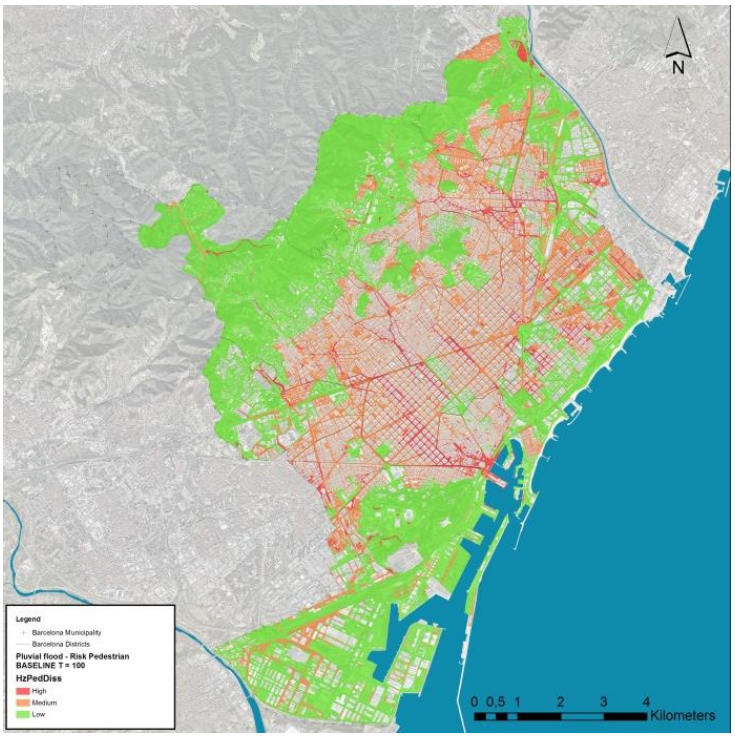

Map 15. *Risk map for pedestrians in the future scenario, with a T100 return period.*

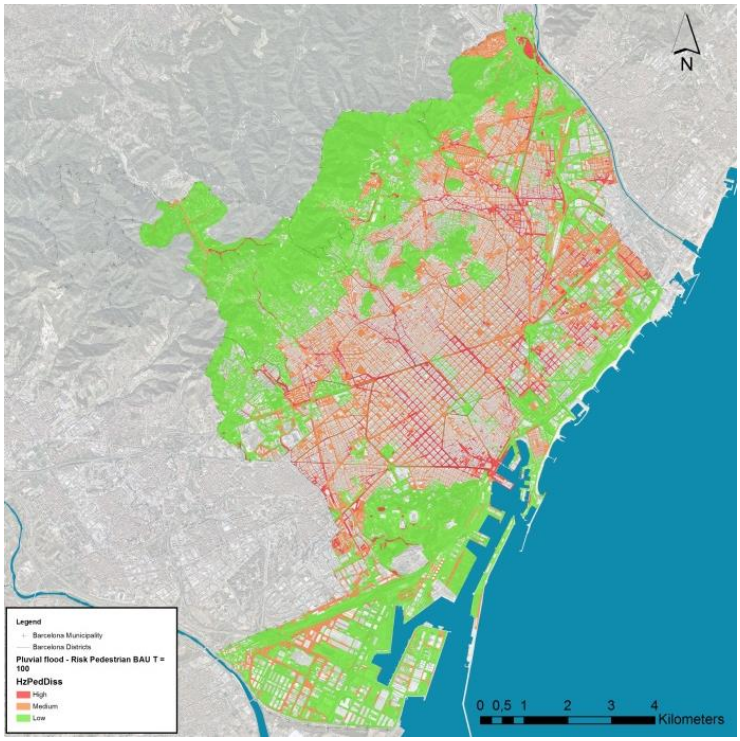

In general, and taking into consideration the conclusions shown in the risk maps, the results for the high-risk areas for the entire city are summarised in the following figure:

Figure 11. *High-risk areas (as a %) for pedestrians in the current and future scenarios, for the most significant return periods.*

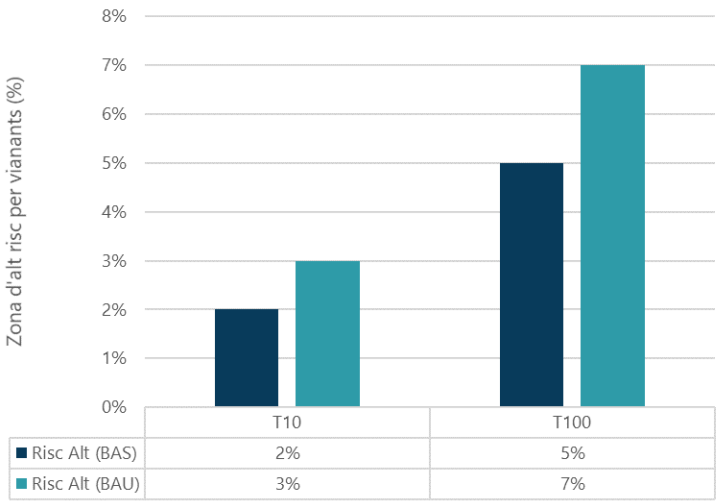

Furthermore, with the aim of highlighting the effect of climate change, in terms of the increase in high-risk areas in Barcelona, the variation in risk areas for pedestrians is shown.

Figure 12. *Increase in high-risk areas (as a %) for pedestrians forecast for climate change, for the most significant return periods.*

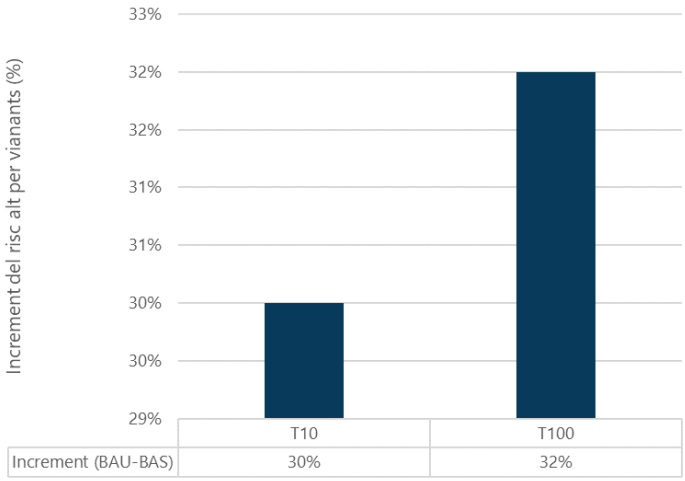

The previous graph shows that the increase in the maximum intensity of torrential rainfall due to the effects of climate change causes an increased risk to pedestrians of around 30%.

Furthermore, the previous risk maps make it possible to define the most problematic areas of the city for pedestrians, according to their high-risk areas, for both the current and future situations, and the effect of climate change on the increased risk can be observed.

Firstly, the areas with the highest concentration of high-risk areas are identified, which are practically the same as the most important critical points of the city due to network malfunctioning, except for those places with a low population density (which are therefore not high-risk areas). In order to facilitate understanding, they have been classified into hubs:

- Hub 1: formed by the Esquerra de l'Eixample, the neighbourhood of Sant Antoni and El Raval, which begins in the area of Diagonal - Pl. Francesc Macià, continuing with Villarroel - Casanova - Av. Roma - Comte d'Urgell - Comte Borrell and finishes in the area around Carrer de Sant Pau: the area around Ronda and Carrer de Sant Pau, Sant Antoni Abat, Paral·lel, Rambla del Raval and Avinguda de les Drassanes.
- Hub 2: Passeig de Sant Joan - Bailèn - Av. Diagonal.
- Hub 3: Vallcarca - Riera de Cassoles - Via Augusta.
- Hub 4: The area formed between Rambla de Badal and Riera Blanca, from Munné - Carrer de Sants, Bacardí, Parcerisa at the height of Constitució, up to Carrer de Quetzal.
- Hub 5: The area of Sant Andreu, starting at Nou Barris and ending at the tracks of La Sagrera. Hub between Carrer d'Alella and Rambla de Fabra i Puig and Rambla de Onze de Setembre, and the Tajo - Cartellà - Riera d'Horta main road.

Map 16. *The major critical hubs in the city*

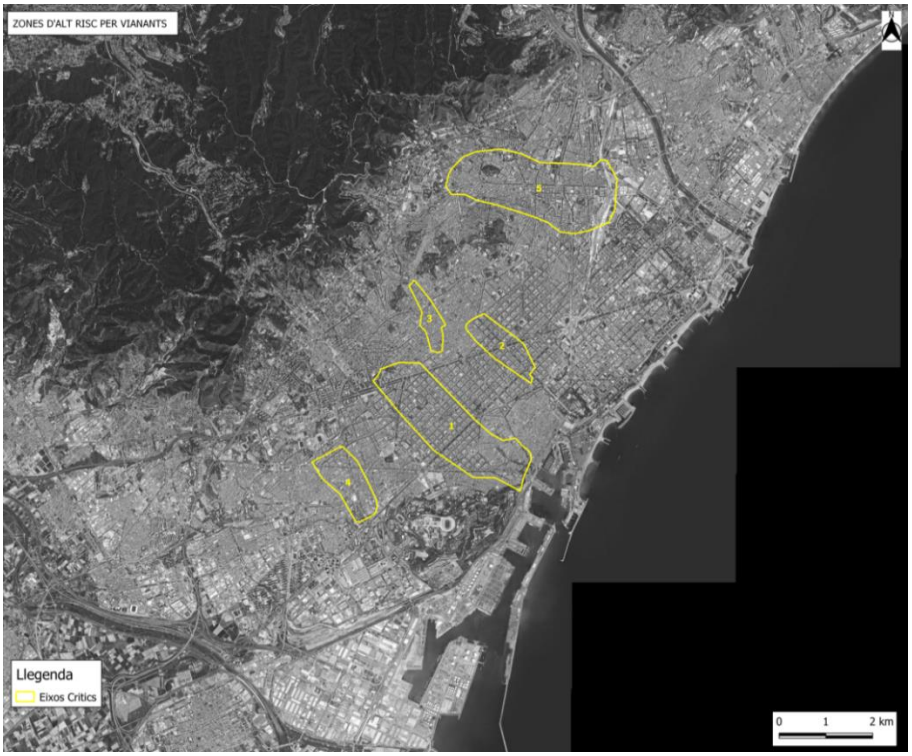

The following figures show the high-risk areas for pedestrians and how they increase, classified according to these hubs.

Figure 13. *High-risk areas (in ha) for pedestrians in the current and future scenarios, for the most significant return periods, in the hubs with the highest concentrations of high-risk areas.*

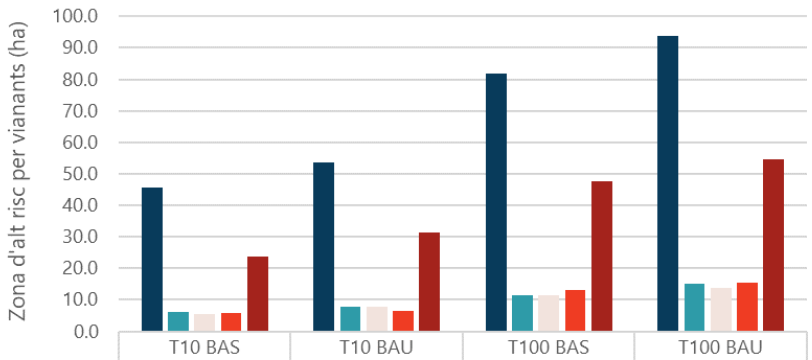

	T10 BAS	T10 BAU	T100 BAS	T100 BAU
Eix 1	45.6	53.5	81.8	93.7
Eix 2	6.2	8.0	11.4	15.2
Eix 3	5.6	7.9	11.3	13.8
Eix 4	5.9	6.7	13.1	15.6
Eix 5	23.6	31.2	47.6	54.6

Figure 14. *High-risk areas (in ha) for pedestrians in the current and future scenarios, for the most significant return periods, in the hubs with the highest concentrations of high-risk areas.*

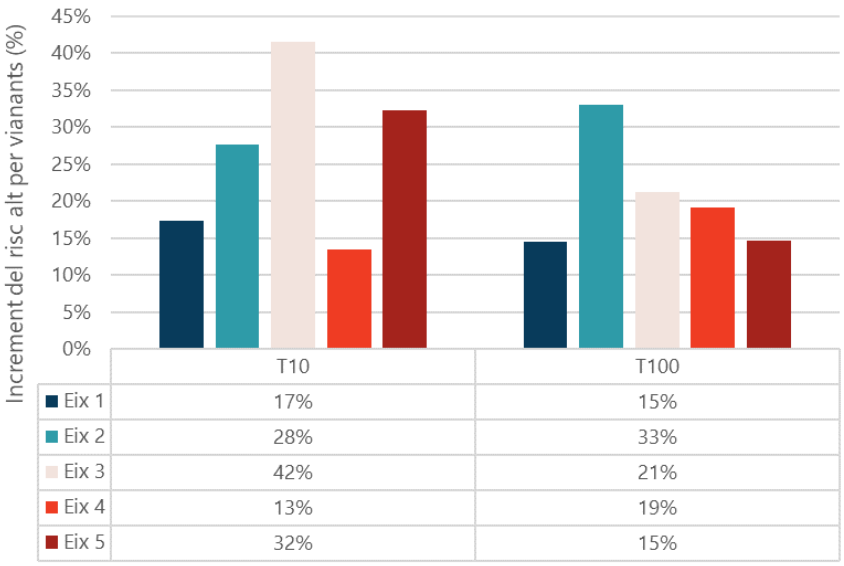

	T10	T100
Eix 1	17%	15%
Eix 2	28%	33%
Eix 3	42%	21%
Eix 4	13%	19%
Eix 5	32%	15%

The results show that for a 10-year return period, climate change may produce an average increase in high-risk areas of 15%, for hubs 1 and 4, of 30% for hubs 2 and 5 and of up to 42% for hub 3.

With regard to high-risk areas for vehicles, the results follow the trend of those obtained for assessing the risk to vehicles and pedestrians, and, therefore, the conclusions and considerations specified above are valid.

Map 17. *Risk for vehicles in the current scenario, with a T10 return period.*

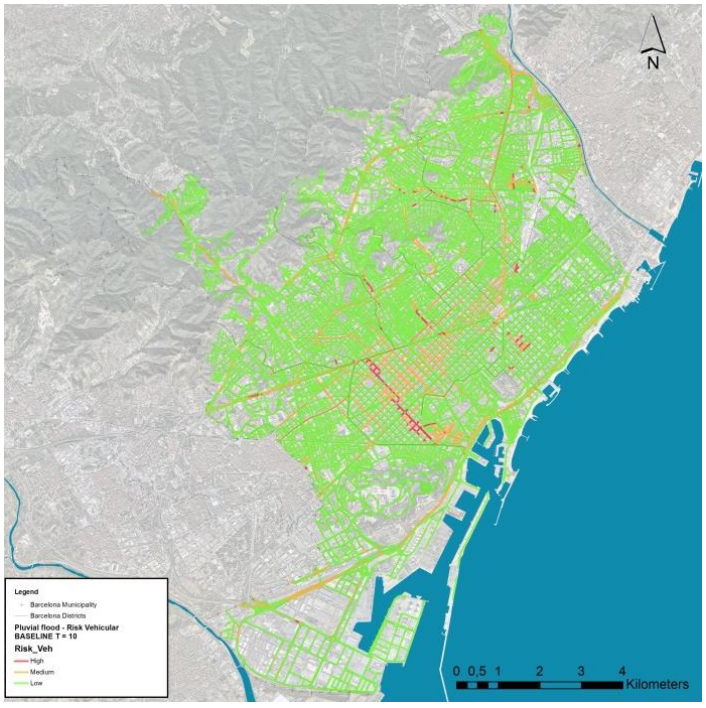

Map 18. *Risk for vehicles in the future scenario, with a T10 return period.*

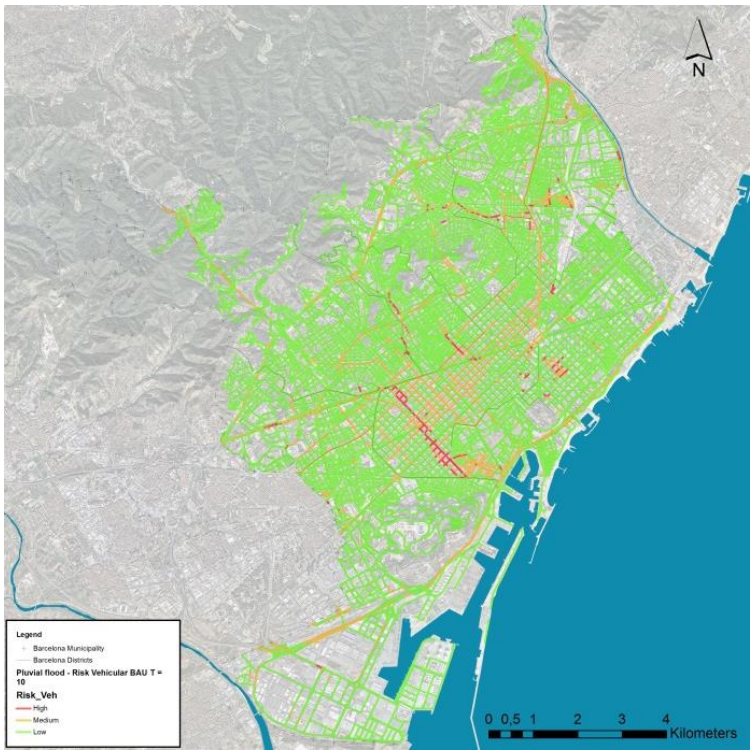

Map 19. *Risk for vehicles in the current scenario, with a T100 return period.*

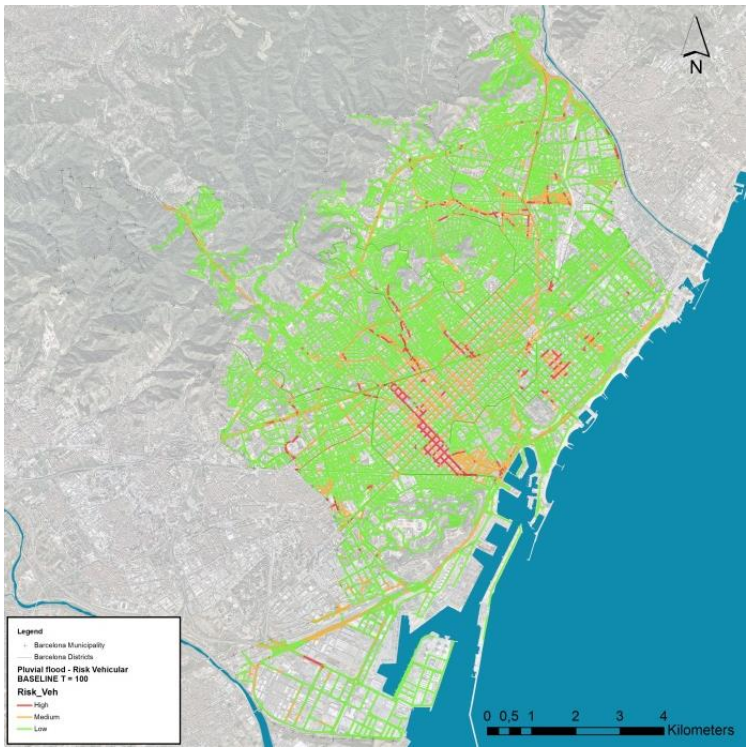

Map 20. *Risk for vehicles in the future scenario, with a T100 return period.*

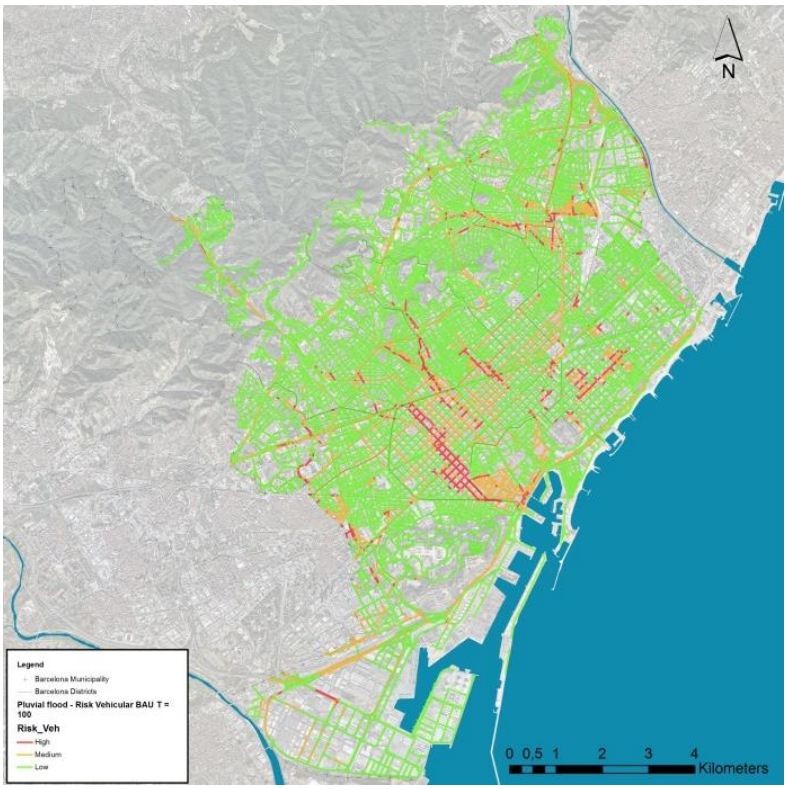

It should be emphasised that the results show that some areas classified as high flood risk have a lower risk for vehicles than for pedestrians. However, the results show that climate change may produce an increase in high risk of around 35% (Figure 13).

Figure 15. *High-risk areas (as a %) for vehicles in the current and future scenarios, for the most significant return periods.*

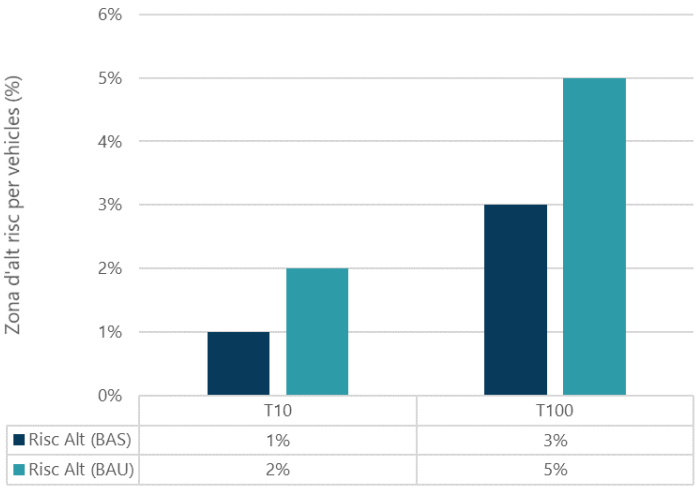

Figure 16. *Increase in high-risk areas (as a %) for vehicles forecast for climate change, for the most significant return periods.*

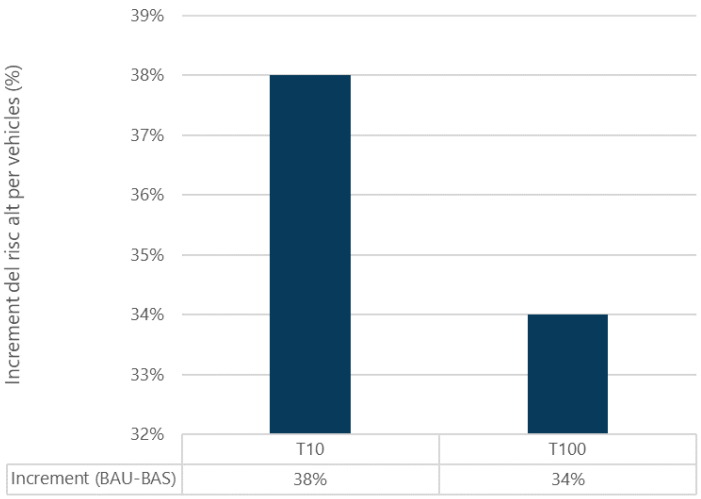

Once the increase in high-risk areas has been assessed for both pedestrians and vehicles, the project goes on to evaluate the introduction of improvements to the drainage system. These improvements have been differentiated into two adaptation scenarios: the first provides for the installation of SUDS (sustainable urban drainage systems) in the city – Adaptation Scenario 1 – and the second provides for the introduction of structural improvements to the drainage system (improving drains, introducing rainwater retention tanks) together with the SUDS – Adaptation Scenario 2—.

Here are the risk maps for pedestrians and vehicles resulting from the model simulation, once Adaptation Scenarios 1 and 2 have been introduced:

Map 21. *Risk for pedestrians in Adaptation Scenario 1, for a T10 return period.*

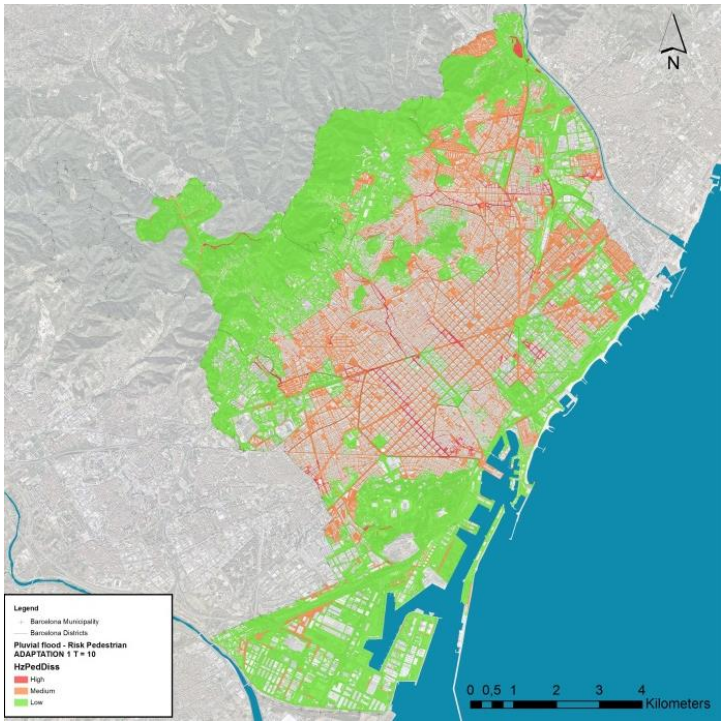

Map 22. *Risk for pedestrians in Adaptation Scenario 2, for a T10 return period.*

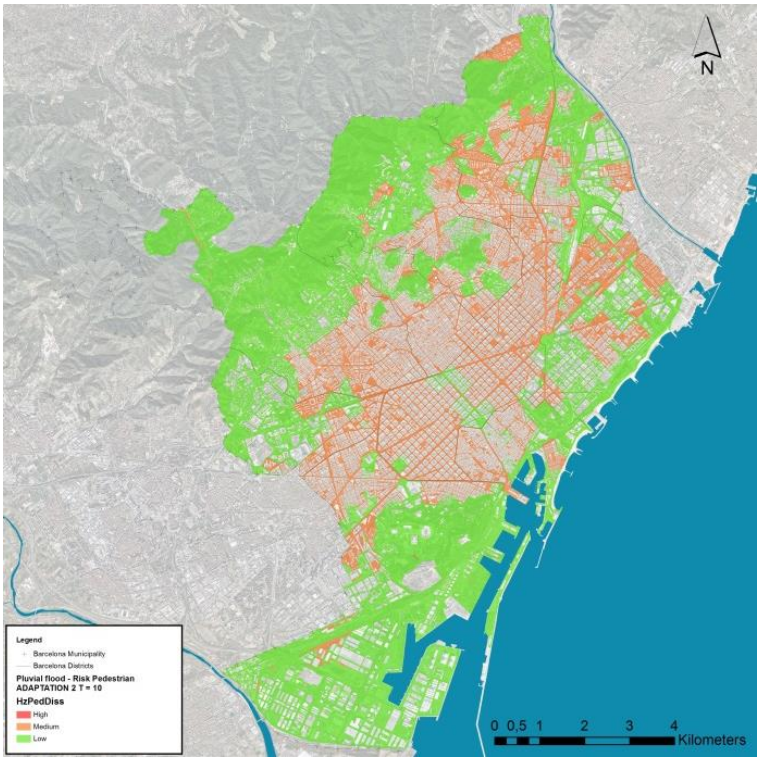

Map 23. *Risk for pedestrians in Adaptation Scenario 1, for a T100 return period.*

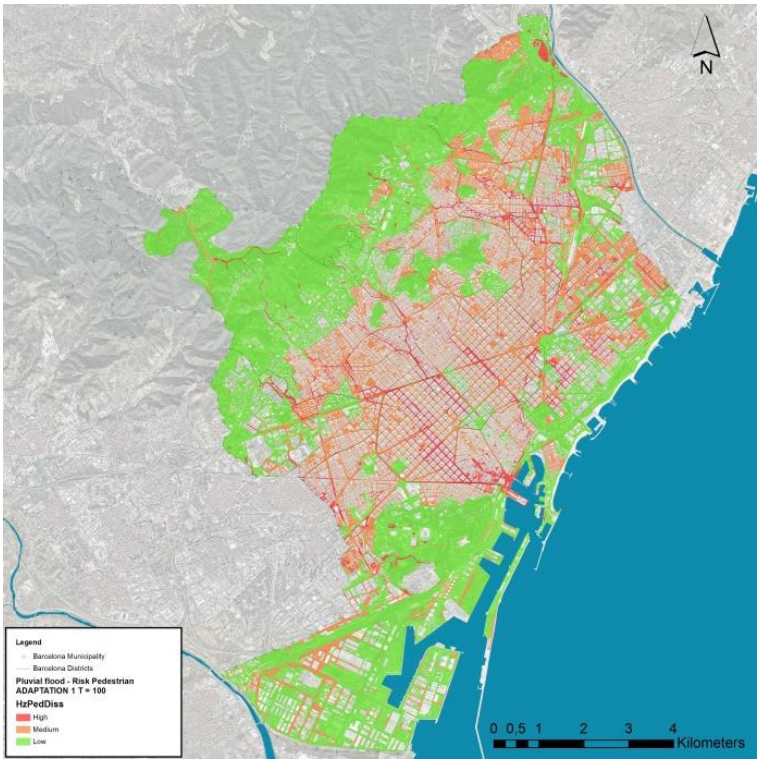

Map 24. *Risk for pedestrians in Adaptation Scenario 2, for a T100 return period.*

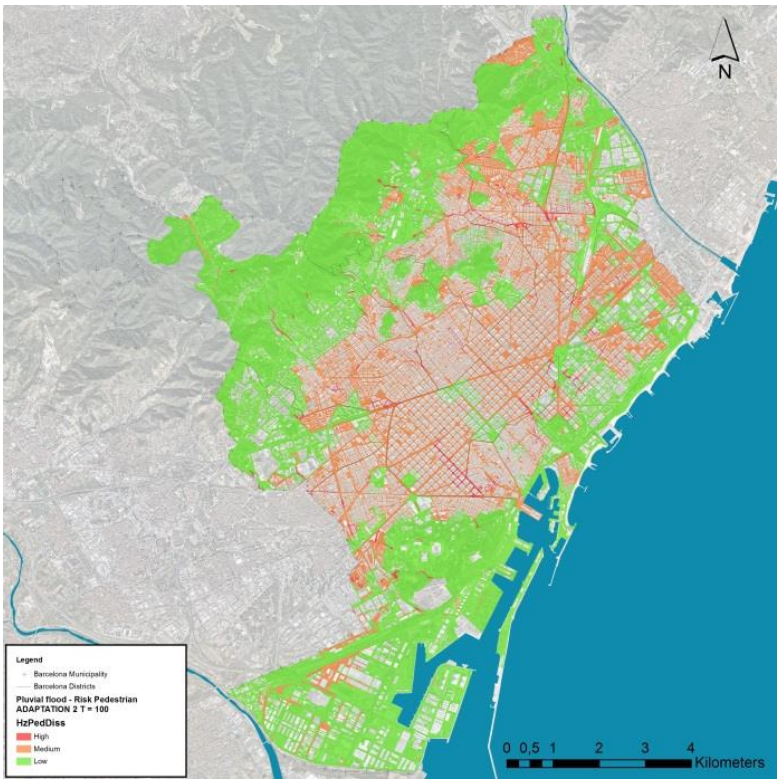

Map 25. *Risk for vehicles in Adaptation Scenario 1, for a T10 return period.*

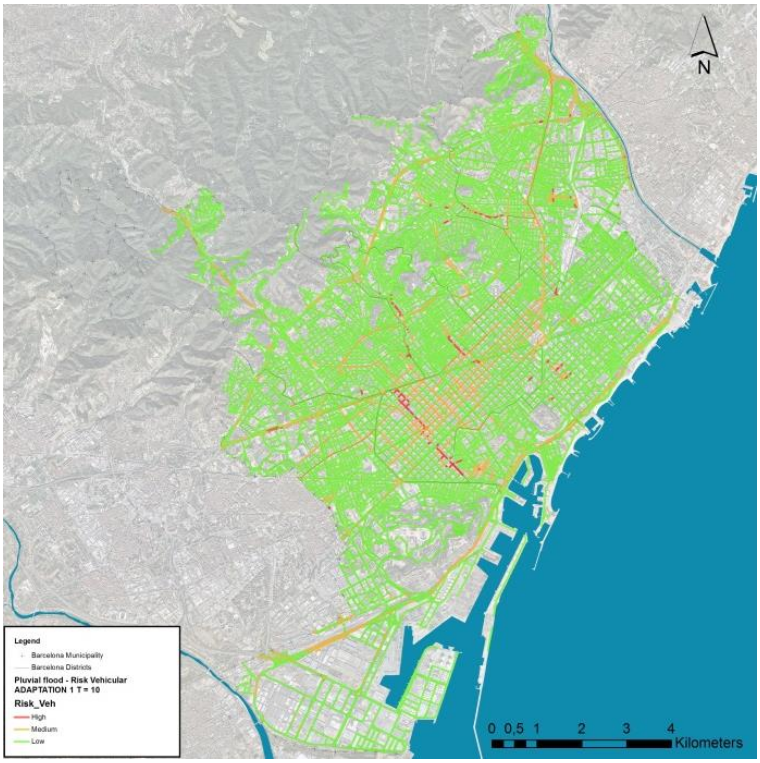

Map 26. *Risk for vehicles in Adaptation Scenario 2, for a T10 return*

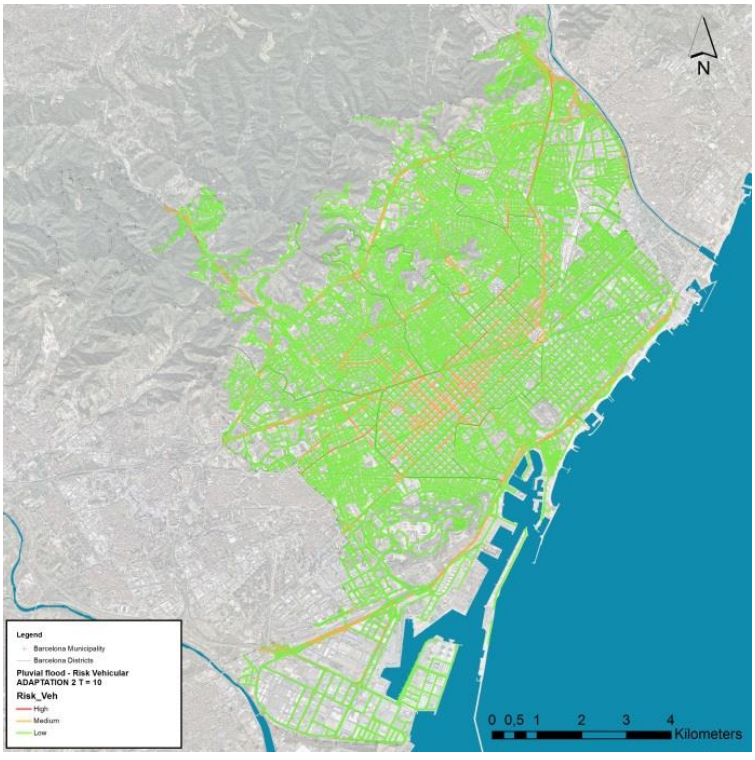

Map 27. *Risk for vehicles in Adaptation Scenario 1, for a T100 return period.*

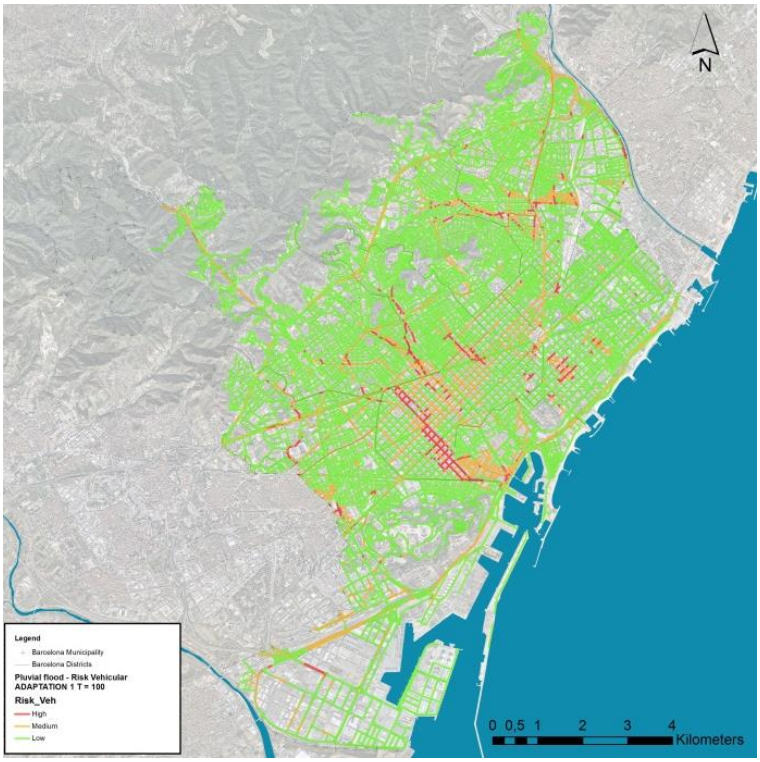

Map 28. *Risk for vehicles in Adaptation Scenario 2, for a T100 return period.*

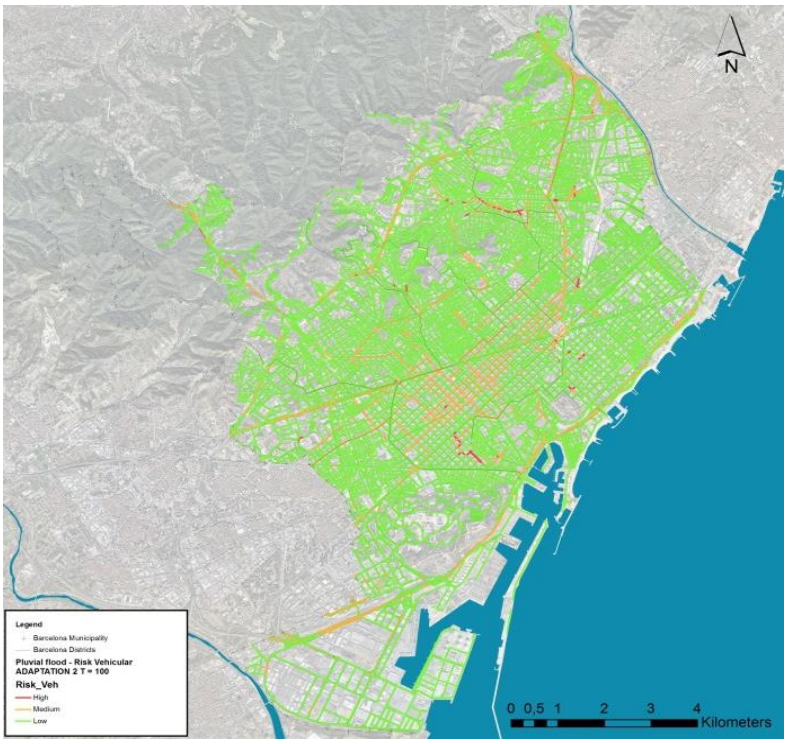

If the future scenario, i.e. the city's current situation affected by the future rainfall conditions caused by climate change, are compared with the different adaptation scenarios, the risk reduction can be obtained as a decrease in the percentage of high-risk flood areas.

The following figures show the reduction in risk obtained for pedestrians and vehicles, respectively:

Figure 17. *Decrease in the high-risk area for pedestrians (as a %) resulting from the measures introduced in Adaptation Scenarios 1 and 2, for the most significant return periods.*

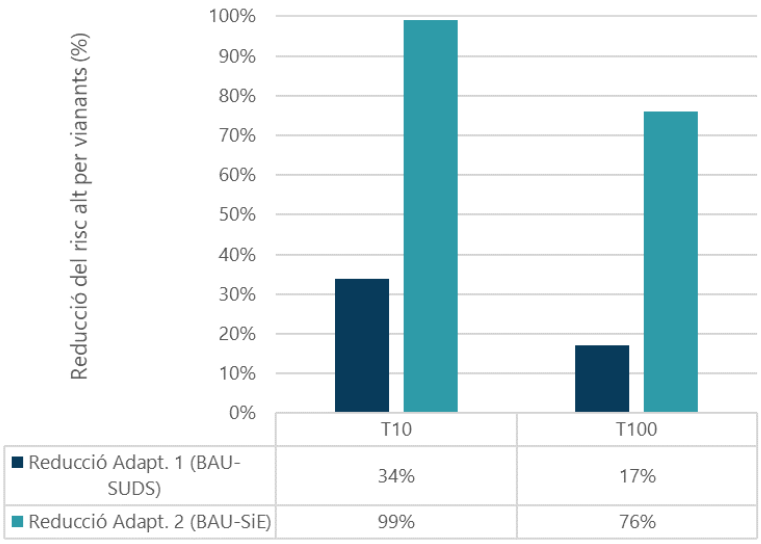

Figure 18. *Decrease in the high-risk area for vehicles (as a %) resulting from the measures introduced in Adaptation Scenarios 1 and 2, for the most significant return periods.*

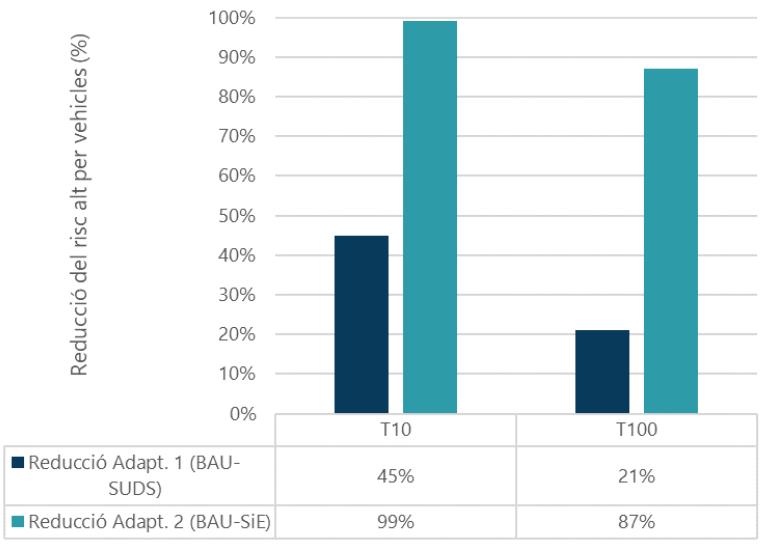

As can be seen, introducing sustainable urban drainage systems (SUDS) throughout the city is forecast to reduce the two risks by 40% in terms of rainfall with a 10-year return period, although it is calculated that for higher return periods, the risk reduction would be 20% or less.

However, the joint introduction of SUDS and structural measures would lead to practically a 100% reduction of the two risks for design storms with a 10-year return period. This figure decreases in proportion to increasing return periods, so that a reduction of nearly 80% is obtained for a 100-year return period.

It should be noted that Adaptation Scenario 2 provides for proposed actions on the city's primary network while considering the secondary network to have sufficient capacity.

Furthermore, a detailed analysis has been carried out on the risk reduction for pedestrians (the most unfavourable case) in the hubs with the highest concentration of high-risk areas.

Figure 19. *Decrease in the high-risk area for pedestrians (as a %) resulting from the measures introduced in Adaptation Scenarios 1 and 2, for the most significant return periods in the hubs with the highest concentration of high-risk areas.*

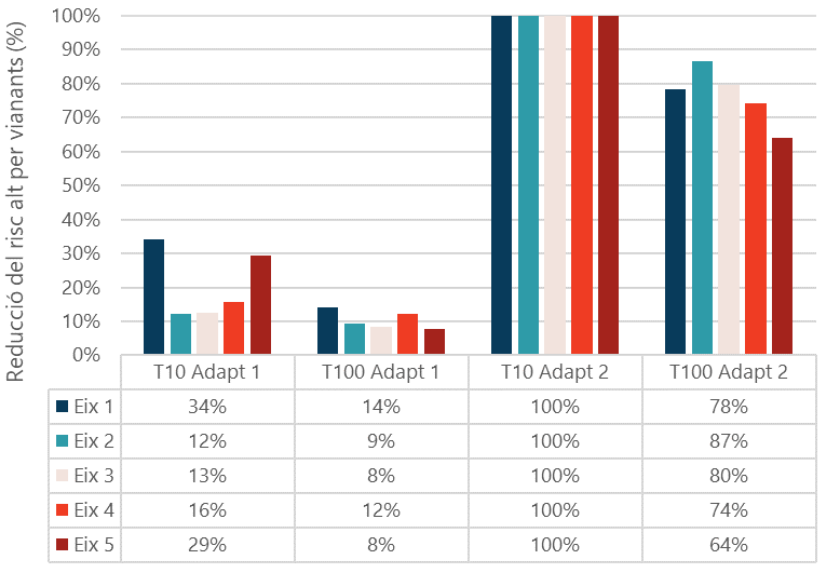

	T10 Adapt 1	T100 Adapt 1	T10 Adapt 2	T100 Adapt 2
Eix 1	34%	14%	100%	78%
Eix 2	12%	9%	100%	87%
Eix 3	13%	8%	100%	80%
Eix 4	16%	12%	100%	74%
Eix 5	29%	8%	100%	64%

Although a similar behaviour in terms of risk reduction for pedestrians is seen on a city-wide scale, some differences between the hubs are identified.

Hubs 1, in the Esquerra de l'Eixample, neighbourhood of Sant Antoni and El Raval, and 5, in the Sant Andreu - Nou Barris area, are the ones that most benefit from introducing SUDS, reducing their risk to pedestrians by nearly 30%, for the most frequent precipitations (10-year return period). By contrast, hubs 2, in Passeig de Sant Joan, and 3, in Riera de Cassoles, are those that benefit least from this implementation, with only a 12-13% risk reduction for pedestrians. It should be noted that hubs 1 and 5 are the largest, and therefore those that have the largest high-risk areas (Figure 16). Consequently, they benefit from a higher risk reduction.

However, deployment of the second adaptation scenario means a complete risk reduction for all the hubs, when 10-year design storms are considered.

3.3 Traffic disruptions

When urban flooding occurs, surface run-off can cause indirect damage by bringing traffic to a halt. The RESCCUE project has assessed the reduction in permitted travelling speeds through the use of various transects in relation of the depths of the water flow present. This type of analysis makes it possible to assess flood risk for the surface transport sector. Furthermore, the modelling results have been used to feed the Transcad dynamic transport model, which is used by Barcelona City Council's Department of Mobility to estimate the impacts produced by urban rainwater flooding on the traffic service.

The hydrodynamic model provides the surface flood depth for each grid cell. These flood depths are used to produce risk maps according to specific hazard criteria. The methodology, developed by the University of Exeter, is shown in the following figure.

Figure 20. *Methodology developed by the University of Exeter in order to produce its flooding-road traffic model.*

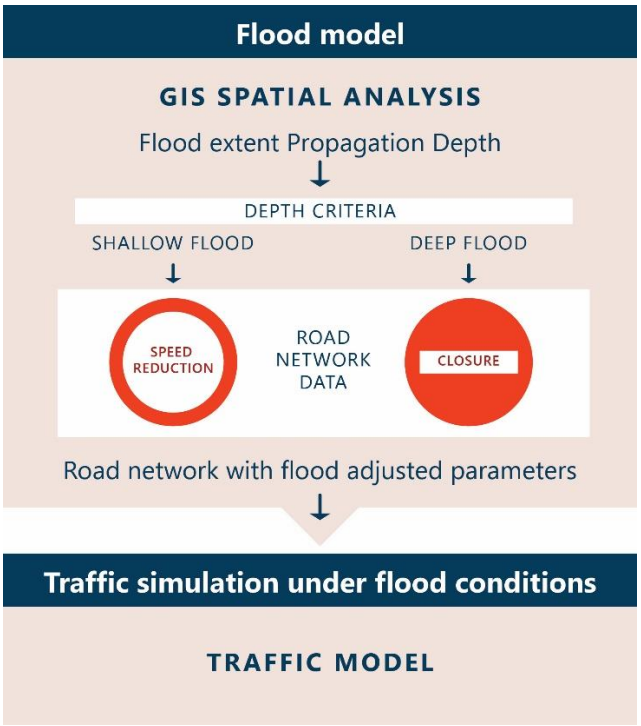

In order to assess the flood risk to road infrastructure, a GIS-based spatial analysis was carried out and the regulations concerning traffic speed reduction were applied. This is shown in the following table:

Flood Depth Range (cm)	Maximum Permitted Speed kmh^{-1}
0.00 – 10.00	Roads maximum speed
10.00 – 30.00	20
+30.00	0 (Road closed)

According to the stated methodology, qualitative risk maps have been produced, classified into three risk levels (**low, medium and high**), for the current scenario and for the climate change scenarios obtained through the use of statistical and temporal regression techniques for 20 future rainfall series provided for 10 general atmospheric circulation models, forced for the RCP 4.5 and 8.5 scenarios and previously validated for a historical control period (1976-2005). Here are the flood-risk traffic disruption maps for the current and future scenarios, for the T10 and T100 return periods:

Map 29. *Surface-traffic disruption for the current scenario, with a T10 return period.*

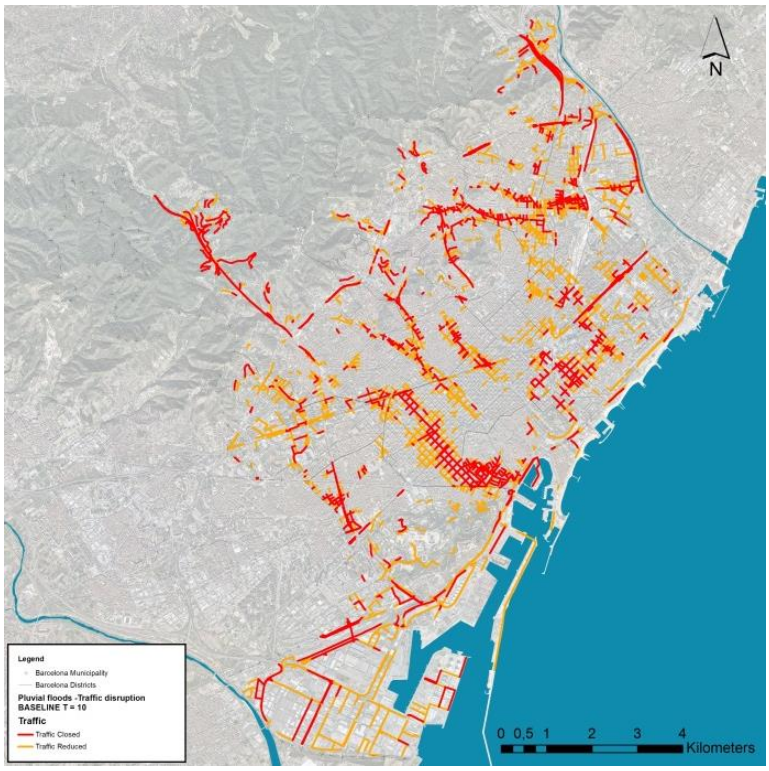

Map 30. *Surface-traffic disruption for the future scenario, with a T10 return period.*

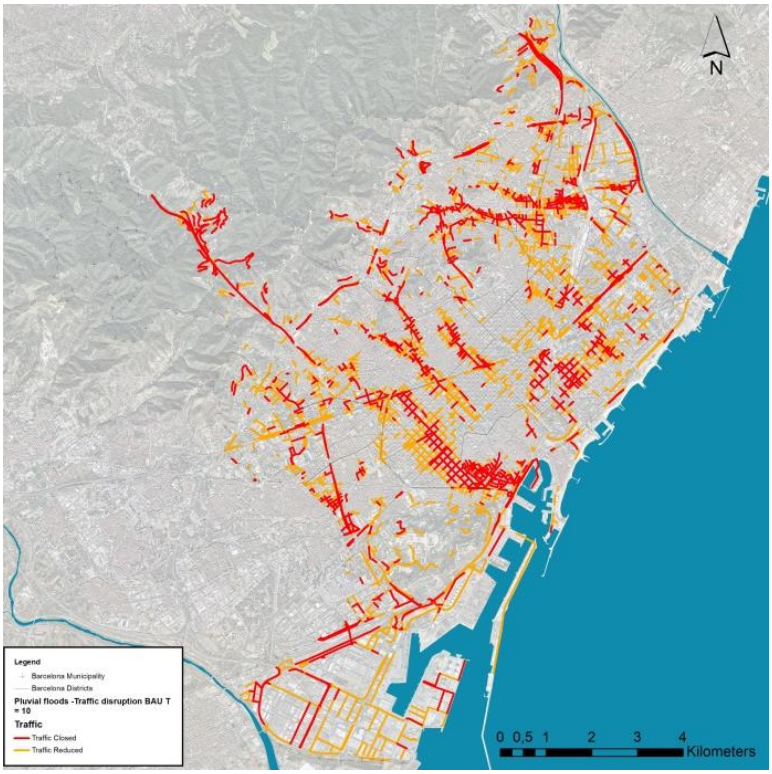

Map 31. *Surface-traffic disruption for the current scenario, with a T100 return period.*

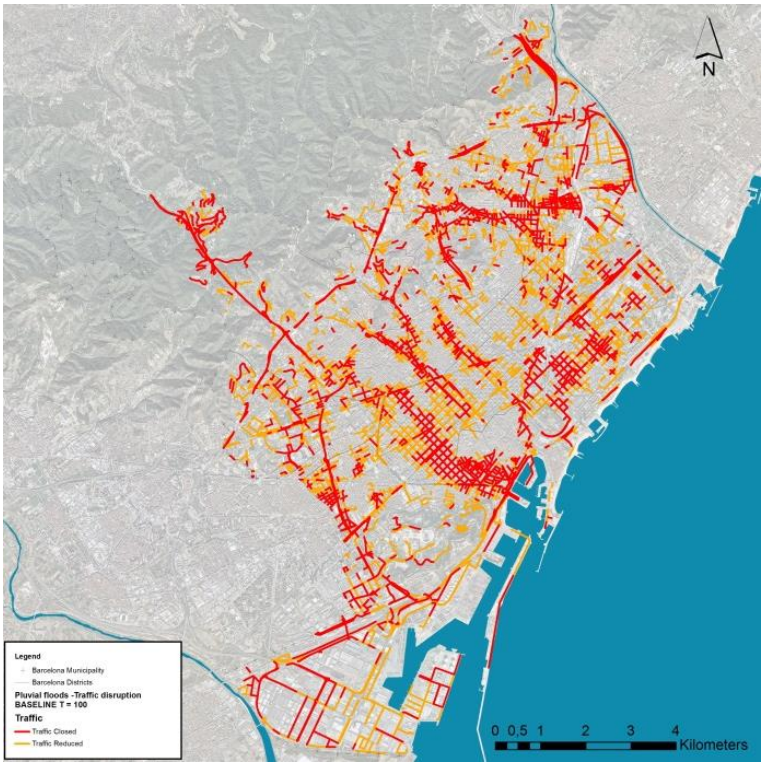

Map 32. *Surface traffic disruption for the future scenario, with a T100 return period.*

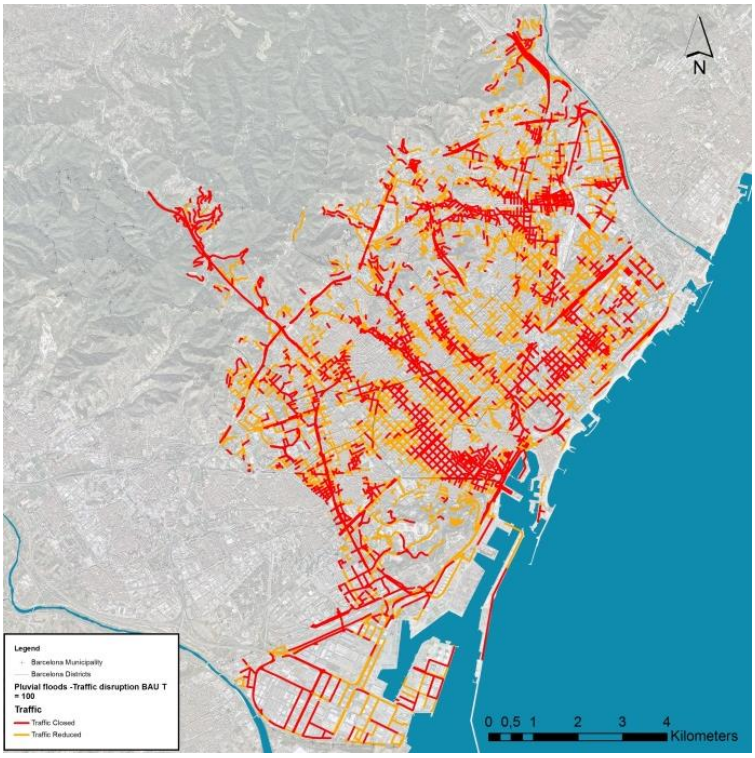

Here are the surface-traffic disruption maps, taking into account the adaptation measures implemented in Adaptation Scenarios 1 and 2:

Map 33. *Surface-traffic disruption maps for Adaptation Scenario 1 (left) and Adaptation Scenario 2 (right) for a 10-year return period.*

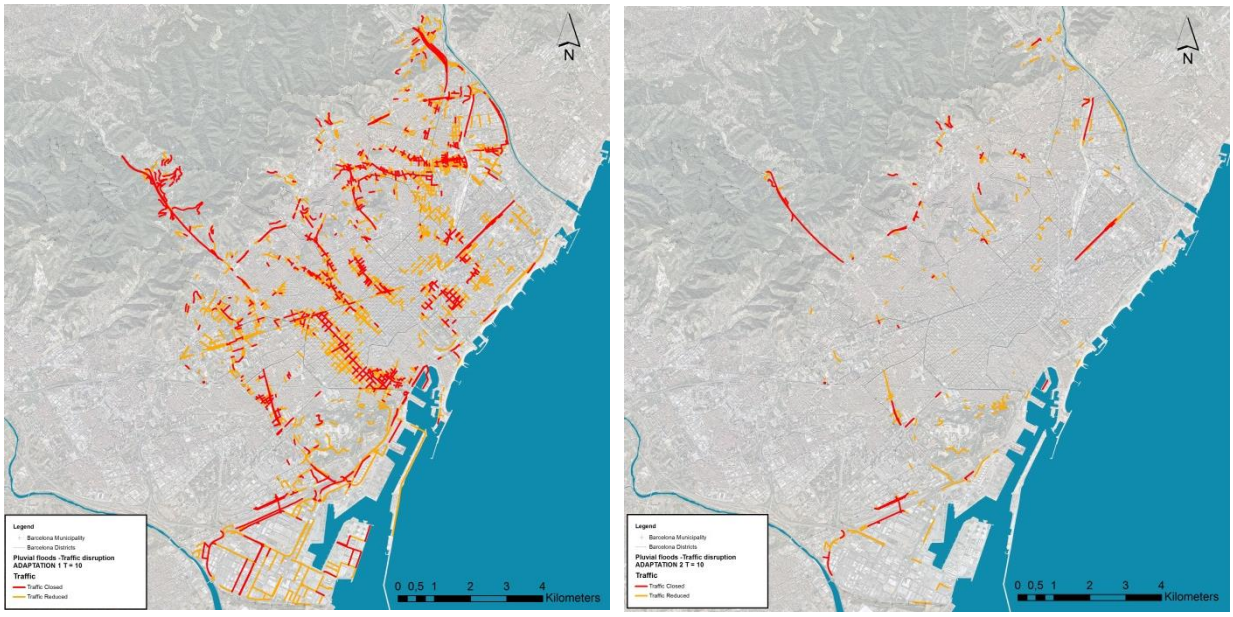

Map 34. *Surface-traffic disruption maps for Adaptation Scenario 1 (left) and Adaptation Scenario 2 (right) for a T100 return period.*

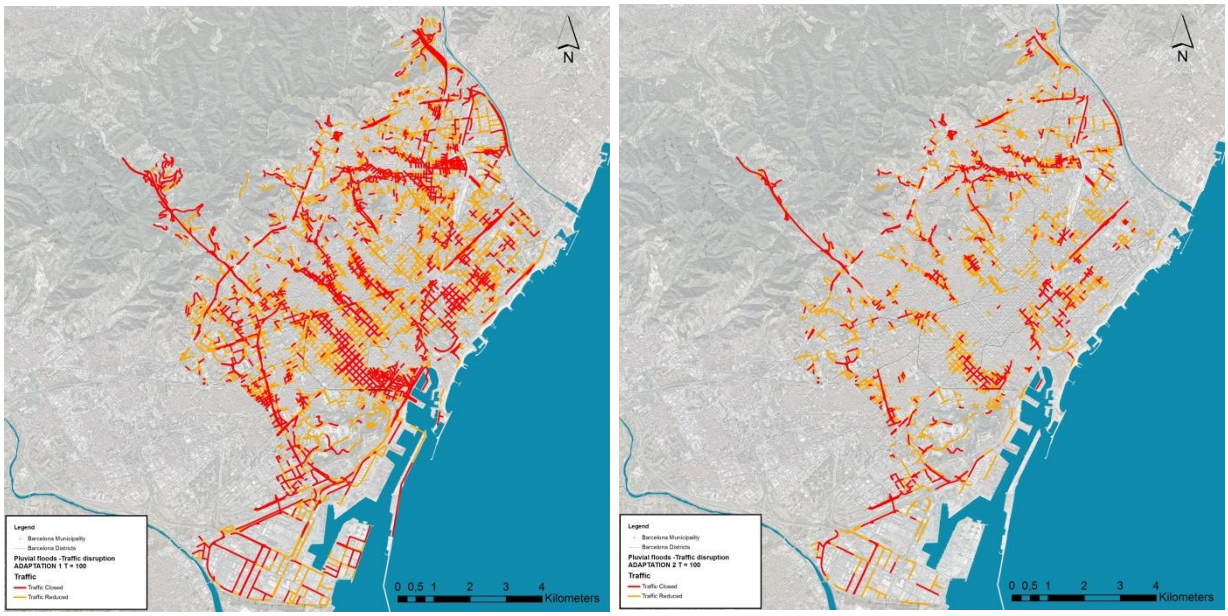

Among other traffic parameters, the Transcad traffic model includes information about the speed limits in each street section. Based on the water flow calculated in the 1D/2D hydrodynamic model, for all the scenarios and return periods studied, and taking into account the previous table concerning the effects of flood risk on traffic, the maximum speed limits are modified for each of the flooded street sections in the traffic model, and the model is run again using these new conditions.

This type of information can be introduced into the traffic model of the city's department of mobility in order to assess the increase in travelling times in the city and, subsequently, perform the analysis of monetisation, increased emissions and consumption, etc.

The following figures show the evolution of surface-traffic disruption on Barcelona streets for the current, future and Adaptation 1 and 2 scenarios, and the 10-year and 100-year return periods.

Figure 21. *Length of streets (as a %) with reduced speed limits or closed due to the effects of flooding in Barcelona city, for the current, future and Adaptation 1 and 2 scenarios, with the most significant return periods.*

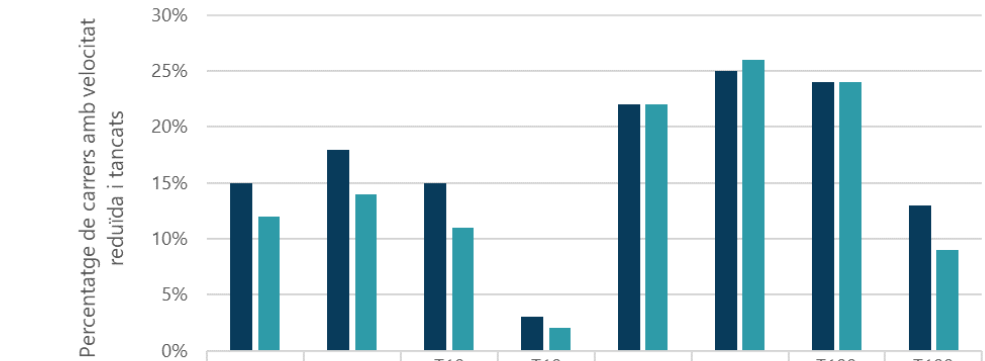

	T10 BAS	T10 BAU	T10 Adapt. 1	T10 Adapt. 2	T100 BAS	T100 BAU	T100 Adapt. 1	T100 Adapt. 2
Velocitat reduïda (%)	15%	18%	15%	3%	22%	25%	24%	13%
Tancat (%)	12%	14%	11%	2%	22%	26%	24%	9%

Figure 22. *Increased length of streets (as a %) with reduced speed limits or closed due to the forecast effects of flooding in Barcelona city, as a result of climate change, with the most significant return periods.*

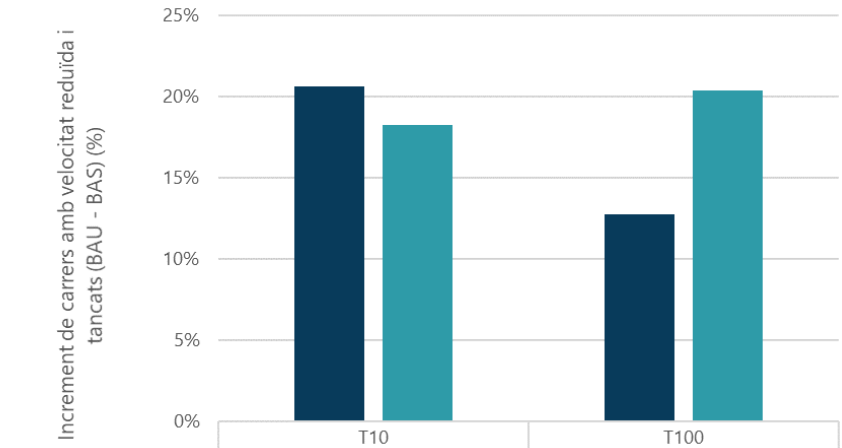

	T10	T100
Velocitat reduïda (km)	21%	13%
Tancat (km)	18%	20%

Figure 23. *Reduction in the length (as a %) of streets with reduced speed limits or closed due to the effects of flooding in Barcelona city, as a result of the measures implemented in Adaptation Scenarios 1 and 2, with the most significant return periods.*

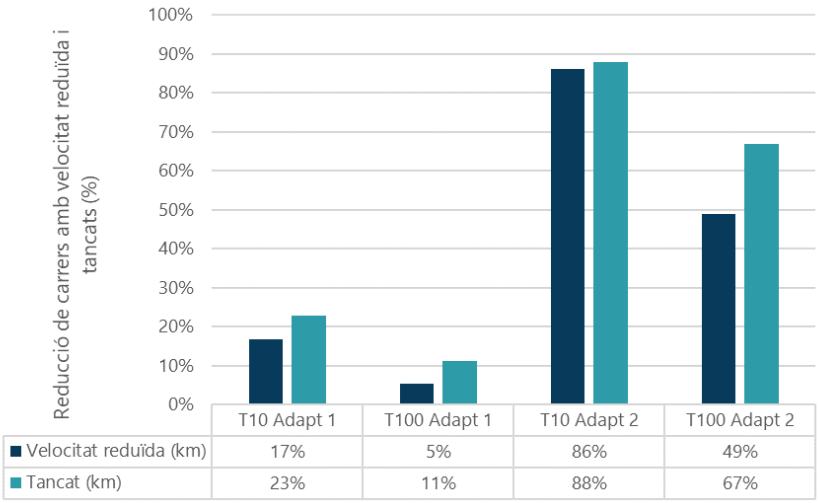

	T10 Adapt 1	T100 Adapt 1	T10 Adapt 2	T100 Adapt 2
Velocitat reduïda (km)	17%	5%	86%	49%
Tancat (km)	23%	11%	88%	67%

The results analysis shows that as the return period increases, the number of affected street sections increases as a consequence. Figure 15 presents the percentage of street kilometres that are classified as closed or with reduced speed limits, and how this percentage increases with the return period. Logically, these return periods also increase in the climate-change scenario and decrease in the adaptation scenarios, thanks to the measures implemented.

Comparing the results of the two scenarios (current and future), it can be seen that, for a total of 1,492 km, the number of streets that may be affected by a reduced speed limit increases by between 13% and 21%, depending on the return period, while the increase in closed streets may rise by nearly 20% for all the return periods.

In regard to the effect of the adaptation measures, the variations of the action scenarios have been considered in relation to the future scenario with climate change. The results indicate that the decrease in the number of affected streets would be nearly 20% (Adaptation Scenario 1) and 90% (Adaptation Scenario 2) for the design return period (T10).

3.4 Stability of solid urban waste containers

Before solid waste is taken to the rubbish dumps, the collection process in big cities starts with regular domestic waste collection by municipal services, which is carried out through the use of street containers. Therefore, when urban flooding occurs, these containers may lose stability, which may cause them to release their contents and contaminate the flood water. This study aims to provide the location of potentially unstable containers in the city, when they are exposed to various flooding frequencies. The risks relating to container stability can be summarised as collisions with other elements or urban property, additional efforts and costs to return them to their proper positions, water contamination, the safety of pedestrians, traffic disruption, possible blockage of the drainage system and an increased probability of cascade effects due to flooding.

The developed methodology[2] considers that container stability may be compromised when the hydrodynamic variables, water depth and velocity exceed a certain threshold. These variables have been combined and compared with the stability thresholds for slippage and overturning for the different containers.

In Barcelona, there are a total of 27,134 containers, which can be classified according to the waste fraction they contain: other (44%), organic (22%), paper and cardboard (12%), packaging (11%) and glass (11%); by their volume in litres (3,200, 3,000, 2,400, 2,200 and 1,800) or how they are unloaded: lateral (62%), bilateral (25%), rear (12%) and underground (1%). Due to the small proportion of rear-load and underground containers compared to the lateral and bilateral types, only the latter two have been taken into account for this study, which is around 87% of all containers. A container may be more or less vulnerable to flooding, depending on its volume, fraction and how full it is. Three content scenarios have been studied: empty, half-full and completely full containers.

Vulnerability is defined by means of stability curves, which have been developed for each type of container. All the containers considered in the study are shown on these maps, indicating their capacity and the type of waste fraction they contain. The stability functions were developed based on an analysis of the forces that act on a container, establishing balance conditions for the various types of instability (i.e. slipping, overturning and floating). These functions depend on the velocity and depth of the water (flow). Furthermore, the characteristics of each container (e.g. volume, dimensions or waste fraction it may contain) determine the form of each function. The obtained stability thresholds are used to analyse the potential behaviour of the containers during flooding in Barcelona, caused by design rainfall for historical periods and for short return periods, i.e. between 1, 10 and 50 years. Here is the urban floodability map corresponding to a 50-year return period for the future scenario:

[2] Martínez-Gomariz, E., Russo, B., Gómez, M., Plumed, A., 2020. An approach to the modelling of stability of waste containers during urban flooding. J. Flood Risk Manag. 13, jfr3.12558. https://doi.org/10.1111/jfr3.12558

Map 35. *Urban floodability for the future scenario, with a T50 return period.*

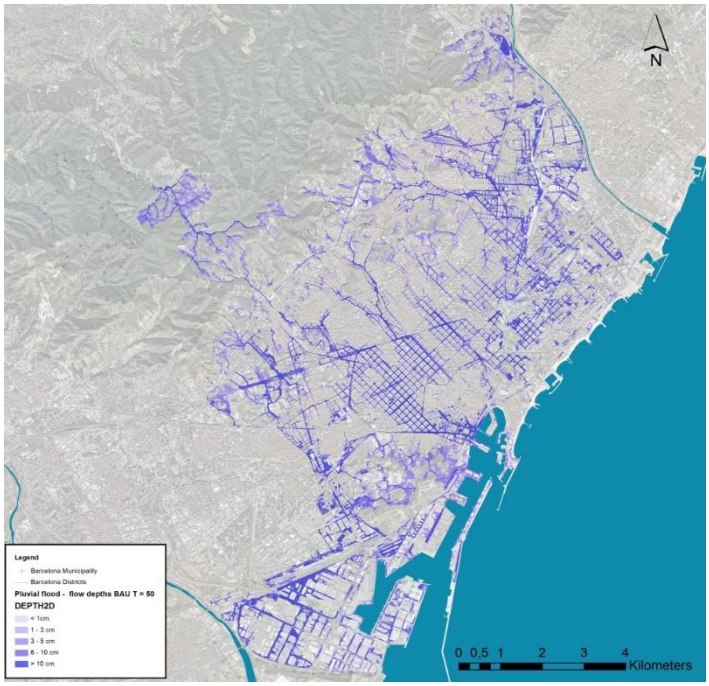

The following figure shows the slippage and overturning stability curves for a 3,200 litre lateral-load container, and waste fraction, for various scenarios: (a) empty container, (b) 50%-full container and (c) completely full container:

Figure 24. *Stability curves for urban waste containers in accordance with how full they are.*

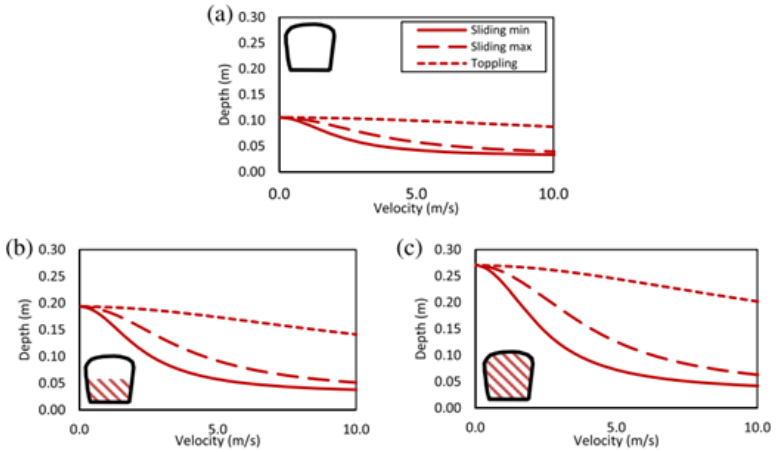

This type of waste carried away by floodwater may further block an already narrow street and increase risk, as they can create an enclosed basin without any outlet for run-off water,

worsening the effects of the flooding. The drain entrances can also become blocked with solid waste if it falls out of the container when it loses stability, thus negatively affecting the drainage system. Furthermore, when a container loses stability, this can cause cascade effects, such as traffic disruption, halting the collection of waste and the potential blockage of the drainage system, as well as causing impacts on people or other assets.

The risk assessment carried out is based on the specific containers exposed to a certain level of risk, determined by water depth and velocity, so that high-risk areas, where a large number of containers are expected to lose stability, have been identified.

The main unknown factor of this study is how full each container may be. Although three different scenarios for container content are considered, the assumption that all of them, at the same time, are filled to the same degree, is a cause of major uncertainty.

The generated maps represent containers that may lose stability according to a variety of instability modes (floating, slippage and overturning), based on various content scenarios (empty, half-full, completely full). The following maps are for a high-risk scenario: empty containers for a 50-year return period and for the current and future scenarios.

Map 36. *Map of effects on urban solid-waste containers for the current scenario (left) and future scenario (right), with a T50 return period.*

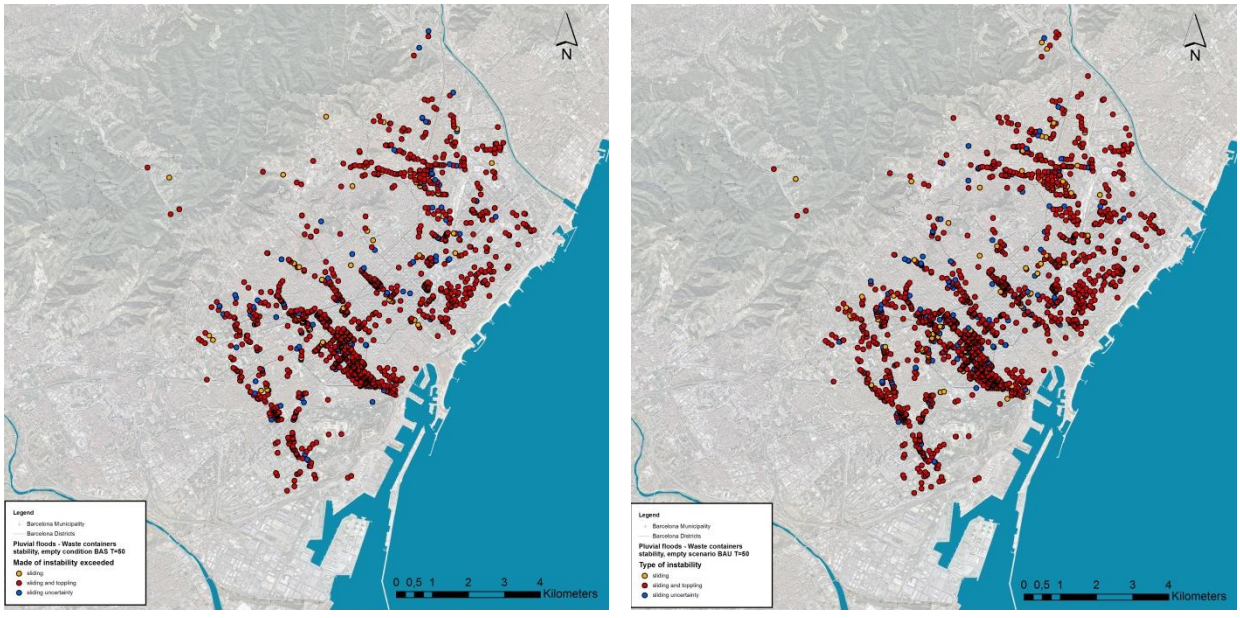

If we present the number and variety of urban solid-waste containers from the previous maps graphically, we obtain:

Figure 25. *Number of unstable, empty urban solid-waste containers (as a %) for the current and future scenarios (left) and the forecast increase in unstable empty containers (as a %) due to climate change (right), for a T50 return period.*

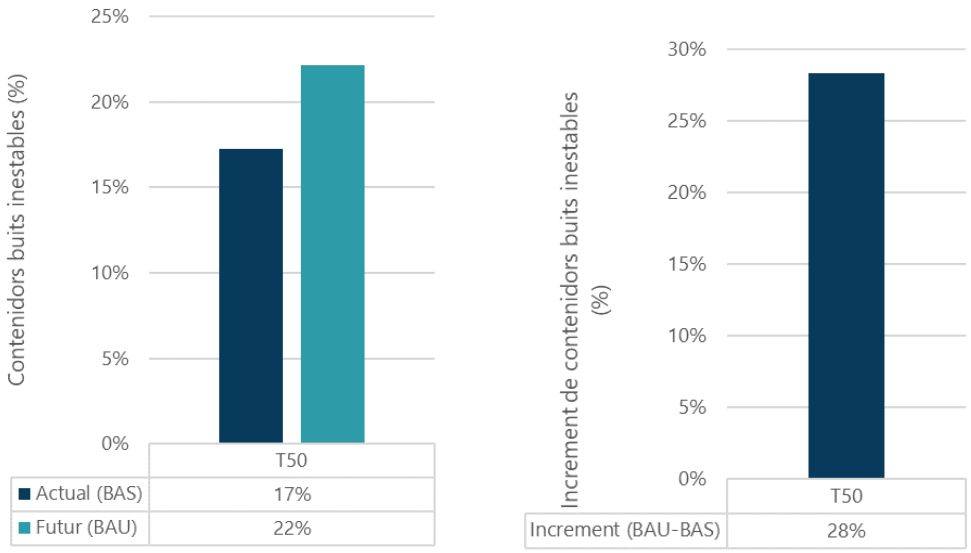

The analysis has shown that with current rainfall for a T50 return period, 17% of all the city's containers lose stability and that this number may increase to 22% under future rainfall conditions, which would mean a 28% increase in the number of potentially unstable empty containers as a consequence of climate change.

In addition to Adaptation Scenarios 1 and 2, a third scenario has been produced for the urban solid-waste sector, which provides for the inclusion of anchoring mechanisms for the various types of container. Furthermore, this third scenario has been combined with the other two, resulting in a total of five different adaptation scenarios. The following maps show the urban solid-waste containers affected by a high-risk scenario: empty containers with a T50 return period, for the five different adaptation scenarios:

Map 37. *Affected urban solid-waste containers for the future scenario, including only the container anchoring mechanisms for a T50 return period.*

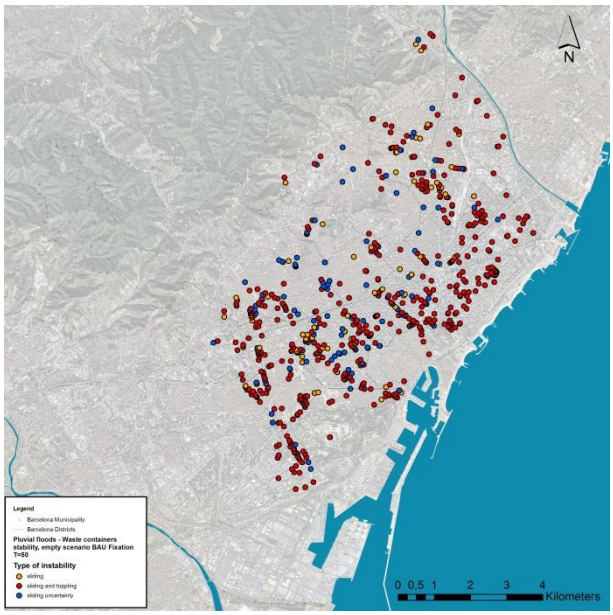

Map 38. *Impact maps for urban solid-waste containers in Adaptation Scenario 1 (left) and Adaptation Scenario 2 (right) for a T50 return period.*

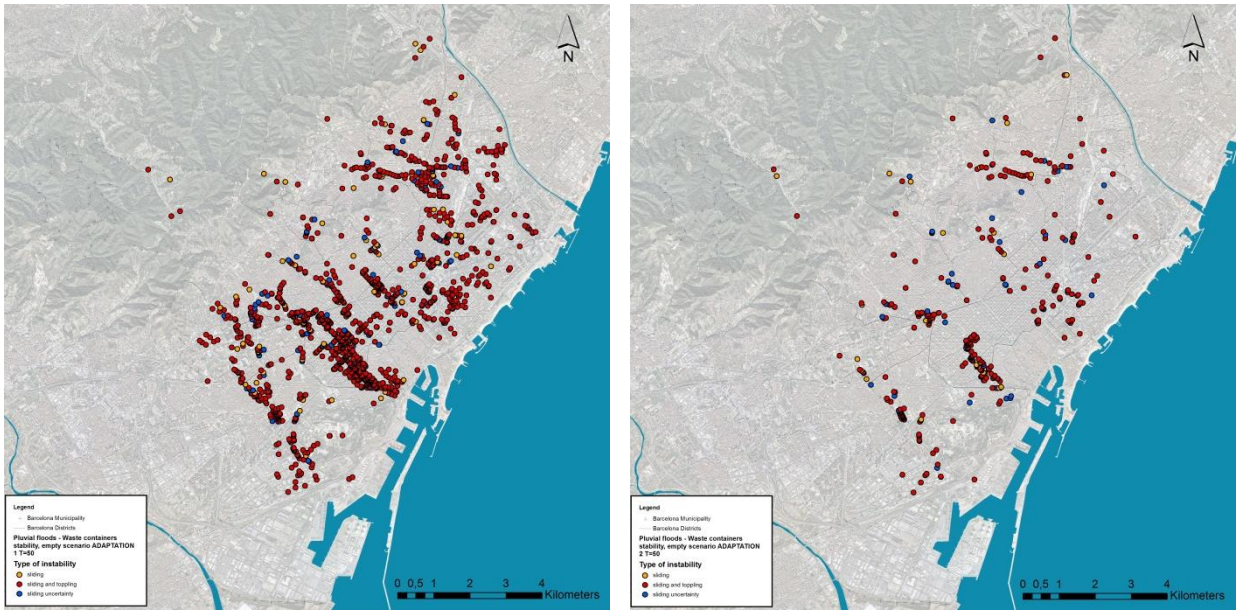

Map 39. *Impact maps for urban solid-waste containers in Adaptation Scenario 1 (left) and Adaptation Scenario 2 (right) for a T50 return period, including container anchoring mechanisms.*

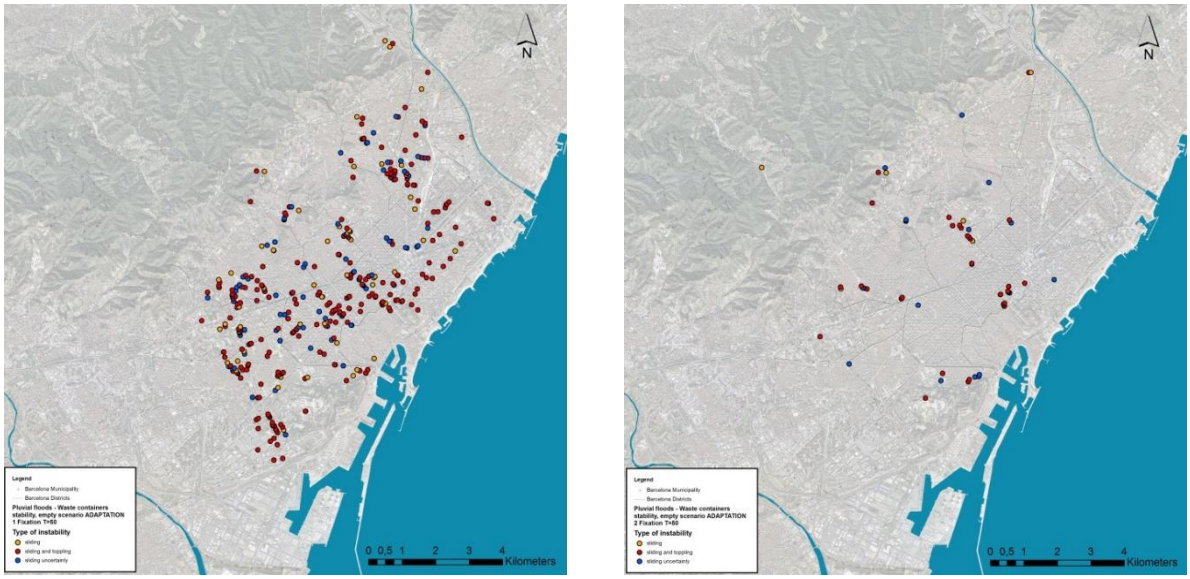

Figure 23 presents the results on the effectiveness of anchoring mechanisms on the stability of urban solid-waste containers, for the SUDS adaptation scenario and the joint implementation of SUDS and structural measures (SM), relating to a flood with a 50-year return period and the scenario of empty containers.

Figure 26. *Decrease in the number of unstable urban solid-waste containers (as a %) as a result of the measures introduced in Adaptation Scenarios 1 and 2, and including the container anchoring mechanisms, for a T50 return period.*

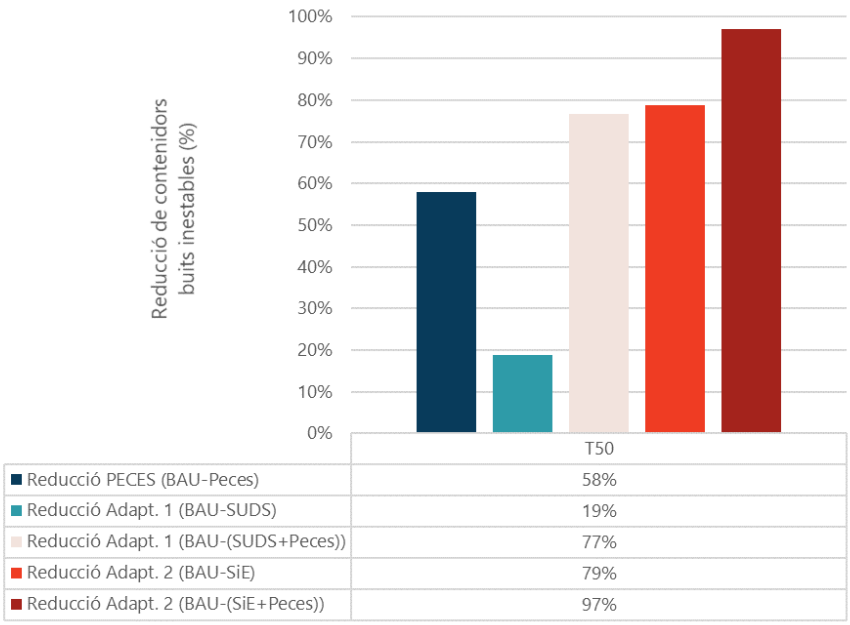

The isolated effect of the anchoring mechanisms produces a 58% reduction in the number of unstable containers. Therefore, this is a very effective, low-cost solution.

Although the joint implementation of SUDS and structural measures (Adaptation Scenario 2) is very efficient (79% reduction), the installation of the anchoring mechanisms together with the SUDS adaptation scenario would be sufficient to avoid any movement in nearly the same number of containers (77%) at a much lower cost. Finally, the movement of empty containers is almost totally avoided when the SUDS, the structural measures and the anchoring mechanisms are implemented together (97%).

3.5 Effects of flooding on property and vehicles: an analysis of direct tangible damage.

In order to estimate the direct tangible damage caused by rainwater flooding in urban areas, the economic impact on property and vehicles has been considered. These are the most affected assets, according to the compensation data provided by the Spanish company Consorcio de Compensación de Seguros (CCS), which is the public body that covers the losses generated by extreme climate phenomena, among others.

The evaluation of property damage was carried out using a methodology[3] based on damage curves, which measure the damage according to floodwater depth. The first step consists of using the floodwater depth in the streets surrounding the property (taken from the hydrodynamic model), based on watertightness coefficients developed for 14 land uses (types of property) in Barcelona, and on whether or not there is a step at the property entrance. As a second step, the flood damage to the properties was assessed, using specific damage curves based on the floodwater depth inside the buildings, developed for the fourteen types of property. Furthermore, a maximum depth was proposed where there are lower floors, so that when that level is reached, water transfer only occurs to lower levels. Various types of property were considered: without basement, with one basement floor and with a maximum of two basement floors. Configurations with or without car parks were also considered, because where there is a car park, the water enters from the floor above, but also directly from the street, an aspect that is also taken into consideration, through the use of watertightness coefficient curves. The model is implemented through the use of SIG tools, in order to establish a water depth inside the buildings and to calculate the corresponding damage.

Figure 27. *Conceptual model for assessing flood damage to urban properties. Source:*[3]

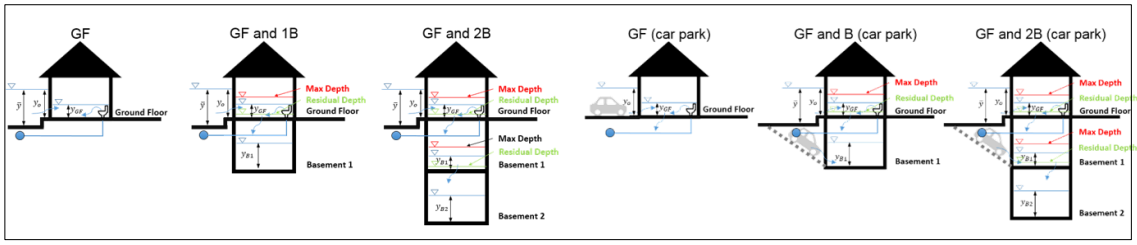

In regard to the damage assessment for vehicles, an innovative methodology has been used, which is also based on the concept of damage curves. The methodology aims to reduce

[3] Martínez-Gomariz, E., Forero-Ortiz, E., Guerrero-Hidalga, M., Castán, S., Gómez, M., 2020. Flood Depth–Damage Curves for Spanish Urban Areas. Sustainability 12, 2666. https://doi.org/10.3390/su12072666
Martínez-Gomariz, E., Guerrero-Hidalga, M., Russo, B., Yubero, D., Gómez, M., & Castán, S. (2019). Desarrollo y aplicación de curvas de daño y estanqueidad para la estimación del impacto económico de las inundaciones en zonas urbanas españolas [Development and application of damage and watertightness curves for assessing the economic impact of flooding in Spanish urban areas.] Ingeniería Del Agua, 23(4), 229–245. https://doi.org/10.4995/ia.2019.12137

uncertainty due to the mobility of the vehicles, proposing a heterogeneous vehicle occupation for the various city areas, based on the information provided by high-resolution aerial photographs. The first step is to adapt the flood damage curves for the five types of vehicles developed by USACE[4] to the case of Barcelona. These curves are converted into a single damage curve weighted according to the percentage of vehicles of each type found in Barcelona, and also taking into consideration depreciation, according to statistical information, by type of vehicle and average age.

Maps of direct tangible damage caused by rainwater flooding in urban areas have been obtained for both properties and vehicles, for the T1, T10 and T100 return periods and the current and future scenarios and Adaptation Scenarios 1 and 2, with the calculated value of damage aggregated for each city neighbourhood. In the case of the T1 return period, the value of damage is null, and for this reason, it is not represented on the maps. The damage to vehicles is not represented on the maps either, as the differences are not very representative in terms of the affected neighbourhoods, and the value of the damage caused to vehicles by flooding is about ten times less than the damage caused to property.

Map 40. *Map of damage value caused to property by urban flooding for the current scenario (left) and future scenario (right), with a T10 return period.*

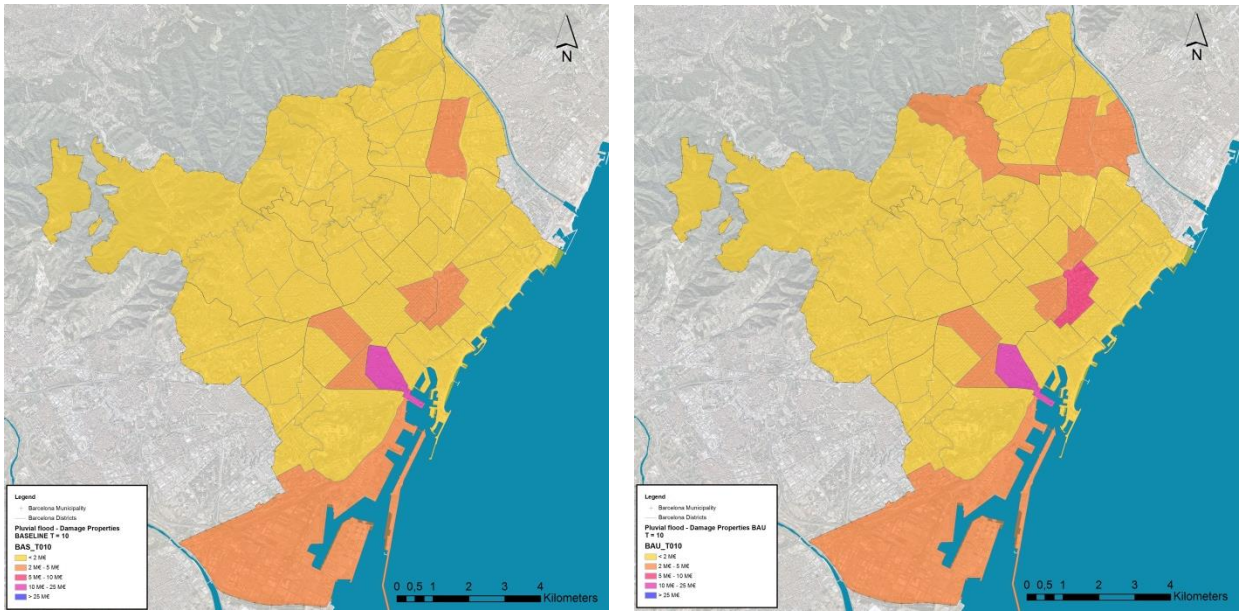

[4] U.S. Army Corps of Engineers (USACE). (2009). Economic Guidance Memorandum, 09-04, Generic Depth-Damage Relationships for Vehicles. Washington, DC. Retrieved from http://planning.usace.army.mil/toolbox/library/EGMs/egm09-04.pdf

Map 41. *Map of damage value caused to property by urban flooding for Adaptation Scenario 1 (left) and Adaptation Scenario 2 (right) for a T10 return period.*

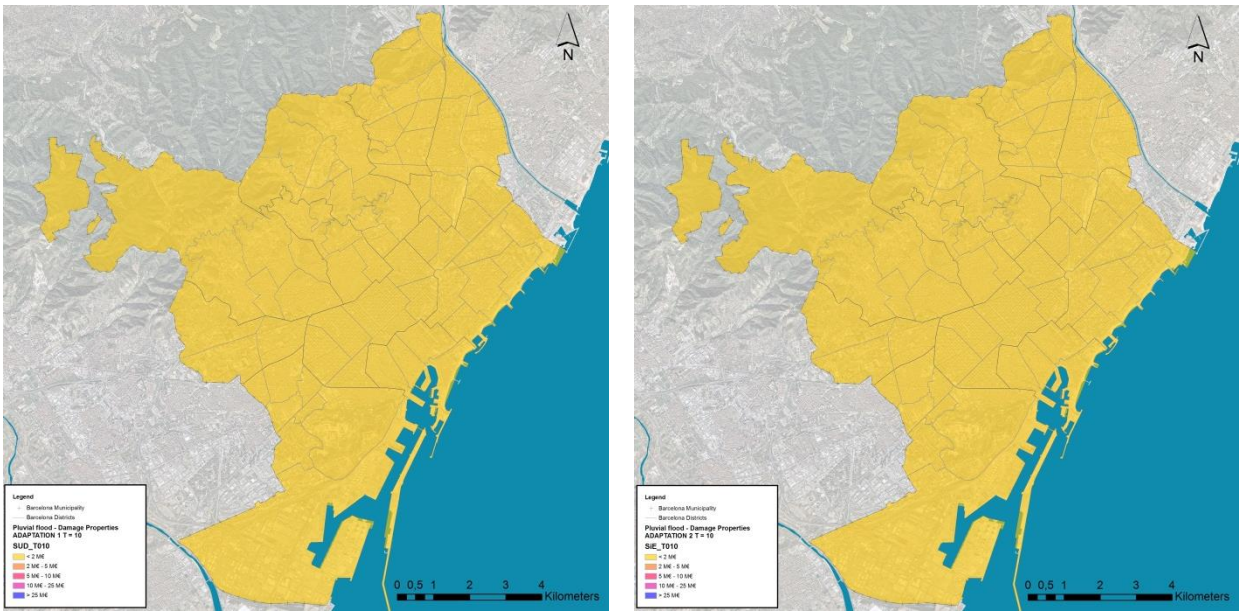

Map 42. *Map of damage value caused to property by urban flooding for the current scenario (left) and future scenario (right), with a T100 return period.*

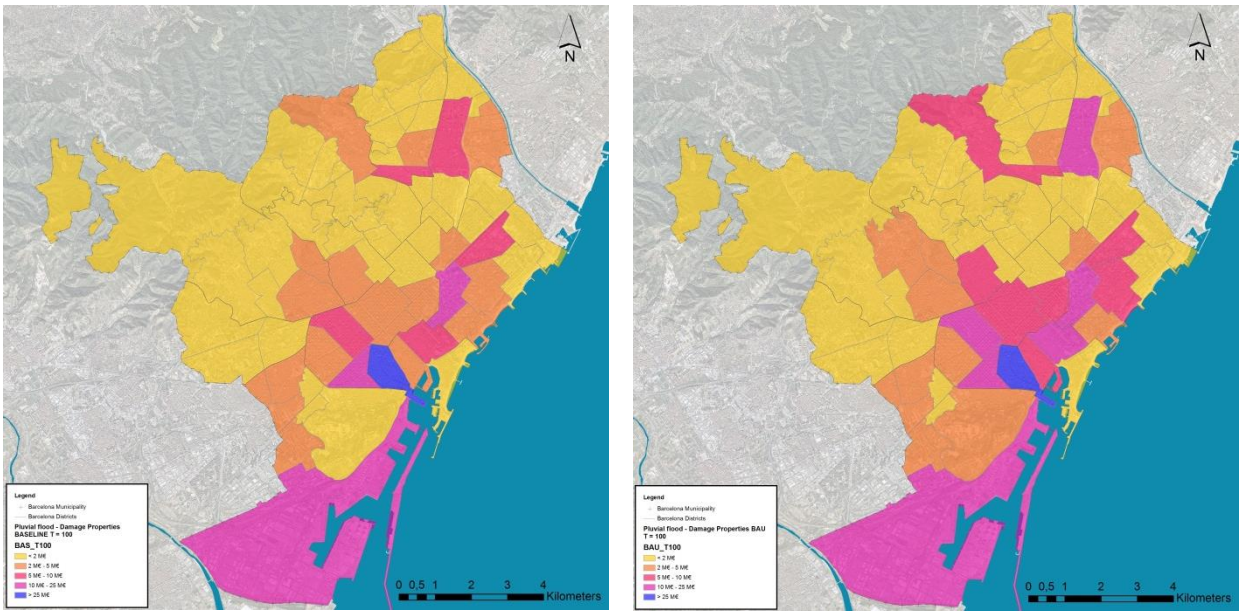

Map 43. *Map of damage value caused to property by urban flooding for Adaptation Scenario 1 (left) and Adaptation Scenario 2 (right) for a T100 return period.*

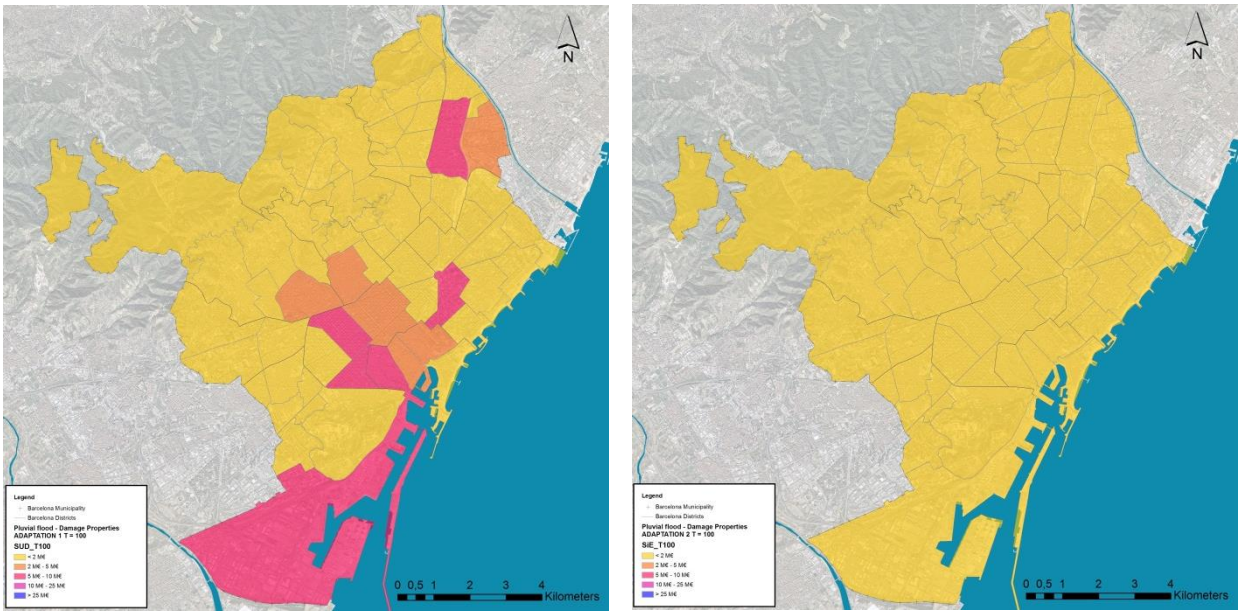

These maps show how the neighbourhoods most affected by property damage are El Raval, el Parc i la Llacuna del Poblenou, Sant Andreu, Sant Antoni, l'Esquerra de l'Eixample, la Marina del Prat Vermell and Zona Franca, and that future rainfall, made worse by climate change, significantly exacerbates the situation in various neighbourhoods, mainly in the centre of the city.

The following associated graphs and tables summarise the obtained results, and show the evolution of the estimated damage to property and vehicles caused by urban flooding in Barcelona city, for the current, future, Adaptation 1 and 2 scenarios, and for the T10 and T100 return periods.

Figure 28. *Value of damage to property and vehicles (in millions of €) due to the effects of flooding in Barcelona city, for the current, future, Adaptation 1 and 2 scenarios, and for the most significant return periods.*

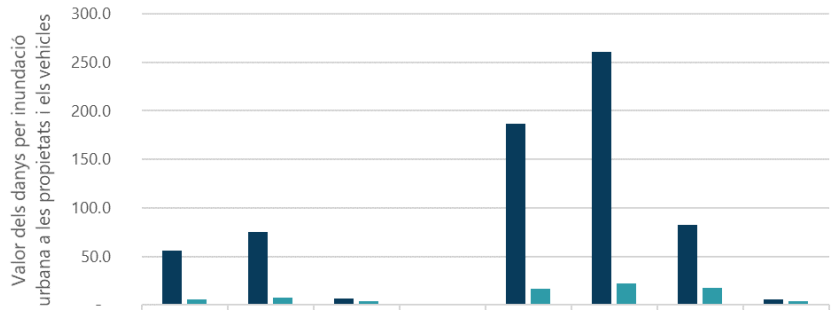

	T10 BAS	T10 BAU	T10 Adapt. 1	T10 Adapt. 2	T100 BAS	T100 BAU	T100 Adapt. 1	T100 Adapt. 2
Propietats (M€)	56.4	75.5	6.5	-	186.3	260.8	82.8	5.5
Vehicles (M€)	5.4	7.4	4.1	0.4	16.5	22.3	17.4	4.2

As the intensity of future rainfall is higher than at present, the value of damage to properties and vehicles in the future scenario is, in general, 35% higher than the estimated value for the current scenario. This difference indicates the potential cost (in relation to direct tangible damage) of not taking action to counter climate change.

Figure 29. *Increased value of damage to property and vehicles (as a %) due to the forecast effects of flooding, due to climate change, in Barcelona city and for the most significant return periods.*

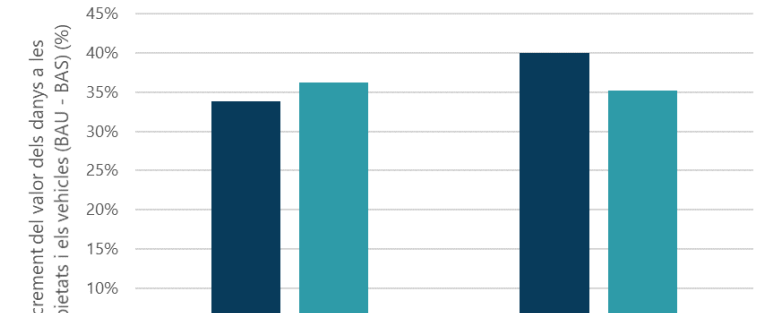

	T10	T100
Propietats (%)	34%	40%
Vehicles (%)	36%	35%

In order to assess the effectiveness of the measures introduced in Adaptation Scenarios 1 and 2, the reduction in tangible damage to property and vehicles produced has been considered, comparing the results of these two adaptation scenarios with those obtained for the future scenario with climate change (BAU). Adaptation Scenario 1 (introduction of only sustainable urban drainage systems, or SUDS, throughout Barcelona) provides a reduction of between 90% and 70% in the value of damage to property and between 40% and 20% in the damage to

vehicles, while the joint introduction of SUDS and structural measures (Adaptation Scenario 2) eliminates nearly all of the damage.

Figure 30. *Reduction in the value of damage to property and vehicles (as a %) due to the effects of flooding in Barcelona city, as a result of the measures implemented in Adaptation Scenarios 1 and 2, for the most significant return periods.*

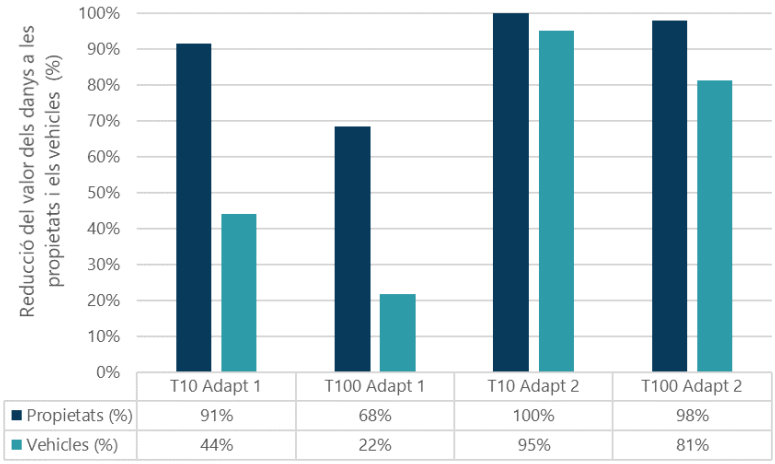

	T10 Adapt 1	T100 Adapt 1	T10 Adapt 2	T100 Adapt 2
Propietats (%)	91%	68%	100%	98%
Vehicles (%)	44%	22%	95%	81%

3.6 Effects on bathing water due to discharges into the receiving environment

Barcelona city's drainage model is characterised by being a unitary system. This means that both waste water and rainwater are channelled through the same sewers to the treatment plants. This unitary model involves a risk, in that the treatment plants do not have sufficient capacity to absorb the excess water caused by torrential rain, and therefore the drainage network then channels the water to discharge points in the sea. These discharges cause a reduction in bathing water quality, which habitually leads to the city's beaches being closed, with the corresponding impacts on activities linked to the Barcelona seashore.

In order to find out more about how these discharges are produced, and their repercussions, a seawater-quality model has been created, with the aim of studying the impact of the unitary system discharges (USD) from the city to the bathing areas. The marine model is used to simulate the spatial and temporal distribution of the *E. coli* bacterium in seawater during and after USD events. *E. coli* is one of the bacteria cited in Spanish and European regulations concerning the quality of bathing water.

Figure 31. *Example of maritime quality simulation after a USD episode (Red = high* E. coli *concentration; Blue = low* E. coli *concentration).*

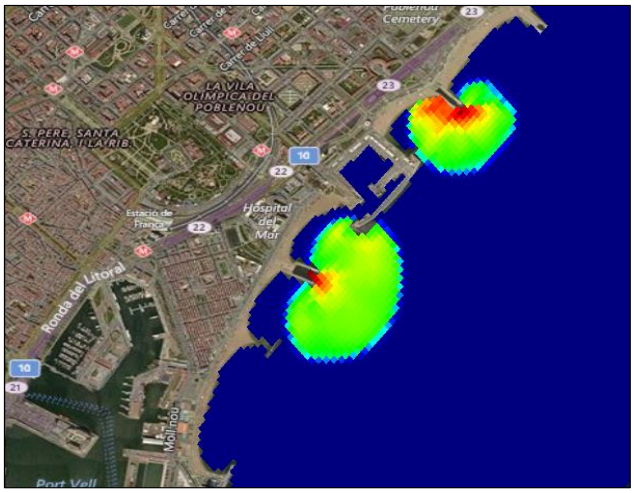

The original model was developed as part of the COWAMA (Coastal Water Management) project, which provided a computer model, operational since 2007, for real-time simulations of bathing water quality at Barcelona's beaches. The marine model includes a new 3D grid, based

on new bathymetric data obtained in 2016, a new calibration and a new validation, with data on *E. coli* concentrations measured during the period from 2014 to 2017.

Figure 32. *New bathymetrics for Barcelona's maritime model.*

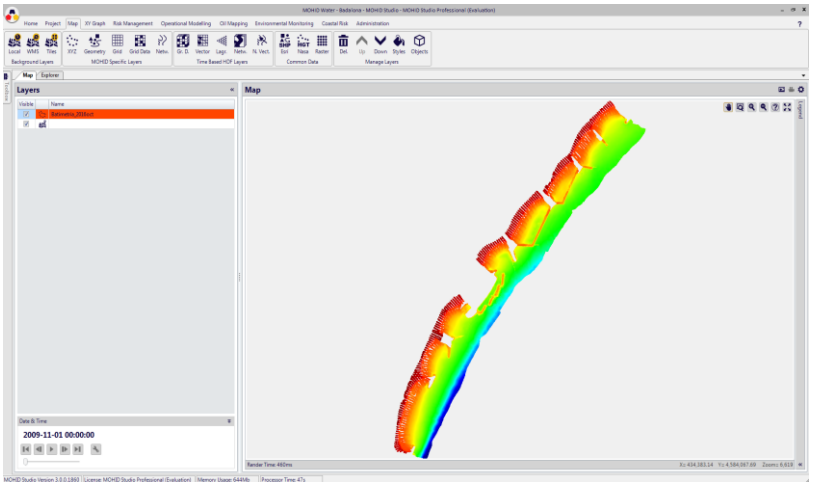

The simulation of water quality near the coastline requires spatial discretisation scales on a scale of tens of metres, while the coastal hydrodynamic processes can be produced on scales of hundreds of kilometres. Therefore, three nested grids were used to simulate hydrodynamic processes, from a large regional scale to a local scale near the Barcelona coastline.

Figure 33. *The three levels of nested grids used in the Barcelona maritime model.*

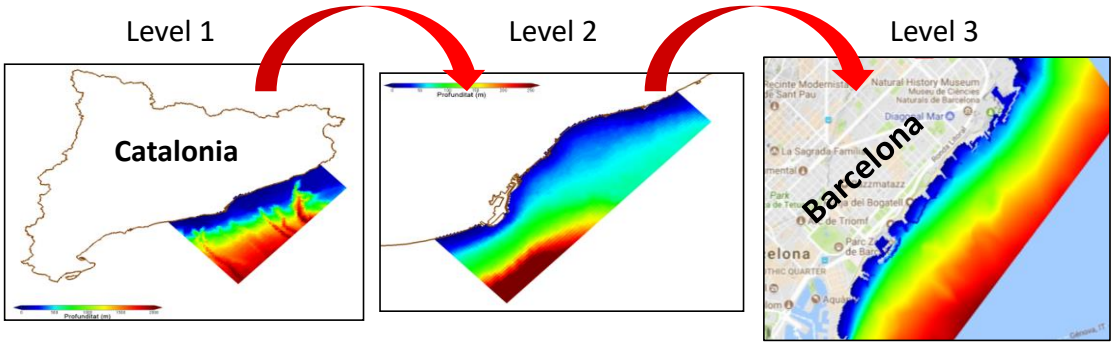

Analogous to the analysis carried out to obtain the design rainfall for the urban flooding model, producing a series of climate change data, the USDs are analysed for the normal hydrological scenarios, but in this case, it is concluded that the future rainfall scenarios do not mean any worsening of the current situation, as climate change will not significantly increase the average

rainfall nor the number of episodes. Therefore, based on the USD analysis, for both the current and climate change scenarios, the series of rainfalls for 2009 were selected, a year which produced 60 USD episodes with a total rainfall of 520 mm.

Figure 34. *Rainfall series for the selected average year (2009).*

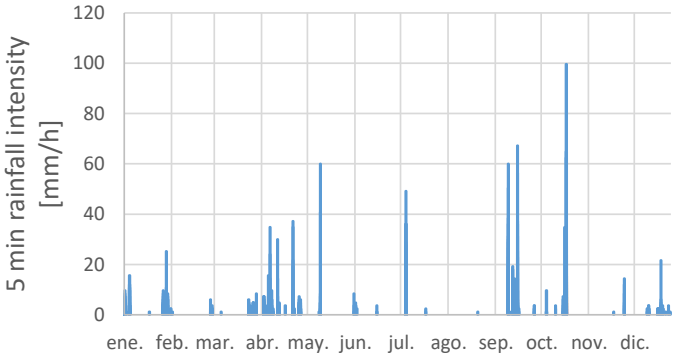

Carrying out simulations through the linked application of the urban flooding model and the maritime model during the bathing season (from 25 May to 15 September), the concentrations of *E. coli* in seawater were obtained. The impacts are quantified in terms of the time during which the bacteriological contamination values (*E. coli* concentrations > 500 cfu/100 ml) were not met, in accordance with the recommendations established in Royal Decree 1341/2007 and the Bathing Water Directive, for the bathing season taken as a reference (2009) for each of Barcelona's beaches. The following graphs show the results for the current and future scenarios (concurring) and for the two Adaptation scenarios.

Figure 35. *Non-compliance time (in days) with the bacteriological contamination values established by the Bathing Water Directive for the bathing season, as a consequence of discharges into the marine environment, for the current/future and Adaptation 1 and 2 scenarios for Barcelona's beaches and the average value.*

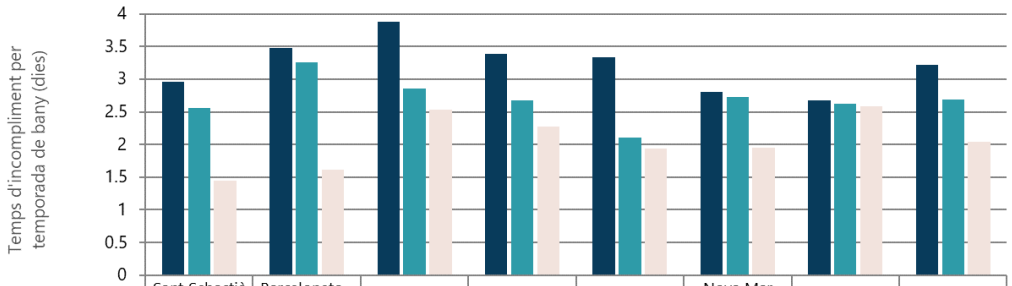

	Sant Sebastià - Sant Miquel	Barceloneta - Port Olímpic	Nova Icaria	Bogatell	Mar Bella	Nova Mar Bella	Fòrum	Mitjana
BAS = BAU (Actual i Futur)	2.96	3.47	3.88	3.39	3.33	2.81	2.67	3.22
Adapt. 1 (SUDS)	2.56	3.26	2.86	2.67	2.11	2.73	2.62	2.69
Adapt. 2 (SUDS + dipòsits)	1.44	1.61	2.53	2.28	1.94	1.95	2.58	2.05

Figure 36. *Non-compliance time (as a %) with the bacteriological contamination values established by the Bathing Water Directive for the bathing season, as a consequence of discharges into the marine environment, for the current/future and adaptation 1 and 2 scenarios for Barcelona's beaches and the average value.*

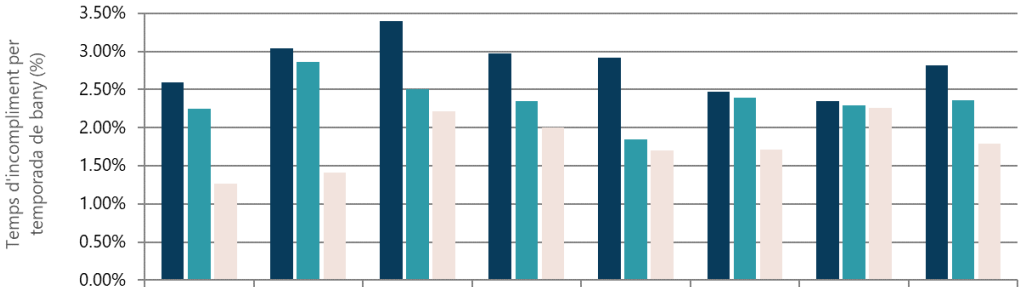

	Sant Sebastià - Sant Miquel	Barceloneta - Port Olímpic	Nova Icaria	Bogatell	Mar Bella	Nova Mar Bella	Fòrum	Mitjana
BAS = BAU (Actual i Futur)	2.60%	3.04%	3.40%	2.97%	2.92%	2.47%	2.35%	2.82%
Adapt. 1 (SUDS)	2.25%	2.86%	2.51%	2.35%	1.85%	2.39%	2.30%	2.36%
Adapt. 2 (SUDS + dipòsits)	1.26%	1.41%	2.22%	2.00%	1.70%	1.71%	2.26%	1.80%

The results of the simulation of the current scenario (coinciding with the future non-adaptation scenario) shows that on average, all the beaches in Barcelona did not meet the Bathing Water Directive's established values for a total of 3.22 days, which is the equivalent of 2.82% of the bathing season. The variation between the various beaches ranges between 2.35 at the Fòrum beach and 3.40% at Nova Icària.

On average, in Adaptation Scenario 1, the SUDS can reduce this time to 2.36%, while in Adaptation Scenario 2 (SUDS and structural measures), the non-compliance time is reduced to 1.8%, slightly above the 1.5% objective established in the Catalan Water Agency's (or ACA's)

circular. However, this 1.5% value was a guideline, so that the proposed actions are considered to comply with the established objectives.

Figure 37. *Decrease in non-compliance time (as a %) with the bacteriological contamination values established by the Bathing Water Directive for the bathing season, as a consequence of discharges into the marine environment, as a result of the measures introduced in Adaptation Scenarios 1 and 2 for Barcelona's beaches and the average value.*

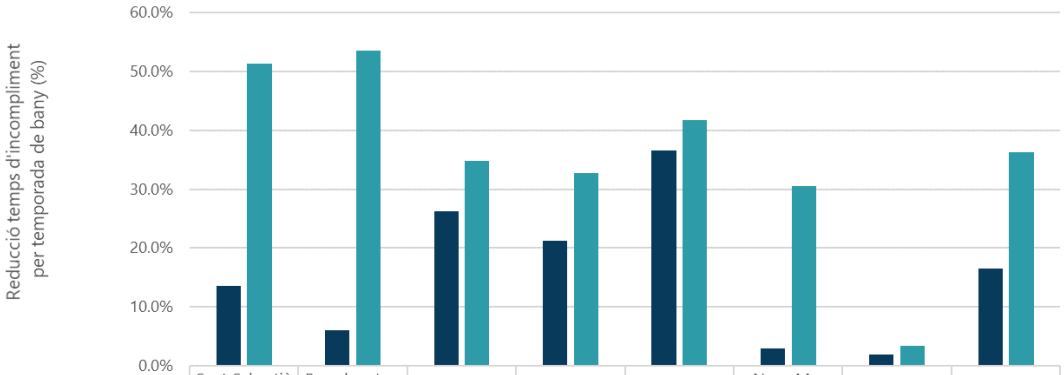

	Sant Sebastià - Sant Miquel	Barceloneta - Port Olímpic	Nova Icaria	Bogatell	Mar Bella	Nova Mar Bella	Fòrum	Mitjana
Reducció Adapt. 1 (BAS-SUDS)	13.5%	6.1%	26.3%	21.2%	36.6%	2.8%	1.9%	16.4%
Reducció Adapt. 2 (BAS-SiE)	51.4%	53.6%	34.8%	32.7%	41.7%	30.6%	3.4%	36.3%

Graph 28 shows that the effect of the adaptation measures is very variable, depending on the beach being studied, so that the difference is practically unnoticeable at the Fòrum beach, while reductions of over 50% are produced for the combination of SUDS + anti-USD tanks on the Sant Sebastià-Sant Miquel and Barceloneta-Port del Fòrum beaches.

However, discharges into marine ecosystems do not only have impacts on health and the environment, but also affect the area's economic activities. Economic losses associated with the closure of the beaches due to high contaminant levels would be expected. This is especially relevant for a city such as Barcelona, where tourism and leisure have a major weighting in the economy, with urban beaches which benefit the local population and tourists.

As with rainwater flooding, the economic impacts of unitary system discharges (USDs) at the city's beaches are classified as indirect damage, because the business losses are caused by the discharges, but the companies are not directly affected. A methodology has been developed to estimate the costs borne by seashore businesses, which considers the number of days the beaches are closed due to high bacteriological contamination caused by USD discharges (data provided by the marine model on USDs at the city's coastal bathing area) and the direct added impact to the associated economy (based on data from the economic analysis on Barcelona's seashore economic activity for 2017).

In order to avoid overvaluation, the study area has been restricted to those seashore districts where there are discharge points, as can be seen on map xx. The affected districts represent 40.5% of Barcelona's total seashore economy.

Map 44. *Map of Barcelona's seashore areas, where the districts affected by USDs are highlighted.*

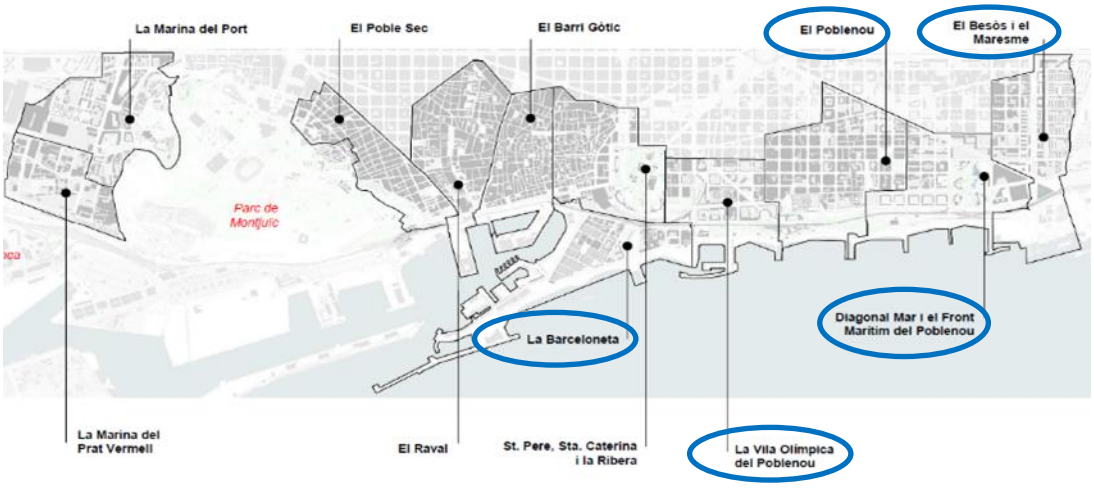

For the purpose of modelling, it has been assumed that during a USD episode in the bathing season, a red flag is raised and beach users cannot swim, and they are therefore advised not to remain on the beach. Under this supposition, the economic sectors included are only those directly related to tourist and leisure activities that may be affected by a beach closure, e.g. small shops, restaurants, and leisure or aquatic activities. Lastly, the model also takes the seasonal factor into account, which considers that 50% of annual tourism revenue occurs during the summer period.

After this hypothesis, and considering a bathing season of 114 days, the indirect damage is estimated to be €510,328 for every day the beach is closed. Using this data and the data concerning the duration of high contamination at Barcelona's beaches for an average year (3.22 days), there is an estimated loss of €1,643,265 per bathing season.

By applying the same methodology to the adaptation scenarios, the results for the following graphs are obtained. It should be noted that the effect of the implementation measures in the adaptation scenarios, especially the structural measures (anti-USD tanks), reduce the seashore business losses by approximately 35%.

Figure 38. *Estimations of indirect damage for business losses and high contamination days during the bathing season, due to the effects of discharges into the marine environment, for current/future and Adaptation 1 and 2 scenarios.*

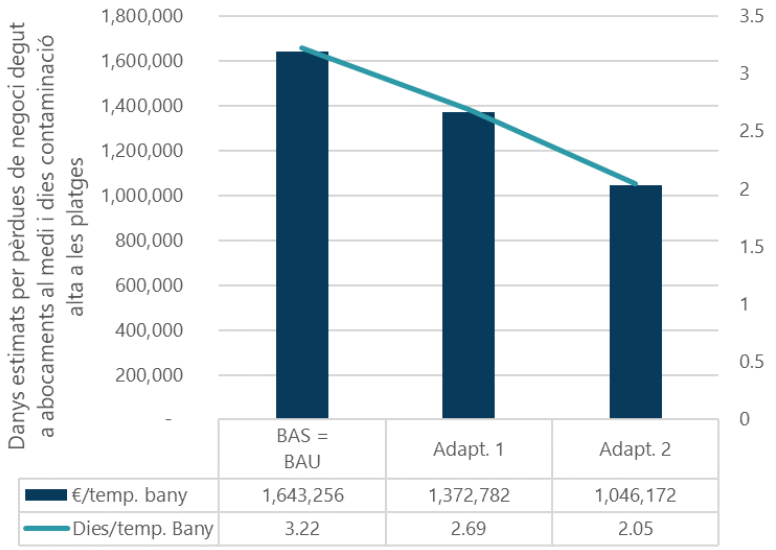

Figure 39. *Decrease in the estimated value of damage (as a %) due to business losses produced by the effects of discharges into the marine environment as a result of the measures introduced in Adaptation Scenarios 1 and 2.*

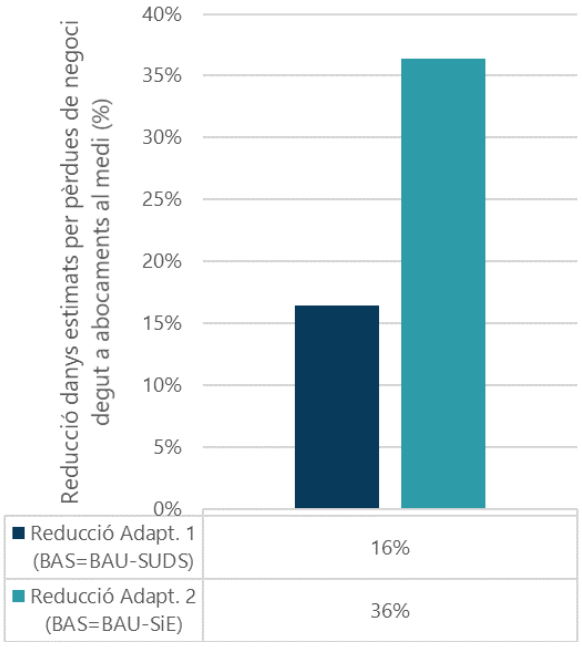

3.7 How the electricity sector is affected

For the impact analysis of urban flooding on the electricity sector, medium voltage (MV) and high voltage (HV) substations located within the city's municipal boundaries have been examined. This area corresponds to the analysis area of the urban drainage model developed for the project. Normally, these types of infrastructure are protected and insulated against flooding when they are established, taking a return period into account. However, this could raise a problem in the future unless the increase in magnitude caused by climate change is taken into account. Consequently, the protection measures may not be sufficient in some cases, and there is a chance of causing power cuts that would affect entire neighbourhoods, or even districts.

One of the major uncertainties of this model was a lack of knowledge concerning the specific location of critical electrical infrastructures (sometimes located on the surface, and sometimes underground or with self-protective elements that are not always known). The impact analysis used a vulnerability curve (known as fragility curve in the electricity sector) for the electricity infrastructure proposed by the U.S. Federal Emergency Management Agency (FEMA). The curve relates the probability of a failure in an electrical structure with the depth of flooding (Figure 29). The results obtained from an analysis of the affected area rate (AAR) at each substation and the fragility curve were calculated in order to obtain a failure probability, and they were subsequently classified into three different risk categories:

- Category 1 (10 cm < WDA <= 80 cm). All substations affected within the 10 and 80 cm are counted. 80 cm corresponds to a failure probability of less than 3%. These do not count in the following category.
- Category 2 (80 cm < WDA <= 160cm). All substations affected within the 80 cm and 160 cm are counted. 160cm corresponds to a failure probability of 50%. These do not count in the following category.
- Category 3 (WDA > 160cm). All substations affected with a 160 cm depth of floodwater, or more, are counted.

Figure 40. *Explanation of the categorisation threshold provided, based on the fragility curve adapted from FEMA, 2009.*

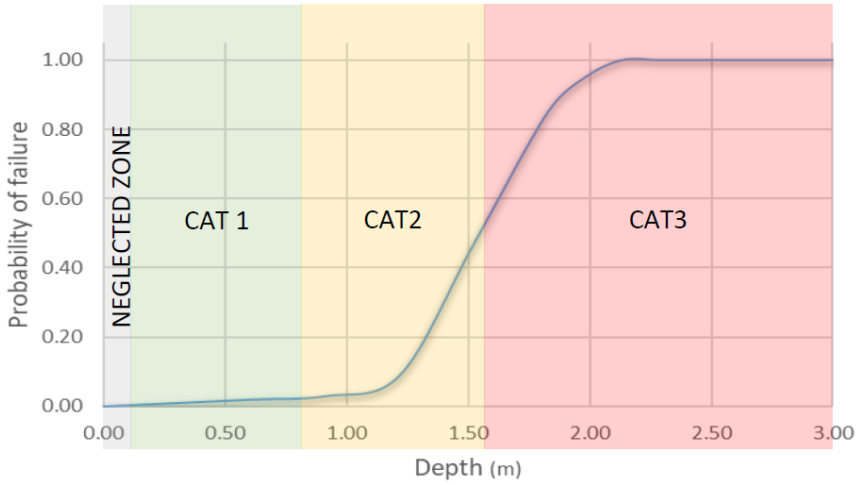

However, Barcelona's electrical substations have only reached the first category.

The following maps show the affected electrical infrastructures in the case of flooding, for the current (BAS) and future (BAU) scenarios. It should be noted that the affected substations in a specific return period will also be affected in a higher return period, but they are superimposed on the return period shown because they both present the same size and, consequently, the same affected area rate (AAR):

Map 45. *Electrical infrastructures affected by urban flooding and the affected area rate for the current scenario.*

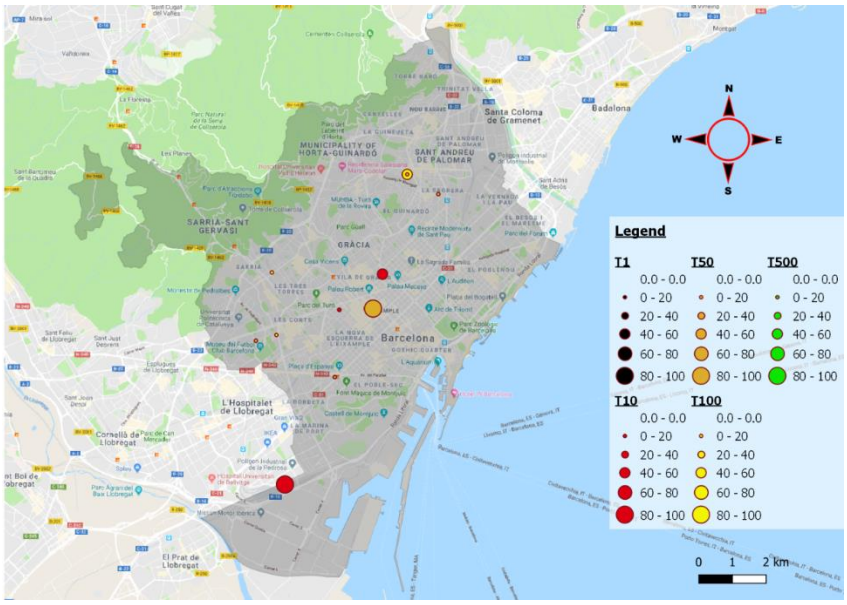

Map 46. *Electrical infrastructures affected by urban flooding and the affected area rate for the future scenario.*

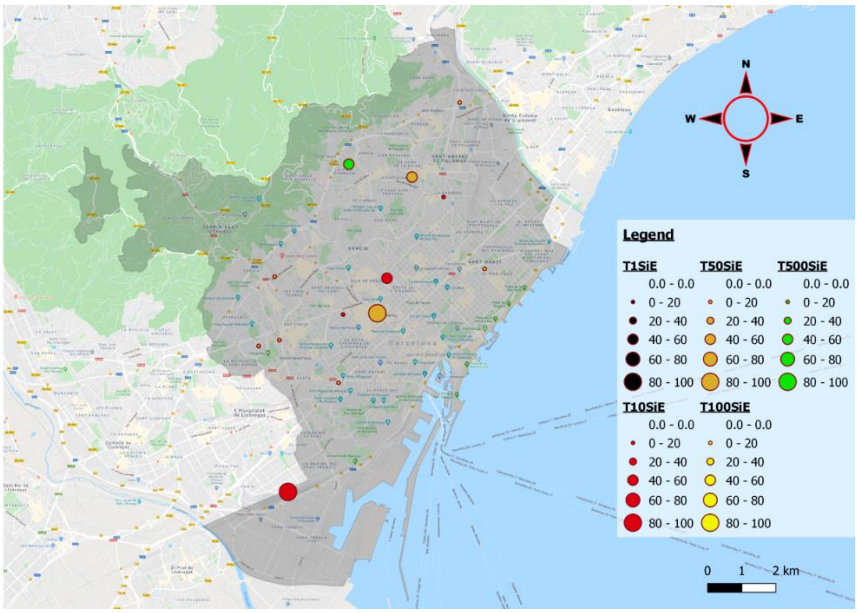

Figure 41 shows the exposure to flooding of substations of various voltages. There are no effects for the T1 return period; it is in the T10 return period that two locations of each type (MV and HV) start to become affected in the BAS scenario, with one MV substation more in the BAU scenario. From T50 onwards, the number of MV substations exposed to flooding risk increases to nine in both scenarios, and to three high-voltage substations potentially affected in T500, for BAS, and to four for BAU. Therefore, the clear increase produced from the reference scenario to the normal scenario for the substations exposed to flooding risk should be noted.

Figure 41. *Number of affected substations in the current (BAS) and future (BAU) scenarios and their percentage over the total number of substations located in Barcelona.*

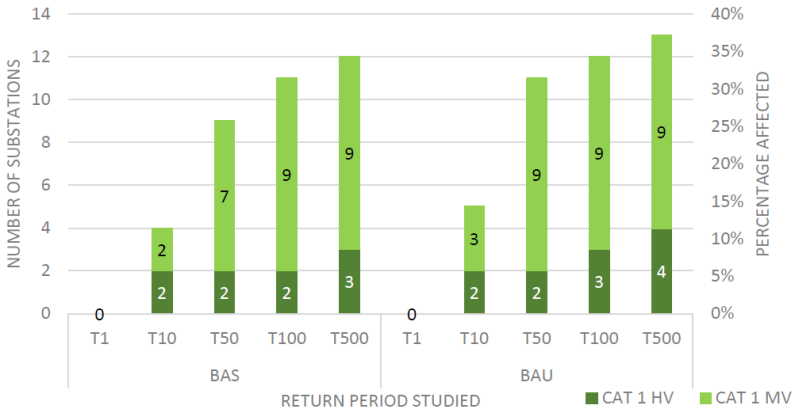

The evaluation of the reduced flooding risk for Barcelona's electricity system was carried out in accordance with the two adaptation scenarios (SUD and SiE) and following the same methodology and criteria adopted for the Baseline and BAU scenarios. Figure xx summarises the numerical results of the locations potentially affected by flooding, after applying the prevention measures contained in the SUD and SiE models. For the SUD adaptation scenario, four substations seem to be potentially affected by flooding at T10 (2 MV and 2 HV), 10 substations at T50 (8 MV and 2 HV), 11 substations at T100 (9 MV and 2 HV) and 13 in the T500 return period (9 MV and 4 HV). This means, in the worst possible case, 37% of Barcelona's substations would be exposed to flooding.

However, when the combination of SUDS and structural measures (SiE) is applied, only one HV station is exposed and only five MV stations are exposed when a T500 flooding event occurs. Therefore, the worst case scenario would be during a T500 flood, in which 18% of Barcelona's substations would be exposed (Figure 42).

Figure 42. *Number of affected substations in the Adaptation 1 (SUD) and Adaptation 2 (SiE) scenarios and their percentage over the total number of substations located in Barcelona.*

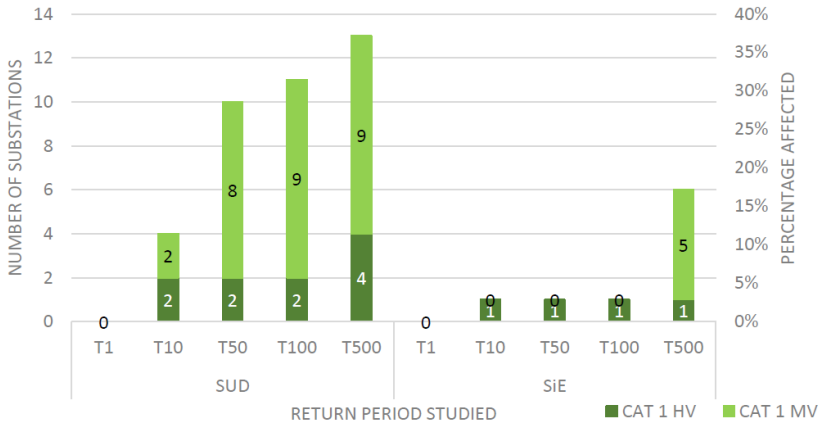

The following maps show how the various electrical infrastructures are affected by flooding in the future scenario, taking into account the Adaptation 1 (SUDS) and Adaptation 2 (SiE) Scenarios:

Map 47. *Representation of the various affected substations after applying the Adaptation 1 (SUD) measures to the BAU scenario, for the various return periods analysed and taking into account the affected area rate (0-100%).*

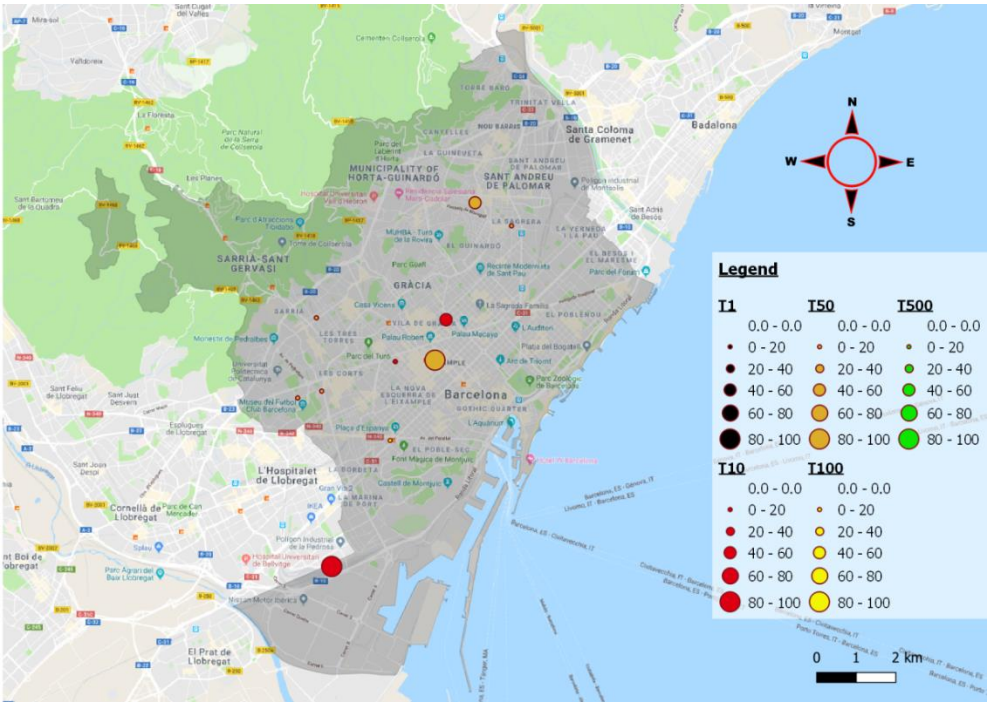

Map 48. *Representation of the various affected substations after applying the Adaptation 2 (SiE) measures to the BAU scenario, for the various return periods analysed and taking into account the affected area rate (0-100%).*

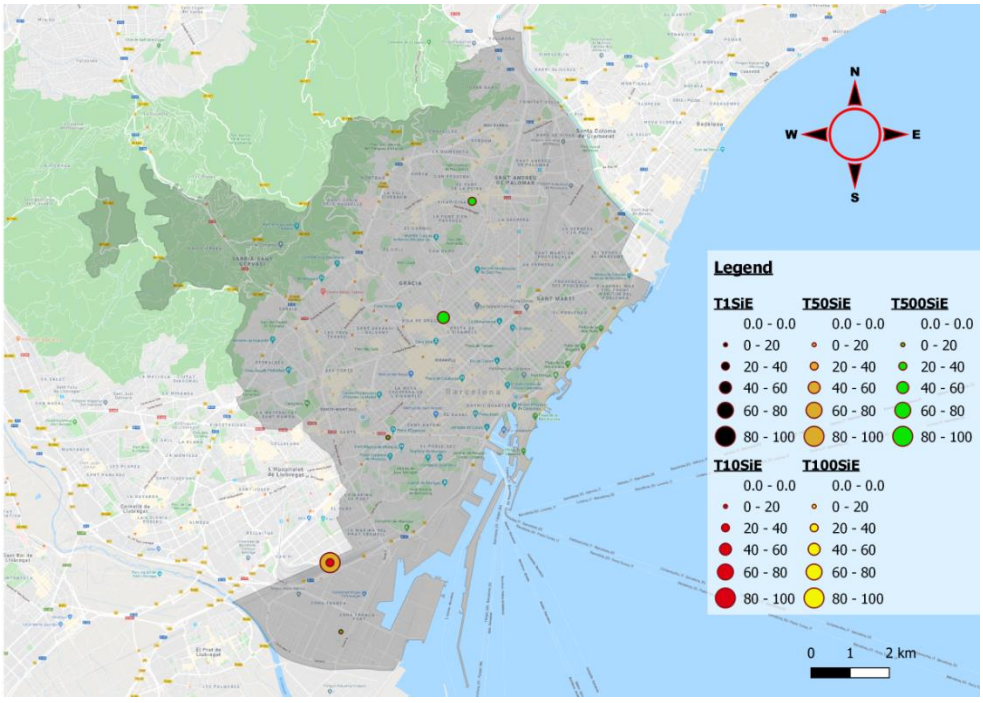

Figure 43 shows the comparison between the BAU scenario and the SUD and SiE adaptation scenarios, once the adaptation measures have been applied:

Figure 43. *Comparison of the BAU-SUD and BAU-SiE scenarios, showing the number of substations that are out of danger in the BAU scenario, applying the various sets of preventative measures and the achieved reduction rate.*

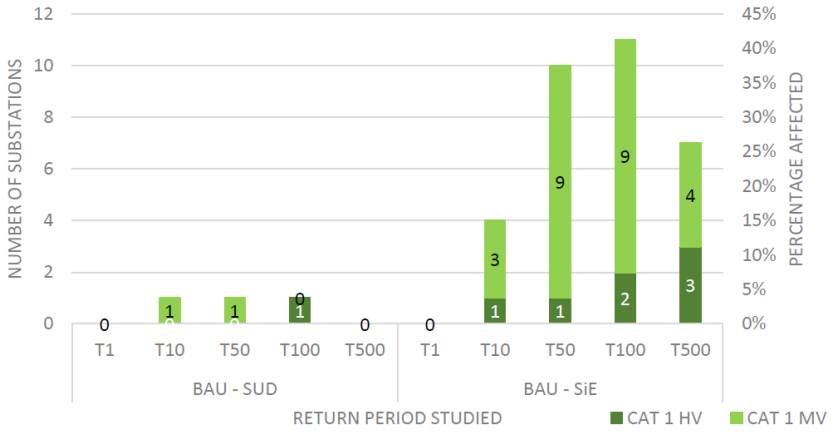

In order to show the effectiveness of the measures being considered, the results are expressed in terms of the reduction in the number of affected locations, after applying adaptation measures and in terms of the reduction rate over the total number of substations. Therefore, when SUDS are applied, it can be seen that one substation is eliminated from flood risk. It can therefore be stated that the SUDS measures are not very effective in regard to the electricity sector. Figure 33 also shows how the reduction in the AAR, achieved for all the return periods, is approximately 10%.

The effectiveness increases considerably when structural measures (SiE) are also applied. Figure 44 shows how the number of affected substations is reduced by 4 for T10, 10 for T50, 11 for T100 and 7 for T500, so that, in the best case scenario, there is a 47% reduction, taking into account both types of substation (MV and HV). When the medium voltage substations are taken into account, there is an average reduction in the AAR of nearly 30% and a 5 cm to 7 cm drop in water depth (WDA) (Figure 39).

Figure 44. *Average reduction in the affected surface area rate and water depth. Average achieved by applying the various sets of preventative measures (SUD and SiE) for each analysed return period.*

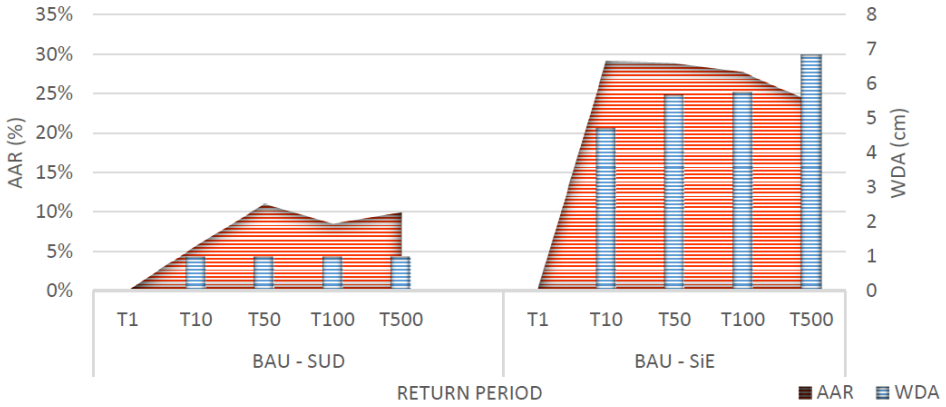

The following maps show the reduction in the flood-affected area, for the various electrical infrastructures, applying the various adaptation measures to the future scenario:

Map 49. *Representation of the substations where the affected area rate was reduced after applying the Adaptation 1 (SUD) measures to the BAU scenario for the various return periods analysed and taking into account the affected area rate (0-100%).*

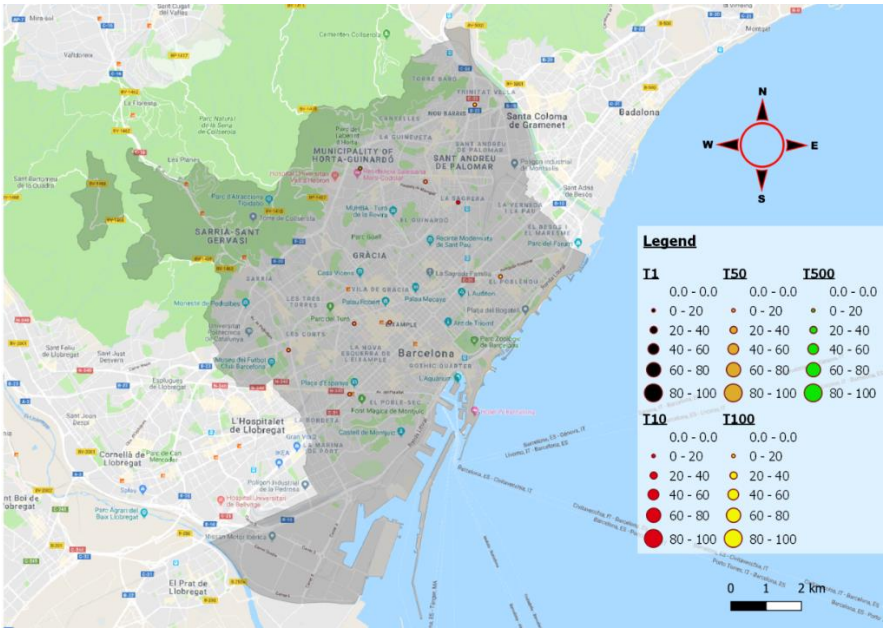

Map 50. *Representation of the substations where the affected area rate was reduced after applying the Adaptation 2 (SiE) measures to the BAU scenario for the various return periods analysed and taking into account the affected area rate (0-100%).*

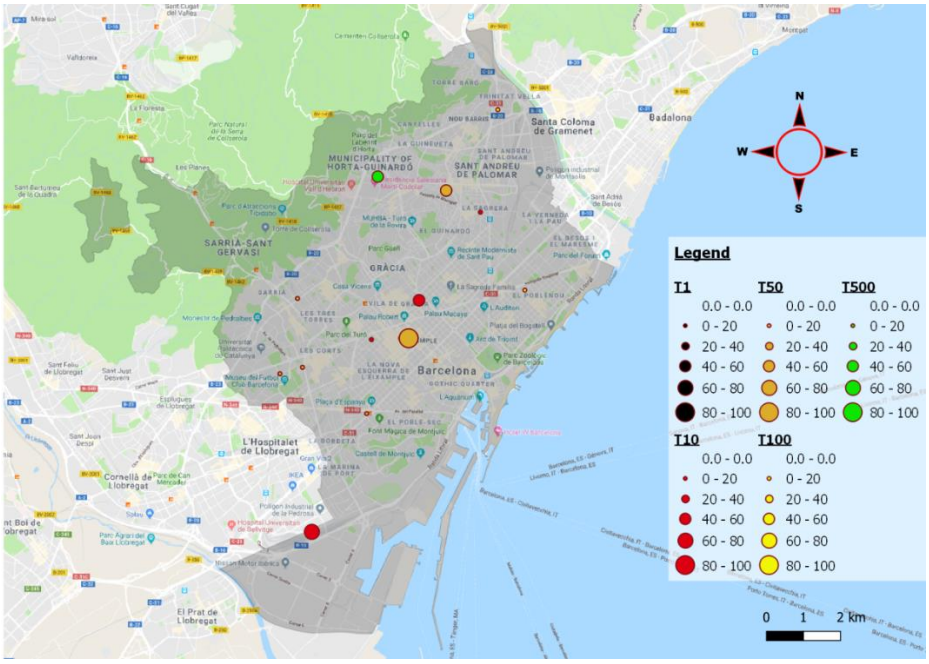

4 Analysis of the impacts derived from the rise in sea level: effects on beaches, infrastructures and coastal services

The aim of this model is to assess the impact of a rise in sea level due to climate change on different coastal areas and structures:

- Groynes of the unitary drainage system's discharge points
- Beaches (real surface area of 30.32 ha)
- Shipyards
- Port breakwaters
- Port quays
- River Besòs delta
- River Llobregat delta
- Discharge drains of the unitary drainage system

The model is based on a simple GIS spatial analysis which, given the future average rise in sea level from a simulation based on the results of climate projections, evaluates the area of permanently flooded structures and seashore areas. It should be noted that the analysis only considers the effect of a rise in sea level, without taking into account sea swell or tides.

The comparative analysis between real and future flooded areas and on the seashore and their associated infrastructures takes as its main hypothesis and starting point that in the current scenario there are no effects to be seen. Therefore, the effects of a rise in sea level on seashore areas is measured in two different future scenarios for the 2071-2100 horizon:

- An average rise in sea level of 35 cm, according to RCP 4.5
- An average rise in sea level of 50cm, according to RCP 8.5

The impacts of a rise in sea level are quantified in terms of:

- The main unitary system (USD) discharge points and drains that may become partially flooded because of the rise in sea level (and furthermore, produce the indirect problem of introducing salinity into the sanitation system).
- Permanently flooded (practically lost) beaches, river deltas, etc.
- Critical infrastructures (sea walls and quays), potentially exposed to floods produced by the rise in sea level.

The maps represent the vulnerable elements potentially exposed to flooding due to the rise in sea level for the two future scenarios:

Map 51. *Main effects for the RCP 4.5 2070-2100 scenario*

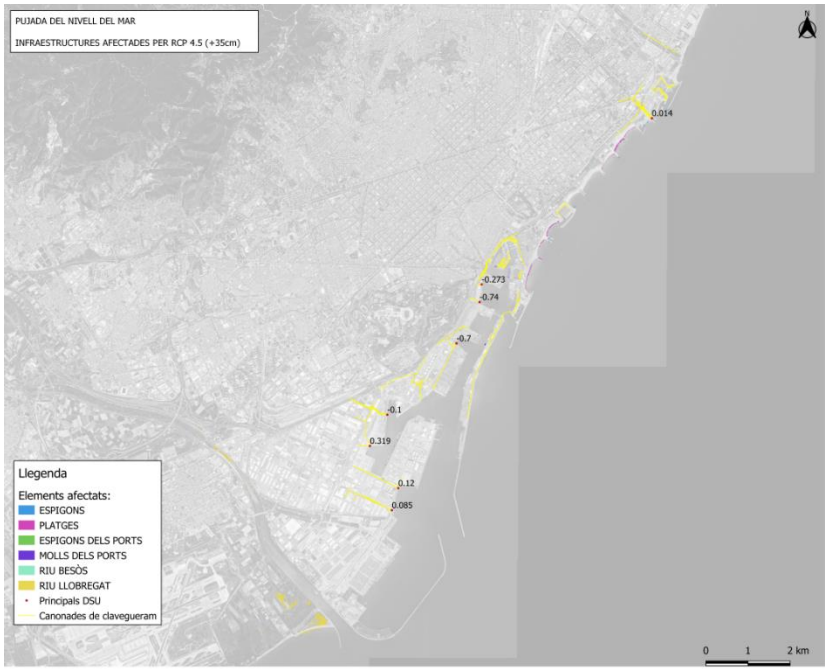

Map 52. *Main effects for the RCP 8.5 2070-2100 scenario*

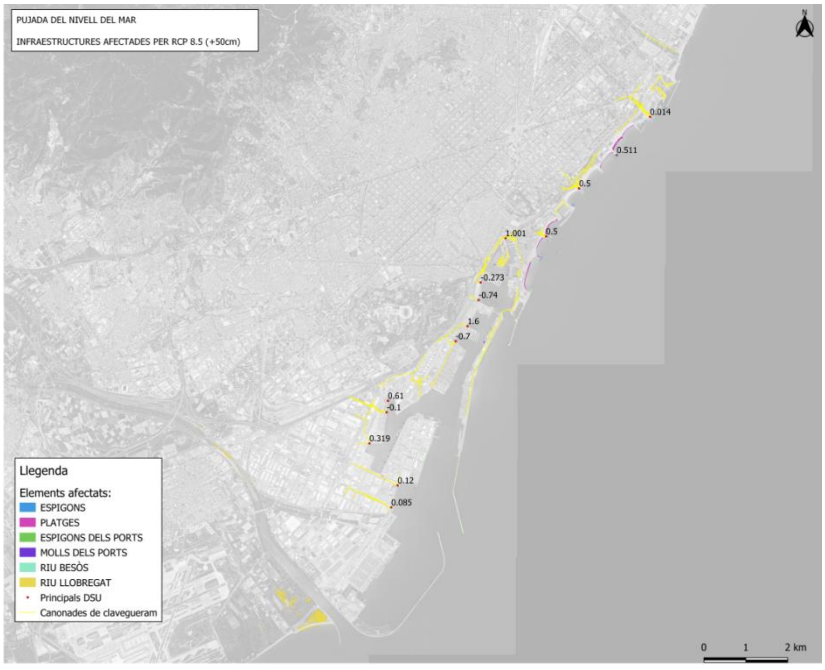

Conclusions

Taking as a reference the current situation, where the beaches occupy a surface area of 30.32 ha, this surface area will be reduced by approximately 3.35 ha (about 11% of the total) in the case of

a 35 cm average increase in sea level and 5 ha (about 17% of the total) in the case of a 50 cm average increase in sea level.

The following table shows the flooded surface areas (in ha) of the various Barcelona beaches, except for Bogatell beach, which would not be affected by either of the two predicted future scenarios:

Beaches	RCP 4.5 (+35 cm)	RCP 8.5 (+50cm)
La Barceloneta	0.29	0.46
Llevant	0.28	0.38
Mar Bella	0.23	0.42
Nova Icària	0.00	0.02
Nova Mar Bella	0.93	1.40
Somorrostro	0.70	0.90
St. Sebastià-St. Miquel	0.92	1.42
General total	3.35	5.00

With regard to the other affected seashore infrastructures, the following table shows how they are affected in the two climate-change scenarios under study:

Data from the GIS model for the rise in sea level	Seashore area (ha) flooded by a 35 cm rise in sea level (RCP 4.5)	Seashore area (ha) flooded by a 50cm rise in sea level (RCP 8.5)
Unitary drainage system groynes for the discharge points	0.72	1.26
Shipyards	0.95	0.96
Sea walls	1.34	3.46
Quays and port areas	0.41	0.56
Besòs delta	0.07	0.16
Llobregat delta	13.16	20.11

5 Impact analysis on water availability.

Barcelona's water supply is guaranteed by the hydrological resources of the Llobregat and Ter catchment areas, and basically depends on the volume of water stored in the reservoir system (Fig. 40).

Figure 45. *Reservoir system of the Ter and Llobregat catchment areas. Source:* [5].

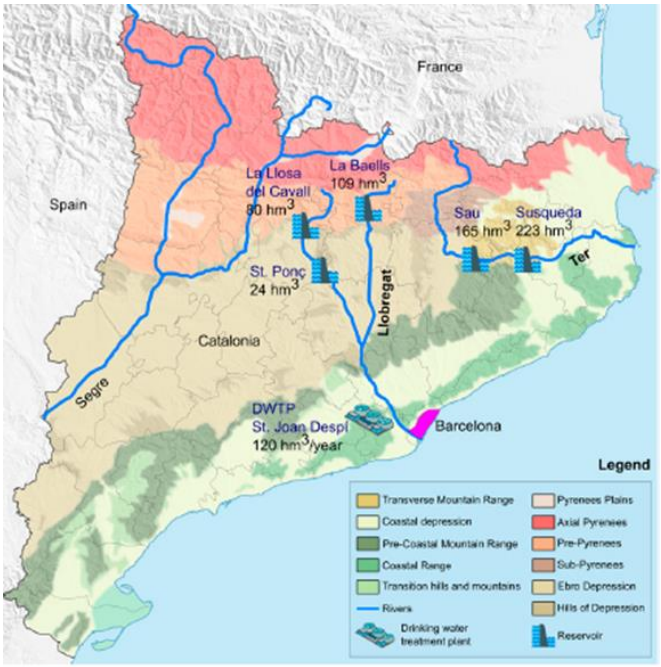

When these volumes are less than some specific values established in the Drought Plan, developed by the Catalan Water Agency (ACA), the city may enter various states of drought, each of which involves a variety of restrictions (leisure activities, irrigation, industrial uses, reducing water pressure in pipes, etc.). Figure 41 shows how the available hydrological resources have decreased over the last 20 years.

[5] Forero-Ortiz, E., Martínez-Gomariz, E., & Monjo, R. (2020). Climate Change Implications for Water Availability: A Case Study of Barcelona City. Sustainability, 12(5), 1779. https://doi.org/10.3390/su12051779

Figure 46. *Decrease in the city's hydrological resources over the last 20 years.*

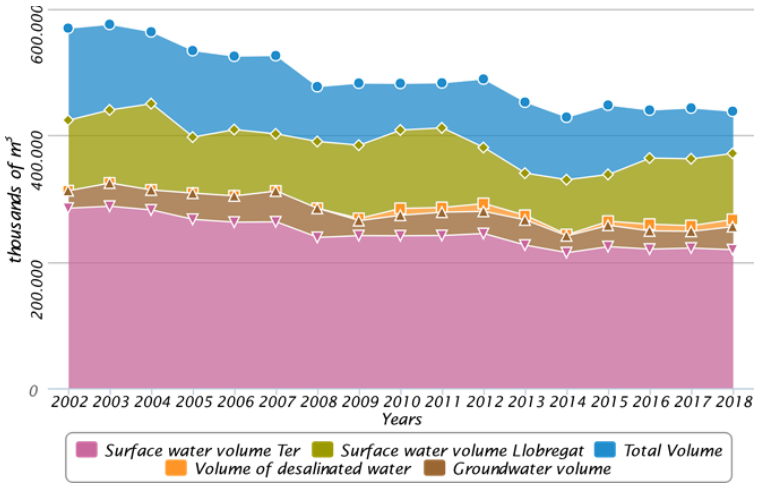

The aim of this hydrological resources and drought model is to represent the water contributions that enter the reservoirs on a monthly time scale, according to rainfall falling on the subcatchment areas for each reservoir.

Figure 47. *Results of the hydrological model simulation used.*

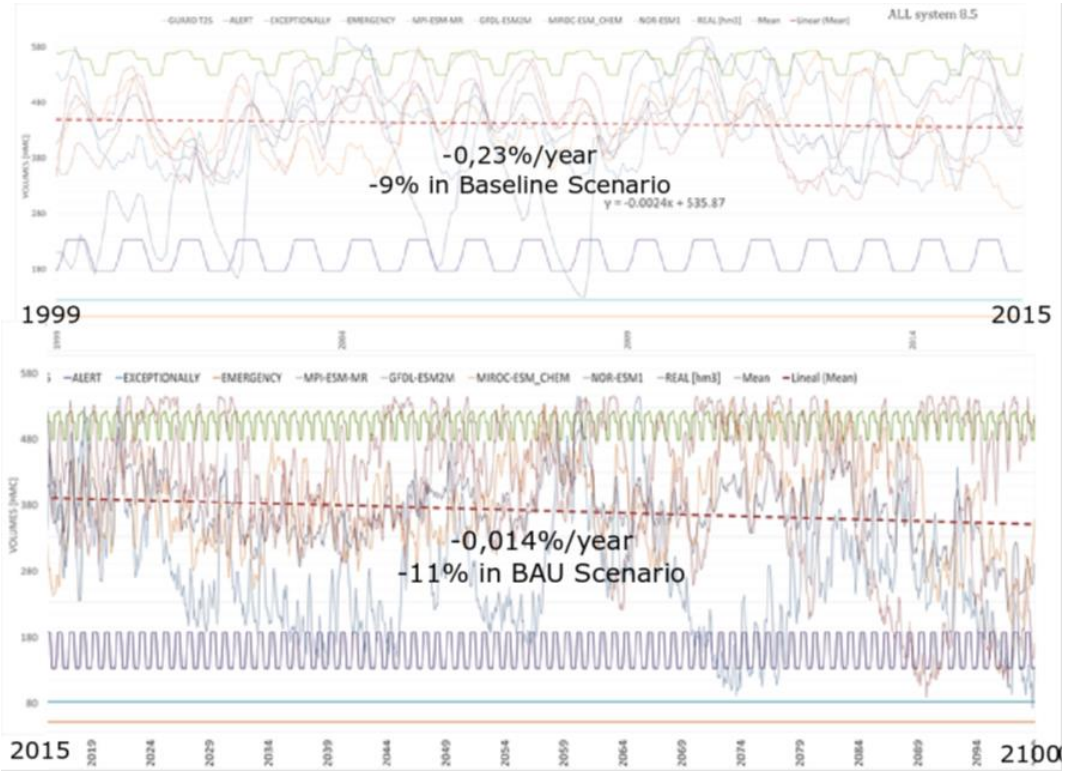

The simulations of the volumes of water entering each reservoir were carried out by applying an integrated hydrological modelling system developed at the Swedish Meteorological and

Figure 48. Results of the hydrological model simulation used.

Hydrological Institute (HBV model). The model applies three different reservoir models: one simulates the behaviour of the land, the second the upper reservoir, and the third the lower reservoir which represents the base groundwater flow and is considered to be appropriate for reproducing the contributions of the reservoirs to the Llobregat and Ter catchment areas.

The result of the simulations carried out indicated that water availability will noticeably decrease in the 21st century in the overall reservoir system. The intercorrelation between the new models provided a trend line for the predicted behaviour of the water in the reservoir system. For 2019-2100, the models predict an average reduction in water availability of 11% for 2100 and of 9% for 2050. These results are in line with other previous studies (Figure 43). These changes in sustainable water availability will have consequences on a city scale, for both the socio-economic conditions and for ecosystems.

Figure 49. *Studies on the expected reduction in hydrological resources in Barcelona for 2050 and 2100.*

Study	Mean Expected Reduction by 2050	Mean Expected Reduction by 2100
Climate change impacts study in Barcelona—water cycle [10]	12%	No Data
RESCCUE Project	9%	11%
Water and climate change. Diagnosis of the impacts predicted in Catalonia [17,37]	7%–15% according to diverse scenarios	No Data

6 Conclusions

- The result of the urban drainage model simulations is an identification of the city's major critical points with historical flooding problems (Map 5, p. 9).
- Taking into account that Barcelona's drainage system already suffers overflows in 24% of the network for rainfall with an average return period frequency (T10), it is estimated that the negative effect of climate change will increase this value by 4%, reaching 28% overflow of the network and values of 44% for rainfall with less habitual return periods (T100).
- Regarding the risk to people, and the effects of flooding on pedestrian and vehicle stability, the high-risk areas will increase by around 30%, which means an increase from 240 to 312 ha of transitable surface area in the city for pedestrians and of 110 to 148 ha for vehicles, for a 10-year return period. If we consider the 100-year return period, these high-risk surface areas total 585 ha at present and this would rise to 762 ha (12.4% of the city's total transitable surface area) for pedestrians. For vehicles, the high risk areas would rise from the present 318 ha to 433 ha for the future scenario (7.1% of the city's total transitable area).
- The effects on the road network, in terms of speed reductions and street closures caused by flooding, also get worse with climate change. Comparing the results for the current and future scenarios, for the city's total 1,492 km of road network, between 13% and 21% of the streets – for the T10 and T100 return periods respectively – would experience reduced speed limits, while the number of closed streets in the future climate-change scenario would increase by around 20% for all return periods, which means approximately 30 km of streets closed for the 10-year return period and around 60 km of streets closed for the 100-year return period.
- On analysing the effects on urban waste containers by evaluating the risk of slippage and overturning caused by flooding with a 50-year return period and taking into account how full they are, we find that 17% of the total number of city containers studied lose stability in the current scenario and that this number could increase to 22% under future rainfall conditions, which means a 28% increase in the number of potentially unstable empty containers as a consequence of climate change.
- The model for seawater contamination due to discharges into the marine environment from the unitary sewer system, which simulates how water quality is affected by *E. coli* bacterial contamination, show that during the bathing season, the city's beaches could suffer up to 3.22 days of red-flag closure due to low water quality.
- The neighbourhoods most affected by damage to property are El Raval, el Parc i la Llacuna del Poblenou, Sant Andreu, Sant Antoni, l'Esquerra de l'Eixample, la Marina del Prat Vermell and Zona Franca. At present, the city suffers damage to property for a value of €56 million for a rainfall episode with a 10-year return period, and €186 million

for a rainfall episode with a 100-year return period. With future rainfall, made worse by climate change, this damage will become significantly more severe, by between 35% and 40% for the 10-year and 100-year return periods, respectively, so that the damage caused is estimated at €75 million and €260 million for the 10 and 100-year return periods, respectively

- The main conclusion derived from the modelling of the city's electricity system is the need to explore this area further, given that the project's results are based on a series of hypotheses and premises produced with estimated data and which do not reflect the reality of the system.
- The main effects of the rising sea level on the seashore occurs at the city's beaches, which will lose approximately 3.36 ha (about 11% of the total surface area) in the case of a 35 cm average rise in sea level for the RCP 4.5 scenario by the end of the century and 5.03 ha (about 17% of the total) in the case of a 50 cm average rise in sea level for the RCP 8.5 scenario by the end of the century.
- The results of the analysis of the supply capacity of the reservoirs in the Ter and Llobregat catchment areas indicate an 11% reduction in hydrological resources by the end of the century, taking into consideration the worst-case scenario for climate change.